EVALUATING THE IMPACTS OF TIDAL STRUCTURES ON THE ABILITY OF MARSHES TO REDUCE COASTAL HAZARD IMPACTS

by

ADA CHIMZULUKEME AGBOGU

(Under the Direction of C. Brock Woodson & Matthew V. Bilskie)

ABSTRACT

Coastal communities are threatened by many hazards, such as storm surge, flooding, saltwater intrusion, and coastal erosion. A tide gate at Hunter Army Airfield in Savannah, GA, has a history of failure and repair that has caused numerous ecological shifts to the low-lying vegetation located between the tide gate and a critical rail line upstream. Field surveys and a hydrodynamic model were used to determine the effects of the tide gate on the surrounding marsh and to quantify how these landscape changes translate into the performance of the marsh ecosystem as natural infrastructure. Four scenarios (natural, present, potential, and damaged conditions) were used in a hydrodynamic model to identify potential issues, including tide-gate overtopping, increased erosion risk, and extended flooding due to flow constrictions. In conclusion, this research helps understand the implications of how traditional infrastructure disrupts ecosystem function and the trade-offs between engineered and natural coastal defense systems.

Keywords: Coastal hazards, Gray infrastructure, Advanced Circulation Model (ADCIRC), Tidal Marsh, Tide gate, Military installation.

EVALUATING THE IMPACTS OF TIDAL STRUCTURES ON THE ABILITY OF MARSHES TO REDUCE COASTAL HAZARD IMPACTS

by

ADA C. AGBOGU

B.Sc., University of Nigeria, 2019

A Thesis Submitted to the Graduate Faculty of the University of Georgia in Partial Fulfilment of the Requirement for the Degree

MASTER OF SCIENCE

ATHENS, GEORGIA

2025

EVALUATING THE IMPACTS OF TIDAL STRUCTURES ON THE ABILITY OF MARSHES TO REDUCE COASTAL HAZARD IMPACTS

by

ADA CHIMZULUKEME AGBOGU

Major Professor(s): C. Brock Woodson

Matthew V. Bilskie

Committee: Whitney A. Pagan

Daniel J. Coleman

Electronic Version Approved:

Ron Wolcott

Vice Provost for Graduate Education and Dean of the Graduate School

The University of Georgia

December 2025

ACKNOWLEDGMENTS

Completing this research would not have been possible without the assistance, contribution, and guidance of so many people whose names may not all be enumerated. Most of all, I would like to thank my major supervisors, Drs. C. Brock Woodson and Matthew V. Bilskie, for taking a chance on me, a humble girl from Nigeria. I am also grateful to Dr. Whitney Pagan who provided tutelage and support, and for that, you have my immense gratitude.

Special thanks to Dr. Daniel Coleman, for his dedicated and unwavering help to my research work. To Madison Lepain, Elizabeth Collins, Holly Mullins and Olorunjuedalo Oguntoyinbo, colleagues who were always available for the field trips to Savannah, I say a big thank you.

To my other colleagues, Aditya Gupta, Becca Stanley, Oscar Villegas Gutierrez, Ebrahim Hamidian, Nashid Mumtaz, Caraline Miller, Saeid Khaksarinezhad, Lina Cardenas, Hunter Kunzelmann, Alex Boland, Liz Collins, Holly Mullins, Frank McQuarrie, I say thank you for the love we shared as a family in COBIA-COAST Lab.

To my family back in Nigeria and those here in the United States, thank you for your support and prayers.

Above all, to the God Almighty, the author of knowledge and wisdom, I thank you for always being there for me especially when the going was tough.

TABLE OF CONTENT

Page

LIST OF TABLES

LIST OF FIGURES

CHAPTER 1

INTRODUCTION AND MOTIVATION

Coastal regions are prone to hazardous events that can negatively affect inhabitants and the surrounding environment (Zhang et al., 2004). These coastal hazards include storm surge, hurricanes, flooding, saltwater intrusion, and erosion and they frequently lead to environmental deterioration, property damage, and loss of life, prompting efforts to prevent or mitigate their impact (Spalding et al., 2014). Anthropogenic activities along coastlines, ranging from industrialization, fertilizer use, urbanization, and overexploitation of resources, are adding pressure on the environment and making the surrounding ecosystem unstable (Hautier et al., 2015). On top of these pressures, climate change is increasing the frequency of coastal hazards, which increases the damage and the costs of repairs (UN, 2022).

Coastal communities often rely on armoring and engineered structures for protection against natural hazards. Such protection is often in the form of gray or conventional infrastructure such as seawalls, dikes, tide gates, riprap, etc. (Figure 1.1, Powell et al., 2019). Conventional infrastructure, usually comprised of steel and concrete, can be expensive to construct and maintain, and often leads to the degradation of the surrounding natural ecosystem. (Waryszak et al., 2021; TNC, 2021). As the effects of climate change become more prevalent, conventional infrastructure often becomes obsolete because it is designed using historical and outdated codes, (International Code Council., 2021) creating the need for a more resilient and nature-friendly protection strategy. In addition, conventional infrastructure is projected to experience further damage with increasing impacts of climate change (Kuwae & Crooks, 2021). As a result, NI approaches began to gain

interest as they proved to be environment and cost-friendly, sustainable, and adaptable (Sutton-Grier et al., 2018).

Figure 1.1: Armoring at the base of the railroad crossing at HAAF

NI are the physical components of nature that provide ecosystem services to support engineering objectives; NOAA, (2024). NI capitalizes on the adaptive capacity of natural systems to enhance coastal resilience. Examples of NI include coral reefs, oyster reefs, wetlands etc. (Beck et al., 2018; Stanley et al., 2024). The actions taken using these natural systems to address, sustainably manage, and solve societal challenges to benefit people and the environment are referred to as Nature-based Solutions (NbS). NbS harness the capacity of nature to adapt and provide ecosystem services to the community (European Communities, 2015). A comprehensive grasp of NbS involves an understanding of the geographical distribution of biomes, biodiversity, their ecological resilience, and knowledge of a variety of native species to offer environmental benefits for climate change mitigation and human safety (Seddon et al., 2020). Some features mimic characteristics of natural

components, but are created by human design, engineering and construction to provide specific services to the environment (Bridges et al., 2015). These features are known as Nature-based Features (NbF) and examples include constructed wetlands, artificial dunes etc., whereas the natural components are the Natural Features (NF) that evolve through the actions of physical, biological, geologic, and chemical processes operating in nature. A combination of NbF and NF is referred to as Natural and Nature-based Features (NNBF) (Bridges et al., 2015).

NI can also be combined with conventional infrastructure to leverage the strengths of both to address social, economic, and environmental challenges (Sutton-Grier et al., 2015). The recognition of these benefits has spurred a re-evaluation of coastal protection strategies, and interest has grown in fusing engineered structures with the resilience of natural systems (Nichols et al., 2019). By combining conventional infrastructure with naturally occurring systems, coastlines are better protected, as the combination of both natural and gray infrastructure offers the benefits of both protective approaches (Singhvi et al., 2022; Song et al., 2024). Integrating these approaches has proven effective and recognized in recent years for both environmental and societal co-benefits (Bridges et al., 2022). However, when conventional infrastructure fails, it can result in the degradation of the surrounding NI. This, in turn, reduces the protective capabilities of the NI (Figure 1.2).

For instance, the damage of gray infrastructure projects can often contribute to the degradation of adjacent wetlands Nunn & Kumar, (2018) by introducing salt water to the wetland when it is already accustomed to a freshwater regime. This action stresses the non-salt-tolerant vegetation which can eventually lead to wrack accumulation and vegetation dieback. Another issue is habitat loss (Orton et al., 2023). Damage to the gray structure may alter hydrologic conditions in ways

that displace or endanger aquatic species, increasing mortality rates and disrupting ecological balance.

Figure 1.2: The left and right image shows dead vegetation because of marsh degradation from saltwater re-introduction.

In other words, altering the natural flow in vegetated areas can compromise their ecological function, highlighting the importance of assessing how human-engineered structures interact with and impact their surrounding environments. Therefore, given the complex interactions between engineered structures and natural systems, this study's overarching objective is to understand better the ecological impacts of the tide gate at Hunter Army Airfield (HAAF), Savannah, GA, on the surrounding tidal marsh ecosystem. To do this, I used field surveys and a hydrodynamic model, ADCIRC, to simulate water movement over the marsh for four landscape conditions (natural,

present, damaged tide gate, potential) that I generated. I then evaluated how the flow-marsh interactions affected the railroad crossing located upstream of the tide gate under those four landscape conditions. Hurricanes Matthew and Irma were used to evaluate system response under extreme conditions. Based on the above overarching research objective, the following specific objectives were:

1.) to understand the evolution of the marsh habitat during disturbances (destruction or repair of the tide gate).
2.) to characterize the marsh on the downstream and upstream sides of the tide gate through time to understand the effects on erosion and flood risk reduction.
3.) to understand how the tide gate alters storm surge and erosion relative to an undisturbed condition.
4.) to provide alternatives to a tide gate if needed for improved infrastructure performance.

CHAPTER 2

LITERATURE REVIEW

Humans have tried both in the past (Watson & Finkl Jr., 1990; Chapman & Bulleri, 2003) and in the present (van der Wulp et al., 2016; Balaji et al., 2017) to intervene in matters regarding natural hazards and climate change by using conventional or gray infrastructure (Coch & Wolff, 1991; Pearlstine et al., 1993; Irish et al., 2013; Cooke et al., 2020). In addition to gray infrastructure, natural infrastructure (NI) has emerged as a vital strategy for coastal protection. NI, such as tidal marshes and mangroves (Krauss et al., 2009), offers significant advantages due to the inherent ability to adapt to dynamic environmental conditions. Recently, solutions combining natural and conventional infrastructure have been employed because the combination offers durability and adaptability (Kawabata et al., 2024), which is very important to combat climate change impacts. However, conventional structures, especially when destroyed or damaged by a natural event, usually affect the natural systems surrounding them (Pearlstine et al., 1993; Souder et al., 2018). Therefore, it is essential to ascertain the effect of conventional structures on NI to ensure the overall condition of the system and the benefits it provides. This section explores the environmental consequences of coastal hazards, elucidating the effects of storms, inundation, and erosion on proximate critical infrastructure and ecological systems. The review further assesses the natural and engineered mitigative strategies for enhancing coastal resilience and examines how human activities affect marsh hydrodynamics, focusing on erosion control and flooding. The numerical model, ADCIRC is discussed in detail to elucidate its suitability and effectiveness in simulating hydrodynamic conditions essential to my research study.

Environmental Impact of Coastal Hazards

Coastal hazards are natural phenomena that expose coastal areas to the risks of property damage, loss of life, and environmental deterioration (Spalding et al., 2014, Bhable et al., 2015). Despite this, many people still prefer to reside near coastlines because of advantages like health benefits (Wheeler et al., 2012; Sandifer et al., 2012; Nash et al., 2022), easy access to water (Barlow & Reichard, 2010; Reimann et al., 2023), and certain food items (Seara et al., 2016; Lakshmi, 2021). The desire to live on the coast underscores the urgent need for effective and equitable strategies to enhance environmental resilience against coastal hazards (Haigh et al., 2018). Proactive measures, such as integrated coastal zone management and sustainable infrastructure, are essential to mitigate risks and ensure that shorelines remain safe and habitable in the face of evolving climate challenges (Bernard et al., 2006; Sandifer & Scott, 2021).

Some of the most costly and deadly coastal hazards are hurricanes which can cause flooding and significant wind damage to properties and infrastructure (National Weather Service, 2020; Welch-Devine & Orland, 2020; NOAA, 2024). For example, Hurricane Katrina remains one of the costliest and most devastating disasters to ever affect the U.S. as it cost many human lives and accrued about $75 billion USD in damages (NOAA, 2020). Beyond human life and property loss, hurricanes can degrade ecosystems by introducing pollutants into waterways (Rothenberger et al., 2018), alter salinity levels, and cause ecosystem degradation (The American Littoral Society, 2012). Hurricanes are a threat as their physical and ecological impacts on human communities and surrounding environments can persist for years (National Weather Service, 2020).

Flooding is another environmental hazard with negative effects on human lives and the economy. For instance, flood events can lead to post-traumatic stress disorder Galea et al., (2005), Golitaleb et al., (2022), depression Waite et al., (2017), and anxiety (Osman et al., 2023). Additionally,

flooding can displace people from their homes and cause severe damage to public spaces, infrastructure, and ecosystems resulting in substantial economic burdens for both the government and communities (Longman et al., 2023).

Another coastal hazard, erosion, which is increasing due to sea level rise associated with climate change and land use change (urbanization), can cause loss of property and critical infrastructure (Borelli et al., 2020; Lim et al., 2021; Eekhout & de Vente, 2022). As waves with high intensity hits the surface material of a structure, particles of that material start to scour and mobilize leading to erosion. The stability of the infrastructure becomes compromised and may eventually lead to structural failure (Hanson & Lindh, 1993; Hewett et al., 2018). Considering the impacts of these coastal hazards, it is essential to adopt proactive measures that address both immediate and long-term risks. Coastal hazard mitigation strategies can provide the needed insight into how we can best protect both the fragile ecosystem and the human population while ensuring resilience against future threats.

Coastal hazard mitigation strategies

The behavior of the coastal landscape evolves across a wide range of time scales (seconds to decades) (Paola et al., 2023). Changes in the coastal landscape are often in response to climatic weather conditions like waves generated by storms but can also be attributed to recurring phenomena such as tides. As a result, communities and ecosystems near coastal regions will continue to face coastal hazards, but strategies can be put in place to secure livelihoods and properties from destruction. These strategies can either be the use of conventional (gray), NI or a combination of the two. Conventional infrastructure involves the design and construction of features such as seawalls, breakwaters, levees, bulkheads, and tide gates, while natural infrastructure includes the surrounding ecosystem and can involve natural and nature-based

features (NNBF) such as wetland construction, wetland restoration, and preservation of existing environments. In some cases, these approaches can be combined as hybrid gray-natural solutions, such as a seawall with planted mangroves on the ocean-facing side.

Gray Infrastructure

Projects involving the use of gray infrastructure typically employ the use of engineered assets to provide either one or multiple services required for the protection of human society. These services can include flood reduction, traditional stormwater management, and erosion control. These rigid structures are usually designed to prevent erosion and provide protection against wave action and highwater levels (UNFCCC, 1999). However, such conventional infrastructure can be very expensive to build and can also have deleterious effects on the surrounding area (Griggs, 2005; Chapman & Underwood, 2011). Reliance on conventional infrastructure has led to a few unanticipated negative outcomes on ecosystems (Brears, 2023). For instance, conventional infrastructure materials like steel and concrete used in the construction of seawalls and dams can be counterproductive as they lack the resilience useful for prolonged environmental protection in a fast-changing climate. Subject to scouring and weathering, the structural failure of this infrastructure can lead to catastrophic damage and the transformation of the surrounding environment (Balaji et al., 2017; Nunn & Kumar, 2018). For example, seawalls on an island in Fiji s developed cracks and began to crumble after some time. Villagers reported that the unstable and dilapidated structure no longer functioned as intended, and water flowed through cracks and into houses (Piggot-Mckellar et al., 2020). Seawalls and similar structures, alone, cannot adapt to changing pressures in the long term. Nature-based solutions, however, can be more sustainable, effective, and adaptable to future societal and environmental needs (Eggermont et al., 2015; Nunn et al., 2021).

Nature-based Solutions (NbS)

Nature-based Solutions (NbS) were identified in 2008 by the World Bank (MacKinnon et al., 2008) and had their first formal research initiative program launched in 2013 (Sowinska-Swierkosz & Garcia, 2021). The NbS concept emanated from the search for innovative strategies to manage natural systems in a manner that fosters both social and environmental benefits (UNEP, 2022). By collaborating with nature rather than opposing it, strategies could be devised for a resilient (Antuna-Rozado et al., 2019), resource-efficient, (European Commission, 2021), and environmentally sustainable economy (Nesshover et al., 2017; Liu et al., 2021). Numerous attempts have been made to define nature-based solutions and a very prominent definition stemmed from the International Union for Conservation of Nature (IUCN). They defined NbS as "*actions to protect, sustainably manage, and restore natural or modified ecosystems, that address societal challenges effectively and adaptively, simultaneously providing human well-being and biodiversity benefits.*" (Cohen-Shacham et al., 2016). The Friends of Ecosystem-based Adaptation (FEBA), a global collaborative network of organizations state that nature-based solutions offer decreased vulnerability for exposed low-income communities by bolstering food and water security and generating income (FEBA, 2022). Also, with NbS, ecosystems can be restored and preserved, aiding in the mitigation of flood and landslide occurrences and strategies offered by NbS can be adopted locally, thus enhancing autonomy and resilience in communities (FEBA, 2022).

Natural Infrastructure (NI)

Natural infrastructure consists of natural ecological systems that provide societal benefits such as storm protection or erosion control. NI is considered a sustainable and resilient approach that can provide necessary steps needed to tackle socio-environmental problems as they can adapt and provide long-term solutions to climatic change impacts (Zhao et al., 2016; Girardin et al., 2021).

NI provides ways to strategically and intentionally preserve or restore elements within a natural system to provide additional societal benefits (Kurth et al, 2024; NOAA, 2024). NI can be resilient Hovis et al., (2021), Bechauf et al., (2022), cost-effective Pirro et al., (2023), and sustainable (Sutton-Grier et al., 2018). However, if NI is damaged or degraded, the loss of ecosystem services can lead to severe environmental and economic consequences. The adoption of nature-based practices has demonstrated numerous advantages Seddon et al., (2019), Dick et al., (2020), Spano et al., (2021) Simelton, et al., (2021) but if projects are not well-designed or do not support surrounding ecosystem function, they may disrupt ecological balance when they fail and can lead to system instability, ultimately diminishing their long-term benefits (Albert et al., 2020).

Hybrid Infrastructure (fusing NI with hard structures)

Hybrid solutions are adaptative strategies combining natural and gray infrastructure (Sutton-Grier et al., 2015). Theese hybrid approaches can deliver improved protection to our coastlines and shorelines (Elliot et al., 2007; Steven et al., 2020). Since engineered infrastructure and NI each possesses distinct strengths and weaknesses, leveraging a blend of these approaches allows for the capitalization of the strength of both while attempting to mitigate their respective weaknesses (Gedan et al., 2011; Sutton-Grier et al., 2015; Waryszak et al., 2021). Newly constructed or restored NI may initially be vulnerable as ecosystems take root (Abelson et al., 2020). During this critical establishment phase, the integration of gray infrastructure can serve as a protective strategy, shielding the nascent natural system temporarily from the impacts of intense weather events. By mitigating the effects of extreme conditions, the gray infrastructure helps ensure the natural system has sufficient time to stabilize and develop its full protective and ecological functions (Sutton-Grier et al., 2015; Oppenheimer et al., 2019; Newton et al., 2020; Smith et al., 2020).

An example of a hybrid system is a living shoreline, a coastline protection method that involves habitat restoration alongside some form of engineered structure (NOAA, 2015). Another form of hybrid system is when NI (e.g., mangroves) is placed before the gray infrastructure (e.g., bulkehad or revetment) to lessen the impact of the incoming wave energy and facilitate sediment accumulation on the engineered structure thereby improving longevity and performance. Such hybrid solutions provide a sustainable and cost-effective way of addressing sea level rise (Currin et al., 2008; Manis et al., 2015). While hybrid infrastructure offers a promising pathway to enhancing the durability and effectiveness of coastal defense systems, the interplay between gray and NI are critical. When gray structures are compromised by coastal hazards, the nearby natural systems are often left to bear the brunt of the hazard impacts.

Impacts Of Failed Hard Coastal Defense Structures On Natural Infrastructure (NI)

The need to protect critical infrastructure is usually the driving force behind the design and construction of most hard defense structures (Griggs & Patsch, 2019; Cooper et al., 2020). However, these hard defense structures often disrupt natural coastal systems, especially when damaged (Giannico & Souder, 2005). This damage can lead to unintended consequences for surrounding ecosystems like mangroves and marshes (Figure 2.1). One effect of failed coastal defense structures is the alteration of hydrology and vegetation dynamics within the affected ecosystems (Environmental Protection Agency, 2020; Sanitwong-Na-Ayutthaya et al., 2023). Such hydrological disruptions can have profound implications in regions with extensive marshland coverage, such as Georgia, where tidal marshes not only support diverse ecosystems but also serve as critical buffers against coastal erosion and storm surge impacts.

Figure 2.1: A healthy NI system dominated by salt-intolerant vegetation (left) compared to the same area affected by saltwater from the downstream after the damage of an existing gray structure (tide gate) by a storm event (right).

Marsh Ecosystems

In Georgia, marshes are very common, occupying approximately 4.9 to 7.7 million acres (Georgia DNR, 2006). Marshes are characterized by herbaceous vegetation, inundated during high water events, and are regarded as NI because they help attenuate waves during storm events. A type of marsh, known as freshwater marshes, are wetlands with less than 0.5 ppt salinity (North Carolina Wetlands, 2017) that are intermittently flooded (Adam, 2015; Mcowen et al., 2017; Fegherazzi et al., 2019), and tend to have a higher diversity of plant species (Odum, 1988). Another type of marsh, saltmarshes, are wetlands that are usually flooded and drained by saltwater brought about by the rise and fall of tides (NOAA, 2024). Predominantly dominated by emerging plants and grasses, saltmarshes range from very slender fringes on steep coastlines to flat expanses of land several miles wide. Dominant plant species for salt marshes along the US East and Gulf coasts are the saltmarsh cord grass (*Spartina alterniflora*), spike grass (*Distichlis spicata*), and salt meadow cordgrass (*Spartina patens*), while common fresh marsh plants include pickerelweed (*Pontederia cordata*), soft rush (*Juncus effuses*), arrow arum (*Peltandra virginica*), and buttonbush (*Cephalanthus occidentalis*) (Bertness & Shumway, 1993). This vegetation can significantly affect

the flow of water within the estuarine ecosystem (Cai et al., 2023). Saltmarshes are typically characterized by a dendric-like network of tributaries that transport sediment and water to the ocean and these tributaries self-organize to distribute the tidal flow across the entire system evenly (Dai et al., 2021).

Salt marshes occur around river mouths, bays, and protected lagoons. Salt marshes serve as nursery and spawning grounds, migration pathways, and feeding grounds for a variety of marine life (Cattrijsse & Hampel, 2006) and are regarded as one of the most productive ecosystems on the planet, playing various roles in ensuring a functional and stable global ecosystem (Knutson et al., 1982; Turner et al., 2004; Visser, et al., 2019; NOAA, 2021). Generally, salt marshes are in middle and high latitudes along the coasts in low-energy shoreline areas forming the interface between terrestrial and marine environments (Visser et al., 2019). These marshes are essential parts of estuarine ecosystems providing ecosystem services that protect and cushion coastlines from intense surges and waves (Costanza et al., 1997; Gedan et al., 2008; Sherman & Hartman, 2021; Taylor et al., 2021; Jing et al., 2023).

Coastal Marshes and Threats to their Ecosystem Services

Coastal marshes provide ecosystems services such as wave attenuation and storm surge reduction. Ecosystem services refer to the benefits humans get from surrounding environments. The ecosystem services provided by marshes are at risk due to anthropogenic activities Broome et al., (2019) that have led to environmental changes and have contributed to marsh depletion around the world (Purcell et al., 2020). Apart from human activities, Krebs et al., (2023), stated that sea level rise could also impact marsh habitat loss. Historically, the function and importance of coastal marshes were treated with less regard as they were not viewed as a significant source of hydraulic resistance or as a system that impeded the transport of high wave and wind energy (Kemp et al.,

2000; Duan et al., 2002). Now, marshes are widely recognized as critical NI and have been shown to reduce sediment suspension, stabilize channels, provide habitat for organisms, improve water quality, and sequester carbon (Luhar & Nepf, 2013; Drake et al., 2015; Alizard et al., 2018; Schuerch et al., 2022; Irwin et al., 2018; Van Coppenolle & Temmerman, 2020; Temmerman et al., 2023; Adams et al., 2021; Woods, 2021; Yu et al., 2022). By applying restorative strategies on the coastlines, the ability of marshes to reduce storm surge could be enhanced. This nature-based approach not only promotes resilience toward climate impacts but also offers a sustainable solution for coastal protection.

Coastline protection via wetland restoration is being used to dampen the effects of coastal hazards but can be challenging to implement successfully (Long Island Sound Habitat Restoration Manual, 2004; Barbier, 2011; Li et al., 2018). Degraded salt marsh ecosystems can be restored either by reintroducing tidal exchange or adjusting sediment levels (Day et al., 2007; Day et al., 2021) or both (Billah et al., 2022). Wetland restoration projects are most successful when restored sites mimic their original surrounding environment in their designs, especially in terms of hydrology and morphology (Middleton, 1999; Kentula, 2000). When successfully restored, wetlands can provide the ecosystem resilience along the coasts needed to combat climate change and reduce the cost of coastal protection in the long term (Van Zelst et al., 2021).

Vegetated and unvegetated wetlands play a crucial role during storms (Gedan et al., 2011). Often regarded as the ‘kidney’ of the environment, wetlands thrive in porous and spongy soils, allowing them to absorb a large amount of water during precipitation (Mitsch & Gosselink, 2015). As a result, they tend to reduce the effects of erosion and flooding in coastal areas. As wetlands slow down the intensity of flowing water, damage that could have been done to ecosystems and

infrastructure, may be averted. However, the protection can be increased when wetlands are combined with man-made structures. A vital benefit of wetlands is their ability to retain water.

Wetland vegetation reduces the intensity of the incoming wave energy and disperses the energy over a wide area (Shepard et al., 2011). This process also slows down the flow velocity and in turn, may diminish erosion. Wave energy is proportional to the square of the height of the wave:

$$E = \alpha H^2 \text{.....Equation 2.0}$$

and the total energy of the wave per unit area is:

$$E = \frac{1}{8}\rho g H^2 \text{.....Equation 2.1 (Stewart, R. H.; 2007)}$$

where E is the nergy per unit area (J/m^2), ρ is the density of water (sea water) (approximately 1029 kg/m^3), g is acceleration due to gravity (9.81 m/s^2), and H is the wave height (in meters).

Wetlands decrease the wave height as waves pass through due to the friction produced by the surface contact. The wave height reduction between two points can then be calculated as:

$$\Delta E = E_1 - E_2 = \frac{1}{8}\rho g(H_1^2 - H_2^2) \text{.....Equation 2.2}$$

where E_1 and E_2 are the energy per unit area (J/m^2), and H_1 and H_2 are the wave heights (in meters) at points 1 and 2 respectively.

The mitigation of storm impacts depends on the abundance and density of vegetation found in the marsh as the vegetation produces resistance that decelerates the mean flow by producing drag, a resistive force that dissipates the energy carried by flowing water (Wu & Marsooli, 2012; Marsooli & Wu, 2014; Foster-Martinez et al., 2018; Rizalihadi et al., 2019; Brooks et al., 2020; Zhang & Nepf, 2021; Zhang & Nepf, 2024).

Plant Density and Drag Coefficient

Drag is the force generated by a fluid flowing over or around an obstruction. This resistive force can be caused by different features such as channel morphology Kranenburg et al., (2019), Bo & Ralston, (2020), topographic roughness Warner & MacCready, (2014), bed composition, Grant & Madsen, (1982), and vegetation (Nepf, 1999; Horstman et al., 2021). Drag exerts a force on the flow capable of dampening incoming wave energy and surges. This is one reason why vegetation is regarded as a solution to flooding and erosion problems as it reduces flow velocity (Rupprecht et al., 2017). Vegetation transforms mean kinetic energy into turbulent kinetic energy at the scale of branches and plant stems (Nepf, 1999). This conversion of energy heavily impacts turbulence intensity and vegetative drag. The force of the vegetative drag can be defined as the drag force per fluid mass as:

$$F_D = \frac{1}{2} C_D \rho a U^2 \quad \text{.....Equation 2.3}$$

Where C_D is the bulk drag coefficient, ρ is the density of the fluid, a is the vegetation density in meters, and U is the uniform flow speed. The coefficient of drag is a function of plant density and usually depends on the Reynolds number, defined as the ratio of inertial to viscous forces in a flow:

$$\mathrm{Re} = Ud/\nu \quad \text{.....Equation 2.4}$$

Where U is the flow speed, d is the characteristic linear dimension (generally plant stem diameter), and ν is the kinematic viscosity (Nepf, 1999).

Salt marshes can attenuate waves and dissipate energy during harsh storm conditions and other hydrologic events (Garzon et al., 2019, Möller & Spencer, 2002; Zhu et al., 2023). Incoming waves are attenuated by marshes although the attenuation rate depended on the height of incoming waves

and marsh elevation between stations. Additionally, the amount of vegetation affects wave attenuation (Garzon et al., 2019; Schoutens et al., 2019; Coleman et al. 2022). Schoutens et al., (2019) gave a more detailed description of the effects of vegetation during seasonal cycles through monthly monitoring of the growth of *Bolboschoenus maritimus*, a dominant saltwater marsh species in the Elbe estuary located in Germany. Flow and tide attenuation rates were highest in the summer and lowest in the winter as the aboveground biomass was usually washed away by the first storms.

The measure of the elasticity of the plant leaves, known as Young's modulus, is also an important consideration as this determines the ability of the plant leaves to stretch and deform during a stress event such as a storm (Fig., 2.2; Zhu et al. 2023). Experiments showed that vegetation with rigid stems reduced more wave energy than vegetation with very flexible stems. Rominger & Nepf, (2014) further investigated the role of blade flexibility on drag force and demonstrated the association between blade flexibility and mass transfer to blades. With the use of modeled blades of different materials, the flexural rigidity of the blades was varied to make adjustments to suit real-life scenarios. Houser et al., (2015) emphasized the importance of blade rigidity in estimating energy dissipation during storm events. Their experiment showed that the "no-swaying" model, a term used for the rigid blades, was observed to produce higher drag force than the flexible blades. Similarly, Dalrymple et al., (1984) detailed the physical structure of the marsh vegetation and noted that marsh plants are predominantly flexible and can sway and bend in the presence of hydrodynamic forces. Their experiment also showed that the flexibility of the plant is essential to note since flexible stems remove less wave energy than rigid stems.

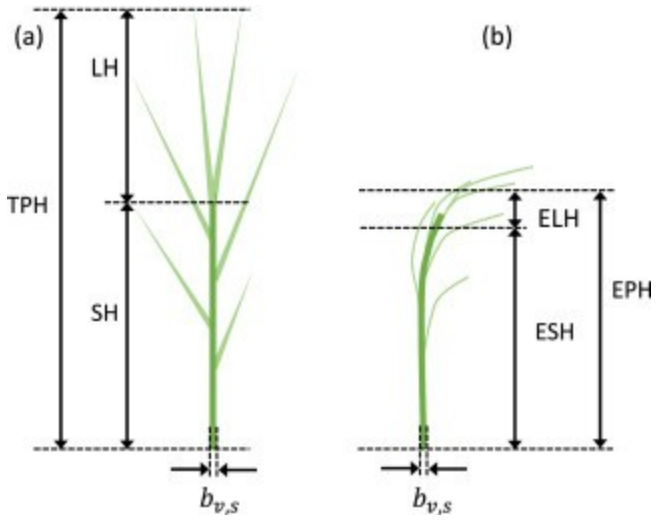

Figure 2.2: (a) Diagram of physical vegetation heights which includes stem height (SH), total plant height (TPH), and leaf height (LH). (b) Diagram of effective vegetation heights which includes effective leaf height (ELH), stem diameter $b_{v,s,}$ effective stem height (ESH), and effective plant height (EPH) .

Anderson & Smith, (2014) affirmed the usefulness and capabilities of marshes for wave attenuation using artificial stems of *Spartina alterniflora* (polyolefin tubing) in a large-scale flume (64.1m × 1.5m × 1.5m). This experiment provided wave energy dissipation capacity of *Spartina*. Focusing on the complexities of drag through a vegetation canopy provided information regarding wave irregularities at different heights, stem densities, periods, and water levels. The results indicated that as stem density increased, there was an increase in wave attenuation. The STWAVE (Steady State Spectral WAVE) model was used to estimate the drag coefficient.

Figure 2.3: Artificial Spartina alterniflora array in a flume used to run simulations for real-life scenarios (Anderson & Smith, 2015).

In the Yangtze estuary in China, an experiment was done to investigate the attenuation capacity of vegetation when plants are flattened since the stem of the native saltwater marsh species, *Scirpus mariqueter* is prone to breaking during the winter (Ge et al., 2018). With two experimental flume set-ups containing models of standing and flattened vegetation respectively, both scenarios could effectively dampen wave energies in higher wave conditions. However, the wave damping capacity reduced as water depth increased (Ma et al., 2023).

Bottom drag, also referred to as bed shear stress, is the resistive force exerted by the seabed on flowing water due to friction, and acts in addition to plant-induced drag. This drag is produced by different components ranging from the morphology of the coastal landscape to soil-bed composition, topographic roughness, as well as vegetation (which is a summative effect of the drag on individual plants). Drag varies as a function of flow direction, flow speed, fluid viscosity, fluid density, and other hydraulic parameters (Ortals et al., 2021). The coefficient of drag C_D, often expressed as bottom drag, can be related to the roughness length scale using:

$$Zo = z\, e^{(-\mathrm{k}/\sqrt{Cd,bot})} \quad \text{……Equation 2.5}$$

This type of drag emanates from marsh landscapes, leads to the formation of a boundary layer at the interface, and creates a characteristic logarithmic velocity profile:

$$u(z) = \frac{u*}{k}\left[In\left(\frac{z-d}{Z0}\right)\right] + \beta \quad \text{.....Equation 2.6}$$

where Z_0 is the bed roughness height, u(z) is the fluid velocity at reference height *z,* k is the von Karman's constant (k = 0.41), u^* is the shear velocity at *z*, d is the local water depth, and $\beta$is the correction coefficient. The drag coefficient, $C_{D,}$ is a means of evaluating the influence of vegetation on the hydrodynamic processes in tidal areas (Leonard & Richard, 2004; Wang et al., 2021).

The drag force produced by bed roughness in tidal environments plays a vital role in sediment transport and hydrodynamics (Ortals et al., 2021). Variations in seabed composition ranging from fine sediments to larger obstacles like rocks or vegetation, can significantly influence the movement of water (Nepf, H., 2012; Ban et al., 2017). While natural forces like bed roughness can alter flow, human interventions such as tidal structures can have an even greater impact. These engineered structures, while primarily designed to control the flow of water, can disrupt sediment transport (Caltrans Division of Research Innovation & System Information, 2016) and lead to unintended outcomes such as reduced ecosystem resilience and habitat loss.

Effects of Tidal Structures on the Surrounding Ecosystem

Water control structures are manmade devices designed to maintain and regulate water levels and facilitate the conveyance of water into different areas (Biehn, 1997; Rogers et al., 1992; Kimball et al., 2015; Bice et al., 2023). These structures are responsible for allocating and transporting water within open channels and for restricting hydrological connectivity (Kimball et al., 2015). Examples of such structures include stilling basins, culverts, dams, and tide gates (Environmental Protection Agency, 2020).

Water control structures are usually implemented in tidal wetlands to control water levels, support agriculture, and prevent flooding and erosion. This is useful in coastal areas, which are prone to flooding and where managing them can be challenging due to their complex nature. Tide gate structures control water flow by restricting water levels on the shoreward side while enabling runoff to flow outwards during intense precipitation, thus averting tidal flow beyond the tide gate structures (Walsh & Miskewitz, 2013; Molnar, 2016). These structures also affect the natural mixing and transport processes within the tidal wetlands (Giannico & Souder, 2005; Dokou & Karatzas, 2012).

Tide gate integration into coastal ecosystems can alter the ecological balance, resulting in adverse effects (Harrington & Harrington, 1982; Zhao et al., 2020). Physical effects of tide gates include upland flood mitigation, variation in turbulence, velocity, and freshwater discharge that fluctuates between pulsing, flushing, and water stagnation (Giannaco & Souder, 2005). Consequently, these variations in water circulation can lead to changes in water temperature, soil moisture content, channel morphology, and sediment transport. Furthermore, these hydrodynamic variations can disturb surrounding habitat, obstruct fish migration and change the composition of aquatic plants (Rytwinski et al., 2017).

Coastal Modeling

Coastal modeling is a way to capture, understand, and predict the complex flows that occur along our coasts (Li, H., 2019). Coastal modeling involves using physical and mathematical equations to generate a set of solutions that represent processes such as tides, storm surge, waves, etc., that occur on our coasts (Huge, J., 2025). By simulating these hydrodynamic processes, we can understand how water control structures affect the surrounding flow patterns and seek appropriate strategies to reduce potential impacts on our coastlines. Among available numerical models,

ADCIRC is commonly used to model tides, wind driven circulation, and assess the extent and occurrence of coastal flood hazards (U.S.A.C.E., 2022).

Advanced Circulation Model (ADCIRC)

ADCIRC is a numerical modeling system designed to simulate coastal flows and storm surge. ADCIRC is typically run in a two-dimensional depth-integrated numerical arrangement although a 3-dimensional model is possible (Luettich & Westerink, 1992; Luettich & Westerink, 2004) and uses an unstructured triangular mesh that allows for high resolution in regions with complex bathymetry and shorelines. ADCIRC solves the shallow water equations for surface water elevation and depth-averaged velocity (Kolar et al., 1994) using finite element methods in which each element contains approximated solutions obtained by a set of basic polynomial functions. These functions lead to a system of equations for solving the unknowns (water level and velocity – u, v) at each node and at each time step. ADCIRC uses an implicit or explicit time-stepping scheme for outputting the solutions of the shallow water equations (Blain & Rogers, 1998). To maintain numerical stability, the Courant Number is used to ensure that the specified time step and grid resolution allow waves to propagate accurately across each element (Pe Kinnmark & Gray, 1985).

The equations involved in the coastal modeling include continuity:

$$\frac{\partial H}{\partial t} + \frac{\partial}{\partial x}(UH) + \frac{\partial}{\partial y}(VH) = 0 \text{……..Equation 2.7}$$

where: U and V are depth-averaged velocities in the x and y directions, u and v are the vertically-varying velocities in the x and y directions, $H = \zeta + h$ is total water column depth, h is the bathymetric depth (the distance from the geoid to the sea bed), and ζ is the free surface deviation from the geoid,

and conservation of momentum (Navier-Stokes) equations:

$$\frac{\partial U}{\partial t} + U\frac{\partial U}{\partial x} + V\frac{\partial U}{\partial y} - \boldsymbol{fV} = -\frac{\boldsymbol{\partial}}{\boldsymbol{\partial x}}\left[\frac{\boldsymbol{Ps}}{\boldsymbol{\rho o}} + \mathbf{g}\,(\zeta - \alpha\eta)\right] + \frac{\tau sx}{\rho oH} - \tau_* U \quad \text{.....Equation 2.8a}$$

$$\frac{\partial V}{\partial t} + U\frac{\partial V}{\partial x} + V\frac{\partial V}{\partial y} - \boldsymbol{fU} = -\frac{\boldsymbol{\partial}}{\boldsymbol{\partial x}}\left[\frac{\boldsymbol{Ps}}{\boldsymbol{\rho o}} + \mathbf{g}\,(\zeta - \alpha\eta)\right] + \frac{\tau sy}{\rho oH} - \tau_* V \quad \text{.....Equation 2.8b}$$

With bottom stress, τ_* expressed as

$$C_f(U^2+V^2)^{1/2}/H \quad \text{.....Equation 2.9}$$

and C_f is the bottom friction coefficient.

This conservation of momentum equations is used by ADCIRC to determine the depth-averaged velocity (Blain & Rogers, 1998; Luettich & Westerink, 2004; U.S.A.C.E., 2022). ADCIRC includes wetting and drying, boundary conditions, and flow resistance via vegetation that allows the model to realistically capture hydrodynamic behavior in wetland systems.

Wetting and Drying

Wetting and drying in ADCIRC allow elements to become wet or dry based on water levels, an essential feature for modeling coastal areas (Dietrich et al., 2004). The topography and bathymetry are also used as slight variations in elevation around an area can significantly affect flow patterns (Luettich & Westerink, 1995). As the water level rises above a minimum allowable water depth those areas are considered flooded, and as the water recedes and falls below the minimum allowable water depth, the area is considered dry (Luettich & Westerink, 1999). ADCIRC makes note of the nodes and elements at the grid boundaries considered wet or dry, as these intricate flow movements aid in capturing ocean area, tidal fluctuations, flood, and erosion patterns.

Boundary Conditions

Tidal exchange occurs when coastal waters interact with the open ocean (Li, H., 2019). Within ADCIRC, this interaction is addressed by applying boundary conditions and tidal forcing at the grid domain. The model uses tidal constituents derived from astronomical data to analyze the periodic rise and fall of tides. Tidal constituents are applied at the open ocean boundary to allow ADCIRC to simulate tidal flow dynamics. The model also incorporates wind and atmospheric pressure data as these can affect currents within the coastal zone and in estuaries (Westerink et al., 1994). The model estimates water level, circulation, and transport patterns to enhance the understanding of sediment transport and ecosystem resilience (Pandoe & Edge, 2008; Orescanin et al., 2016).

Resistance to flow via Vegetation

Resistance to flow is influenced by vegetation (Zhang et al., 2015; D'Ippolito et al., 2021) As water flows through a vegetative terrain, the flow energy declines due to friction. ADCIRC incorporates vegetation by using frictional parameters that simulate how wetlands such as tidal marshes, mangroves, etc., slow down flow velocity. This roughness estimate is modeled using Manning's *n* coefficient, which quantifies how various types of land cover increase friction and decrease flow speed. In the model, Manning's n is converted into an equivalent quadratic friction coefficient at every node, which is then used to compute the bottom shear stress (ADCIRCWiki Contributors., 2020). This bottom stress term is then added to the momentum equation to represent the frictional resistance to flow (Westerink et al., 1994).

The friction coefficient equation is written thus

$$C_d(t) = gn^2 \ / \ \sqrt[3]{h + \eta(t)} \quad \text{.....Equation 2.10}$$

Where C_d is the drag coefficient, t is the time, g is the acceleration due to gravity, n is the Manning's n, h is the depth, η is the water surface elevation.

The incorporation of resistance to flow via vegetation into ADCIRC allows for the understanding of the roles natural barriers play in reducing erosion and flood risk in prone regions.

CONCLUSION

Coastal landscapes are shaped by a complex interplay of hydrodynamics, infrastructure, and ecological processes (Cameron & Pritchard, 1963; Appelo & Willemsen, 1987). While gray infrastructure provides structural protection, nature-based and hybrid solutions offer a more adaptive approach to mitigating coastal hazards. In many cases, these strategies can work together to reduce flood risk, stabilize shorelines, and enhance ecological resilience (Song et al., 2024). Water control structures like tide gates serve as engineered controls that regulate flow connectivity, sediment, and nutrient concentrations, however, the installation of these structures often comes at the cost of ecosystem resilience (Darnault & Uyusur, 2008). Coastal modeling provides a framework for analyzing these interactions, with ADCIRC serving as a critical tool for simulating tidal dynamics and assessing the long-term impacts of infrastructures on the ecosystem. As research continues to bridge the engineering and ecology fields, the challenge remains to balance protection with preservation, ensuring that coastal systems remain functional and resilient even as climatic changes accelerate. Moving forward, the remaining chapters describe the research focus on understanding the effects of a tide gate on the surrounding landscape and how these changes affect the ability of the landscape to act as NI.

CHAPTER 3

EVALUATING THE IMPACTS OF TIDAL STRUCTURES ON THE ABILITY OF MARSHES TO REDUCE COASTAL HAZARD IMPACTS [1]

[1] A.C. Agbogu, D.J. Coleman, M.V. Bilskie, and C.B. Woodson. To be submitted to a peer-reviewed journal

ABSTRACT

Coastal hazards (e.g., hurricanes and extreme storms) can cause severe problems for ecosystems and human communities. To reduce the impacts of coastal hazards, a combination of gray and natural infrastructure (NI) is often used. However, damage to gray infrastructure can negatively impact adjacent natural systems. At Hunter Army Airfield (HAAF), Savannah, GA, a tide gate damaged in 2017 by Hurricane Irma was reinstalled in 2022 to protect an upstream railroad bridge from flooding and erosion. The tide gate has experienced multiple failures and subsequent repairs, causing drastic shifts in salinity for the upstream habitat. The system is currently adjusting to a freshwater regime, causing changes in the vegetation and possibly affecting the ability of the natural system to reduce flow speed and attenuate floods. To better understand these changes, we used field surveys and a hydrodynamic model to determine the effects of the tide gate on the surrounding marsh area and to quantify how these landscape changes translate to the performance of the marsh ecosystem as NI for flood protection and erosion control. Based on the landscape changes four scenarios were developed: a current condition, one without tide gate, a damaged tide gate, and a potential stable state. By comparing modeled flow velocities and water levels across these various landscapes, we identify potential issues such as tide gate overtopping, increased erosion risks, and extended flooding due to flow constriction. Ultimately, our work helps to understand the implications of altering the natural regime of an ecosystem and provide guidance for other coastal communities navigating the tradeoffs created by the co-existence of engineered and natural coastal defense systems.

INTRODUCTION

Coastal communities are threatened by a multitude of hazards, such as storm surge, flooding, saltwater intrusion, and coastal erosion (Spalding et al., 2014). These hazards, which may intensify due to climate change, frequently lead to environmental deterioration, property damage, and loss of life, prompting efforts to prevent or mitigate their impact. People living on the coasts often use conventional infrastructure like seawalls and dikes for protection and shoreline stabilization (Coleman, et al., 2024). However, such structures, when they fail, often lead to the degradation of the natural systems surrounding them, particularly when they are installed as barriers that restrict and disrupt natural flow (Nunn & Kumar, 2018). With the escalating impacts of climate change, NI approaches are an alternative gaining popularity (Sutton-Grier et al., 2015). NI capitalizes on the adaptive capacity of natural systems to enhance coastal resilience and environmental sustainability while providing similar flood and storm surge protection as conventional infrastructure (Sutton-Grier et al., 2015).

Limitations associated with conventional infrastructure have led to a growing desire and demand for alternative coastal protection approaches. For instance, the rigid materials that conventional infrastructure are composed of, provide limited ability for self-repair after major storm events (Mishra & Rai, 2017; Powell et al., 2019). Moreover, conventional infrastructure requires significant financial investment for regular maintenance Hinkel et al., (2014), Waryszak et al., (2021), and their static nature limits their ability to keep pace with sea level rise, making the structures alone insufficient for long-term coastal protection (Schoonees et al., 2019). When considering their life-cycle design, some conventional infrastructure can be adaptable, however. Bhattacharya et al., (2025) examined how optimal life-cycle adaptation strategies enable coastal infrastructure to be updated or retroffited over time to remain resilient under changing conditions.

The recognition of this potential, alongside their limitations has spurred a re-evaluation of coastal protection strategies, with increased interest in practices that fuse engineered structures with the resilience of natural ecosystems (Nichols et al., 2019). Combining conventional infrastructure with natural or 'nature-positive' approaches can improve coastal and shoreline safety while offering the benefits of both natural and traditional infrastructure (Schoonees et al., 2019). Implementing these features has proven effective and is being recognized for both environmental and societal co-benefits (Bridges et al., 2022).

However, the combination of these two types of infrastructure is not always synergistic; gray infrastructure has been shown to alter or degrade nearby ecosystems (Suedel et al., 2022). For example, a tide gate, a water control structure designed to limit the upstream propagation of tidal flows, can lead to reduced sediment transport and salinity shifts, thus affecting the ability of the ecosystem to reduce hazard impacts (Pearlstine et al., 1993; Giannico & Souder, 2005). This dual nature of tide gates–offering flood protection while altering natural tidal dynamics—highlights the complex interactions of conventional infrastructure and natural ecosystems on coastal hazard mitigation.

While there are practical application of tide gates to address ongoing challenges caused by storm surge and hurricane events Walsh & Miskewitz, (2013), Yasmin et al., (2022), their effects on the natural flow of water can lead to physical, biological, and chemical changes for the surrounding ecosystem (Giannico & Souder, 2005). Tide gates alter upstream turbulence, velocity, and water levels, leading to changes in sediment transport and erosion patterns that can, in turn, compromise the stability of upstream habitats (Giannico & Souder, 2005; Johnson & Hutchins, 2023). The restricted flow can concentrate nutrients and heavy metals, increase turbidity, and alter water pH and salinity (Orton et al., 2023). This ultimately degrades water quality and can threaten aquatic

life (Orton et al., 2023). Tide gates also limit the access of aquatic organisms to habitats crucial for spawning, feeding, and predator avoidance by isolating upstream and downstream communities (Giannico & Souder, 2005). On the other hand, when tide gates are removed or damaged, such as by intense storms, the surrounding ecosystem that has adapted to their presence could be disturbed (Pearlstine et al., 1993; Airoldi et al., 2005). For instance, the natural system that might have adjusted to the presence of a functioning water control structure, such as an adjacent fresh marsh (Bice et al., 2023), may experience a temporary reduction in their capacity to provide environmental protection during periods of tide gate damage due to an influx of saline water located behind the water control structure.

An ecosystem frequently interacting with tide gates is saltmarsh. They are a common native habitat along the coast of Georgia, covering approximately 4.9 to 7.7 million acres (Georgia DNR, 2006), and providing ecosystems services (Nepf, H., 1999; Shepard et al., 2011). Saltmarshes can act as natural sponges, absorbing excess water during storms and gently releasing it afterward, thereby reducing flood heights and runoff (Nepf, H., 2012). As such, they have tremendous value for climate change adaptation and coastal hazard mitigation (Shepard et al., 2011). However, like many other ecosystems, marshes face numerous threats emanating from anthropogenic activities and natural processes such as pollution, land use change, invasive species, and climate change, that can impact their long-term survival (Giuliani & Bellucci, 2019; Zhang & Nepf, 2021).

One such example of human intervention impacting marsh dynamics can be observed at Hunter Army Airfield (HAAF) in Savannah, GA, where a man-made historic tide gate has altered the natural hydrological processes of a saltmarsh-dominated area. The tide gate installation triggered major ecological changes upstream, where the marsh shifted from saltmarsh to freshwater wetlands and low-lying maritime forest. While the structure helps control water levels and limit flooding,

its periodic failures and replacements disrupt the system and triggers ecological shifts that toggle between degraded and healthy conditions, particularly upstream. Such shifts are associated with marsh elevation decline and vegetation mortality, leading to reduced ability of the marsh to attenuate tides and wave energy (Mazhar et al., 2022). For this reason, understanding the net impact of the tide gate on the upstream ecosystem is key to assessing whether damage or repair to the gray infrastructure helps or harms the marsh-tide gate.

In this study, I looked at the periods before and after the tide gate repair to assess the impact of the tide gate on the ability of the surrounding area to provide coastal hazard protection. Within this overall objective, I aim to answer the following key research questions:

1. How does the tide gate presence or absence influence erosion and flood levels in the upstream area during a storm, particularly around the railroad crossing?
2. What is the impact of tide gate failure and delayed repairs on flooding and erosion upstream?
3. Can NI provide protection against flooding and erosion in the absence of the tide gate?

The outcomes of this study will address critical concerns related to erosion, flooding, and storm surge dynamics, particularly upstream of the tide gate. I hope these results will lead to better management of systems that involve combining gray and natural infrastructure.

METHODS

Site Description

The study area is located within Hunter Army Airfield (HAAF; Figure 3.1), in Savannah, Chatham County, GA. Since its inception, HAAF has undergone a series of structural and operational changes, each leaving a distinct mark on the surrounding landscape. It has its origins as the Savannah Municipal Airport, established in 1929 (U.S.Army, 2025). A few decades later, the U.S. Savannah Air Force controlled the site and expanded westward to the tide gate area, after which they installed a concrete tide gate in 1957. This water control structure was placed to regulate upstream inundation at the base. Shortly after, the base was renamed to Hunter Air Force base and a railroad crossing, a secondary avenue used in the conveyance of the army and ammunition, was constructed. After a period of closure, the base reopened in May 1940, as Hunter Field. The facility was taken over by the U.S. Army Air Corps in 1941 for military training use and in 1950, the installation was renamed Hunter Air Force Base.

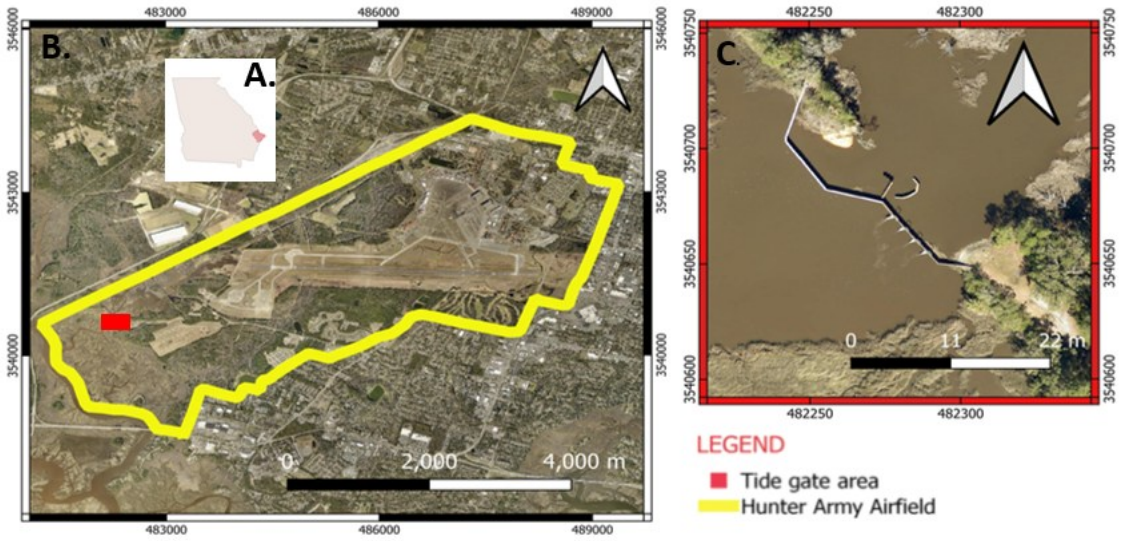

Figure 3.1: A. a map of Georgia indicating Chatham County, the location of Hunter Army Airfield (HAAF), where the study site is situated. B. The highlighted area in yellow indicates the HAAF boundary located approximately 32.011°N, 81.147°W, with the red square indicating the tide gate area. C. Aerial imagery of the tide gate structure within the study area.

The installed tide gate subsequently was damaged and repaired, and in 2002, the army base upgraded to a sheet pile tide gate. However, this replacement was compromised during Hurricane Irma in 2017, necessitating further reinstallation, which was completed in 2022 (Department of Defense, 2021).

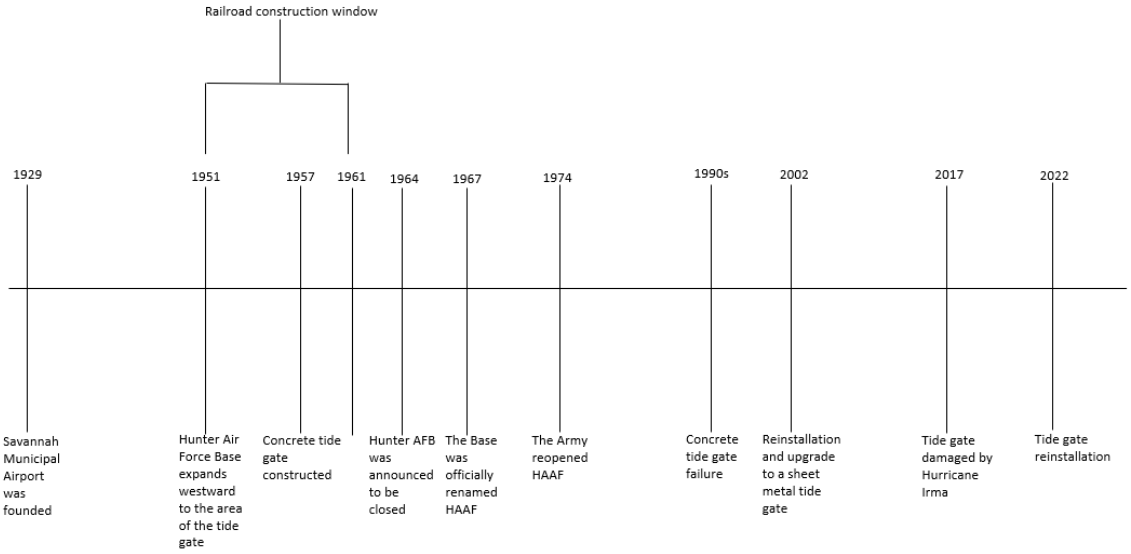

Figure 3.2: Chronological timeline of key developments at Hunter Army Airfield (HAAF), including the operational changes of the base, along with the installation, failure, and replacement of the tide gate structure that caused changes to the surrounding landscape. Spacing is a qualitative indicator of time between events (not to scale).

Before the installation of the water control structure, the area was predominantly characterized by salt marsh vegetation. Following installation, reduced tidal exchange from downstream led to a shift in upstream vegetation composition to non-salt-tolerant plants. Failure of the tide gate would introduce saltwater from the downstream, killing the established non-salt-tolerant plants upstream and re-establishing saltwater vegetation. After the tide gate was reinstalled, the upstream ecosystem began reverting to the non-salt-tolerant marsh as salt water from the downstream became restricted once more. This transition pattern underscores the impact of structural interventions on wetland vegetation and highlights the ecological sensitivity of the natural system to changes in tidal connectivity (Figure 3.3).

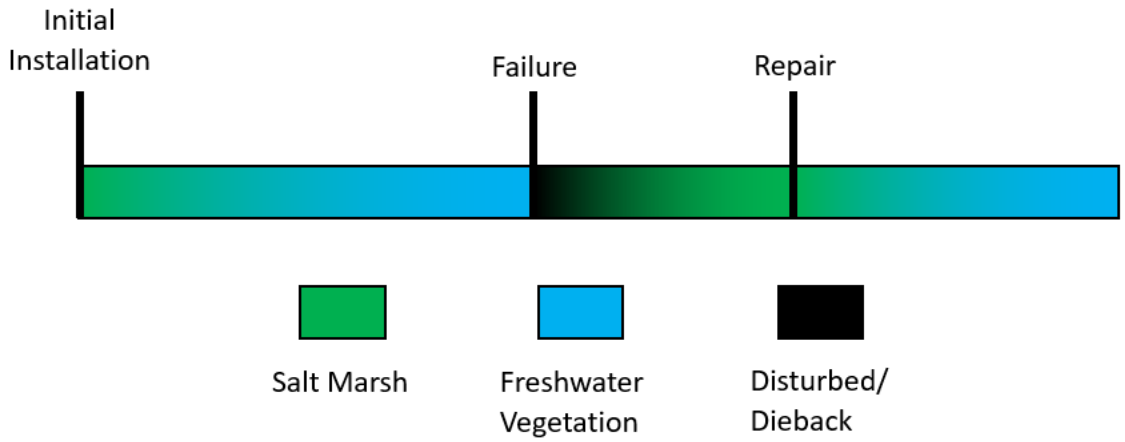

Figure 3.3: Conceptual illustration of the upstream vegetation transitions in response to tide gate installation, failure, and repair. The diagram shows a temporal shift from a salt marsh to a fresh marsh/forest after the tide gate installation. There is a state of disturbed vegetation, which is usually a transition whenever there is a tide gate damage or repair.

The study at HAAF began in May 2023. At that time, the upstream ecosystem was characterized by extensive standing dead stems, wrack accumulation and visible dieback as well as patches of live and dead non-salt-tolerant vegetation (Figure 3.4). The downstream marsh was a dense, monospecific stand of *Spartina alterniflora,* the tide gate was fully functional while the railroad crossing had sandbags placed at the base of the structure as an erosion control measure (Figure 3.5).

Figure 3.4: Photographs taken at the study site during field work in May 17th, 2023.The images show extensive wrack accumulation, standing dead stems, and traces of live vegetation.

Figure 3.5: The railroad crossing at Hunter Army Airfield at the start of the field work, with sand bags at the base of the railroad crossing to protect the base of the structure from intense flow.

Field observations

Four transects were established within the study area with PVC pipes to systematically assess the site conditions. I established one transect near the upstream railroad crossing (Transect A; Figure 3.6) and another in the salt marsh area (downstream of the tide gate; Transect D). Two supplemental transects were located between the railroad crossing and tide gate but are not used for analysis in this study (Transects B and C). Each transect consists of two posts, one near the stream bank and one ~10 m back from the shore. After establishing the transects for the study, I

set up the Real-Time Kinematic (RTK) (< 2 cm vertically) equipment to record precise x- and y-coordinates of each transect as well as the elevation and location of the tide gate.

Field data were collected from 2022 to 2025 once every three months to capture the seasonality and evolution of the site. During each visit, measurements of plant height, width, and density were taken at the posts at transects A and D, as these vegetation parameters can be used to show the relationship between vegetation characteristics and water levels (Riffe et al., 2011; Coleman et al., 2022). At each post along the transects, I recorded total live and dead standing stems found within three randomly placed 0.25 m × 0.25 m quadrats to estimate vegetation density (number of stems per m^2). I then randomly selected 5 stems to measure plant height and 5 stems to measure plant diameter within each quadrat. Plant height and diameter were obtained via a tape measure and digital caliper, respectively. Vegetation measurements for both transects were obtained in May, July, October of 2023, January, April, July, October of 2024, and January of 2025.

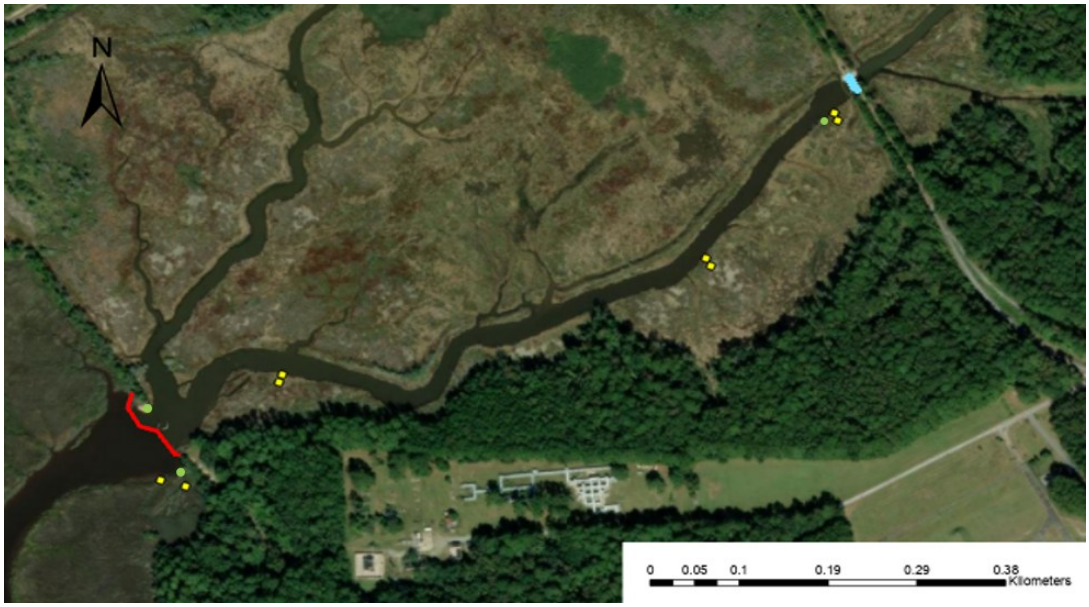

Figure 3.6: Map of the tide gate area showing the monitoring locations. The railroad crossing is represented in blue, while the tide gate is marked in red. Established transects are indicated by yellow circles, corresponding to posts 1 and 2, located in the upstream and downstream areas, respectively. The green circles denote the locations of the pressure sensors deployed at the site from April 19th, 2024, to July 17th, 2024, to monitor hydrological changes across the marsh system. The nomenclature of the transects hereafter will be labeled thus upstream edge (post 1-Transect A), upstream interior (post 2 – Transect A), downstream edge (post 1 – Transect D), and downstream interior (post 2 – Transect D).

Water level observations

To understand tidal dynamics near the tide gate and validate the model results at the boundary level of our mesh domain, I compared water level data obtained from the NOAA tide gage at Fort Pulaski to the water level result from the model at the location of the tide gage. The distance of this tide gage to the study site is ~ 27 km and the tidal range is estimated at 2.11 m, mean higher high water (MHHW) and mean sea level (MSL) were 1.05 m NAVD88 and -0.07 m NAVD88,

respectively. However, given the distance between the Fort Pulaski gage and the study site, and the tidal changes that occur as water flows inland, I deployed three pressure sensors (RBR brand D-Wave solo3) at the study site from April 19th, 2024 to July 17th, 2024, to collect localized water level data and allow for a direct validation of the model performance at the tide gate (Figure 3.6). These sensors were affixed to metal fence posts and placed near the railroad crossing and on both sides of the tide gate. They were driven into the sediment such that the sensor was located in the intertidal zone. For this study, only the sensor located downstream of the tide gate in the area exposed to tidal fluctuations is analyzed. To derive water levels from that sensor, I subtracted the atmospheric pressure from the Fort Pulaski tide gage from the RBR sensor recordings and then converted the resulting pressure to water depth using the hydrostatic relationship. A vertical offset of the sensor, a correction of -0.1095 m was applied to the derived water depth to account for the true position of the sensor in the water column relative to NAVD88.

Model Concept and Domain

The Surface Water Modeling System (SMS) was used to digitize the physical features of the study site from satellite imagery, including shorelines, marsh extent, and the tide gate. These features informed the start of the conceptual model for the study region.

The unstructured mesh domain spans a high-resolution grid near the tide gate (Figure 3.7a) to a low-resolution mesh grid over parts of the North Atlantic Ocean. The minimum mesh size used was approximately 5 m, while the maximum mesh size used exceeded 5000 m near the open ocean boundary. Tidal constituents including O1, K1, Q1, M2, N2, S2, and K2 (see Hagen et al., 2006), were added to this ocean boundary (Figure 3.7c) to enable a well simulated water propagation from the ocean to the marsh where the tide gate is situated. The high-resolution, unstructured, finite element mesh developed comprises 384,932 non-overlapping elements and 206,571 computational

nodes, which represent the discrete locations where water levels and depth-averaged velocities were calculated.

After the mesh generation, two Digital Elevation Models (DEMs) – the Continuously Updated Digital Elevation Model (CUDEM) and Coastal National Elevation Database (CoNED), (obtained from https://coast.noaa.gov/dataviewer/#/), were used to interpolate high-resolution bathymetry and topography data onto the river channel and marsh platform, respectively (Figure 3.7b). The linear method of interpolation found in Bilskie et al., (2015) was used in this study. Located northwest of the tide gate, and at the same height, is an earthen berm which was constructed in conjunction with the first tide gate (Department of Defense, 2021). However, the elevation of the earthen berm was not accurately represented in the DEM, so the elevation was adjusted to match site observations.

In SMS, I generated three meshes that captured the conditions of the study site from pre-tide gate installation to post-tide gate installation, while leaving the rest of the mesh domain the same. In the first mesh configuration, the tide gate was absent, and node elevations along its length were adjusted to match the surrounding bathymetry. The second mesh had the tide gate present, and the RTK-surveyed elevations were assigned to the nodes that outlined the shape of the tide gate. In the third mesh generation, the tide gate was damaged. The node elevations in the damaged part of the tide gate were lowered to match the surrounding bathymetry, while nodes along the portion of the tide gate that remained intact retained the tide gate elevations obtained from the RTK survey. In this study, the four culverts present in the real-life design of the tide gate were not added in any of these meshes.

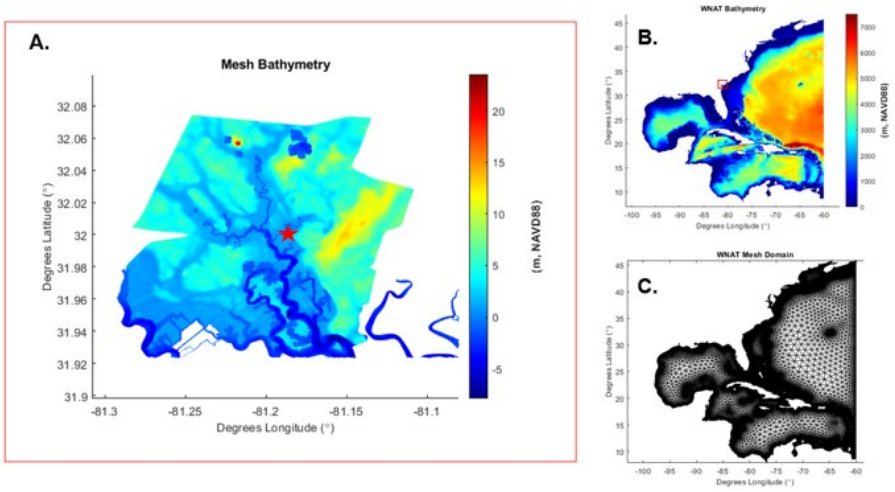

Figure 3.7: (A.) Zoomed in view of the marsh area containing the study site, highlighted by the red box. The star in the map shows the location of the study site in Figure 3.6. (B.) The bathymetry and topography of the Western North Atlantic (WNAT). (C.) The mesh domain of the WNAT.

With the physical framework of the domain established, the next step was to describe the various landscape scenarios brought about by the conditions of the tide gate, after which I characterized the vegetation in each of the landscape scenario.

Landscape Scenarios

I generated the various landscape conditions based on the different vegetation species that have existed from before the first installation of the tide gate through the most recent re-installation, to capture the evolution of the site before and after human intervention as well as the associated ecological and hydrodynamic shifts that occurred in the system. The four distinct landscape conditions I developed include the natural, present, potential stable state, and damaged tide gate (Figure 3.8), and they are described below based on chronological order.

Natural Condition

This condition represents an undisturbed marsh ecosystem characterized by a continuous salt marsh upstream and downstream. This hypothetical condition represents a scenario that probably existed before human involvement. In this scenario, no tide gate was built at the site and/or enough time has passed after the removal of the tide gate to allow the establishment of a natural salt marsh.

Present condition

The present landscape condition represents the study area following the installation of the tide gate or repair of the damaged part of the tide gate. The upstream environment of this condition remains largely degraded and characterized by patches of dead and live vegetation. In contrast, the downstream remains a salt marsh. Under this scenario, the reinstalled tide gate continues to limit saltwater from propagating upstream, thus maintaining a predominantly freshwater environment.

Potential Stable Condition

The potential stable condition comprises a functioning tide gate, a healthy upstream vegetative system, and a salt marsh downstream. This condition represents an ideal scenario in which the tide gate functions as intended. This allows for the development of a low-lying maritime forest upstream while not affecting the downstream salt marsh. Analyzing this condition highlights the potential for integrating engineered infrastructure with natural systems to enhance environmental protection.

Damaged Tide Gate Condition

Following Hurricane Irma, a section of the tide gate was damaged, allowing saltwater to intrude into the upstream system. The extent of the damaged portion of the tide gate was obtained using Google Earth Pro. The influx of saltwater into the upstream area led to the widespread loss of non-

salt-tolerant vegetation, resulting in extensive wrack accumulation, vegetation dieback, and standing dead trees whereas the downstream marsh remains healthy. This condition consists of a healthy marsh downstream, a damaged tide gate, and a disturbed area with standing dead stems upstream. It underscores the vulnerability that can occur after a catastrophic failure of the gray infrastructure and the subsequent impact on the ecosystem.

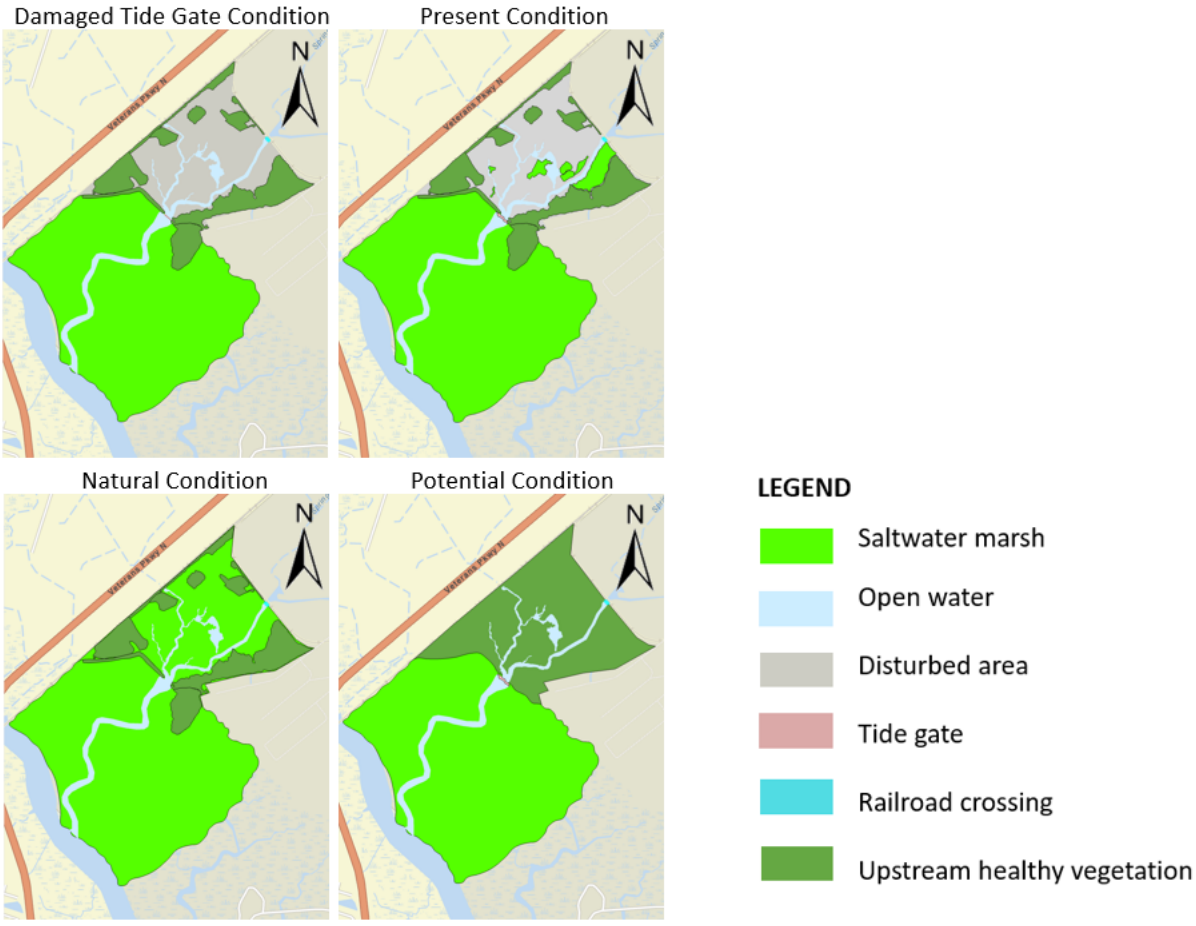

Figure 3.8: The four landscape conditions at the HAAF tide gate area, including the natural, present, potential stable, and damaged tide gate. The figure illustrates changes in marsh extent, upstream healthy vegetation (low-lying maritime forest), disturbed area, and gray structures such as the railroad crossing and tide gate.

Landscape Parameterization

An accurate representation of land cover is essential for reliable hydrodynamic simulations, particularly when assessing flow resistance across diverse landscape conditions. The current National Land Cover Database (NLCD) U.S.G.S., (2018) did not accurately capture the intricate vegetative patterns currently present at the study site. To address this limitation, I used ArcGIS Pro to trace patches of distinct visual characteristics to create custom land cover classes. These custom land covers were assigned unique codes that differed from the original NLCD codes. The area surrounding the study site was extracted from the NLCD 2021 dataset and was replaced with the updated area containing the new custom landcover classes. Land classification variable names were refined based on the names shown in Table 3.1 and their corresponding Manning's *n* values were assigned based on estimates used in similar literature works.

An initial plan for the Manning's *n* estimates was to use the vegetation data obtained during fieldwork for direct site-specific estimation. However, a review of prior work by Passeri et al., (2011) demonstrated that site-specific derivations of Manning's *n* and literature-based estimates for comparable landscape types differ by a negligible degree. Based on this finding, I assigned Manning's *n* values using published estimates from previous studies with similar vegetation characteristics to the land covers I created. This approach ensured that the customized vegetation mosaics remained scientifically robust while maintaining consistency with established practices in coastal modeling.

The customized vegetation mosaics consisted of seven vegetation layers- six upstream and one downstream, as summarized in Table 3.1. While these patches were present across all four landscape conditions (Figure 3.8), Manning's *n* values assigned to each layer were adjusted in the landcover spreadsheet to reflect the unique ecological estimates of each scenario. For example, the landscape condition at the start of the study retained all Manning's *n* values summarized in the

table below, the landscape condition with the tide gate functioning as intended for a prolonged period used Manning's *n* for the forest vegetation mosaic throughout all 6 patches, and the natural state and damaged tide gate conditions (Table 3.2) utilized the salt marsh and degraded area friction values, respectively. These tailored adjustments allowed for the generation of separate landcover files that represented each landscape frictional profile in the hydrodynamic model.

Table 3.1: Manning's *n* values assigned to various vegetation mosaics within the study area to account for surface roughness in hydrodynamic modeling. The values represent the coefficients of resistance to water flow based on different land cover types as informed by published literature. Each category is assigned a code that was different from the codes assigned in the NLCD 2021, with Manning's n values ranging from 0.025 for open water to 0.170 for forested areas.

Vegetation Mosaic	**Names called by authors**	**Code**	**Manning's *n***	**References**
Bare Soil	Bare soil	1	0.1	(U.S.A.C.E., 1994; Bordoni, et al., 2018)
Intertidal Mudflats	Intertidal flats	2	0.030	(Arnaud et al., 2021)
Open water	Open water	3	0.025	(Dietrich et al., 2011)
Coastal Shrubland	Grassland/Herbaceous	4	0.040	(U.S. A.C.E., 2014)
Forest	Mixed Forest	5	0.170	(Dietrich et al., 2011; U.S.A.C.E. 2021)
Degraded Area	Bare land	6	0.03	(Dietrich et al., 2011)
Salt marsh	Saline Marsh	7	0.035	(Dietrich et al., 2011)

Table 3.2: The outline of the various landscape conditions for the study site. These conditions reflect the dynamic interactions between natural and gray infrastructures and provide a framework for assessing marsh resilience and recovery under different conditions.

	Natural Condition	Present Condition	Potential Stable Condition	Damaged Tide gate Condition
Tide gate	None	Intact	Intact	Damaged
Upstream	Healthy salt marsh	Patches of live and dead vegetation	Healthy vegetation	Disturbed area
Downstream	Healthy salt marsh	Healthy salt marsh	Healthy salt marsh	Healthy salt marsh

Hydrodynamic Model Runs

ADCIRC is a two-dimensional depth integrated model used to compute depth-averaged velocities and water levels by solving the shallow water equations at every node throughout the mesh domain (Luettich & Westerink, 2004; Westerink, 2008). The run comprised a 28-day cold start tidal simulation beginning April 19th, 2024, with a timestep of 0.25 seconds to capture tidal fluctuations across the mesh domain. I ran hurricane simulations as well by adding a meteorological file containing wind speed and atmospheric pressure data specific to each hurricane event. These simulations were designed to capture extreme water levels and surge dynamics, including the surge that damaged the tide gate. The wind and pressure files were obtained from Oceanic Weather Inc. (OWI) with 15-minute output intervals to simulate the hydrodynamic response to Hurricanes Matthew and Irma. Each simulation employed a hot start date of September 17th, 2016, and August 20th, 2017, respectively, to ensure a realistic pre-storm condition.

Shear Stress and Critical Velocity

In addition to vegetation measurements, I also obtained soil shear strength data, σ_s. This is a key parameter in predicting sediment stability and erosion potential, and it represents the resistance of sediment particles to external forces before dislodgment occurs (Léonard & Richard, 2004). I measured the soil shear strength directly using a shear vane by inserting the bladed head into the substrate and rotating the device in the soil until the soil failed under applied torque. I recorded the failure point in kilonewtons per square meter (kN/m^2), and the process was repeated five times around each post. The shear vane has interchangeable bladed heads for different soil shear strengths, and each head has its own conversion factor. Heads two, three, and four were used during the measurements in this study.

The soil shear strength readings were converted to Pascals (Pa) and subsequently used to calculate the critical shear stress, (τ_c), by applying an empirical coefficient, (β) expressed as

$$\tau_c = \beta\sigma_s \text{.....Equation 3.2}$$

Where τ_c is the critical shear stress of the soil, β is an estimated empirical coefficient equal to 2.6 $X10^{-4}$ with a standard error of $1.2X10^{-5}$ (Léonard & Richard, 2004), and σ_s is the soil shear strength. After calculating τ_c, I determined the corresponding shear velocity, u_* using the equation:

$$u_* = \sqrt{\tau_c/\rho} \text{.....Equation 3.3}$$

Where, ρ is the water density (1000 kg/m^3 and 1025 kg/m^3 for freshwater and saltwater respectively). u_* was calculated and averaged for all marsh edge and marsh interior readings both at the upstream and downstream transects respectively. For each transect, the lower of the two averages obtained from the marsh edge and interior readings were selected to represent the critical shear velocity for that transect. This approach yielded a representative shear velocity of 0.067 m/s ± 0.003 (Average ± Standard Error (SE)) for the upstream ecosystem and 0.031 m/s ± 0.002 for

the downstream marsh. Since the model used in this study is a two-dimensional depth-integrated (2DDI) model that outputs depth-averaged velocities in the x and y directions, I ensured a direct comparison with these model outputs by converting the shear velocity, u_* into a corresponding depth-averaged critical velocity, $\bar{U}_c$, using the following expression

$$\bar{U}_c = \frac{1}{H} \int_{z0}^{H} u(z)\, dz \quad \text{.....Equation 3.4}$$

Where u(z) is the logarithmic velocity profile in a turbulent boundary layer given as

$$u(z) = \frac{U_*}{k} \ln\left(\frac{z}{z0}\right) \quad \text{.....Equation 3.5}$$

Here, z is the elevation above the bed, and z_0 is the mean roughness height of the channel bed set to 0.007 m (Bergeron & Abrahams, 1992). To apply the above parameters across the study site, I used the nodal attribute file, which includes Manning's *n* information for every node, to assign corresponding shear velocity values. First, I identified the land cover values that corresponded to a Manning's *n* of 0.035 (i.e., the Manning's *n* value for salt marsh; Dietrich et al., 2011) and assigned them the downstream shear velocity value. The river channels had been set to a Manning's *n* of 0.025 (Dietrich et al., 2011) and were then assigned the shear velocity value of 0.0105 m/s. This river channel value was obtained from the critical shear stress values from Sturm, Hong, & Hobson, (2008) and Thoman & Niezgoda, (2008), because I was unable to directly measure the soil shear strength of the river channel in our study site. All remaining areas in the study site were then assigned the upstream shear velocity value.

Using a vertical resolution of 0.01 m, a set of *z* values were generated from z_0 to H to compute the corresponding logarithmic velocity profiles using Equation 3.5. These profiles were numerically integrated using the trapezoidal rule to calculate $\bar{U}_c$ (Equation 3.4) at every location in the mesh for each time step. H was obtained by summing the modeled water surface elevation (WSE), the

height of the water surface above a datum, denoted as η, and the bathymetric depth, the vertical distance from the reference datum to the seabed. Finally, I then compared the modeled depth-averaged velocity to the $\bar{U}_c$ to assess whether flow conditions exceeded the critical threshold for sediment mobilization.

Hydroperiod

Hydroperiod reflects the frequency and duration of inundation at a given location and serves as a key indicator of ecosystem health and vegetation dynamics. The tide simulations under the four landscape conditions were evaluated to see how the tide gate alters inundation patterns across the study site. The hydroperiod analysis utilized WSE data extracted from ADCIRC and for each node, I compared the WSE time series data against the corresponding ground elevation (bathymetric depth) to determine inundation periods, with values exceeding ground elevation assigned a binary indicator of 1 (inundated) and those below assigned 0 (non-inundated). Next, I calculated the inundation duration in seconds by summing these inundated binary indicators across all time steps for each node and multiplying each by the output interval in seconds.

RESULTS

Field Observations

Differences observed in the stem diameter, plant height, and plant density, between the upstream and downstream transects can affect flow patterns and alter water levels within the study site (Figure 3.9). Stem diameter in transect A (upstream) ranged between 3 mm to 20 mm, and had an average stem diameter for the upstream edge and marsh interior of 7.76 ± 4.58 mm (Average ± SE) and 6.47 ± 3.46 mm respectively, whereas, the stem diameter in transect D (downstream) stayed below 10 mm, with an average stem diameter of 7.51 ± 2.16 mm at the marsh edge and 7.30

± 2.35 mm at the marsh interior. Notably, in January 2025, the upstream edge and interior plant diameter increased to 18 mm while the downstream plant diameter remained at 8 mm (Figure 3.9a). Mean plant height for the upstream edge was 71.89 ± 37.2 cm and the upstream interior had a mean plant height of 49.89 ± 42.34 cm, which was the lowest of all locations. The marsh edge and interior for the downstream transect had mean plant heights at 90.67 ± 59.29 cm and 95.62 ± 50.73 cm, respectively (Figure 3.9b). Plant density was lowest at the upstream edge (post A1) with an average density of 121.74 ± 19.50 stems/m^2 and no instances where stem density exceeds 200 stem/m^2. The interior at post A2 showed higher densities than post A1, averaging 297 ± 55.07 stems/m^2, and displayed a notable period of greater than 600 stems/m^2 in April and July 2024. The locations at transect D tended to be more like one another than the two locations at transect A. This is indicated by the presence of overlapping error bars in Figure 3.9c. The stem density for the downstream edge and interior stayed between 200-500 stems/m^2 with average values of 371 ± 34.67 stems/m^2 and 314 ± 23.70 stems/m^2 respectively (Figure 3.9c).

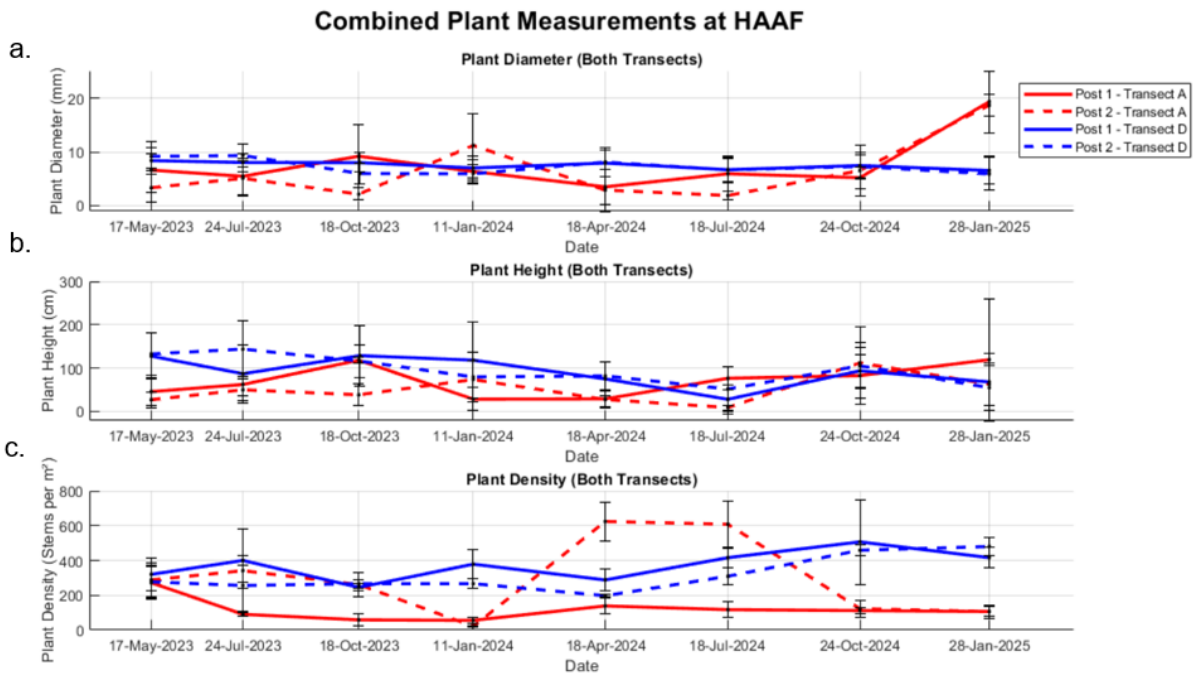

Figure 3.9: Temporal variations in vegetation characteristics: plant diameter, height, and density, at the interior and marsh edge for both the upstream and the downstream transects, respectively from May 2023 to January 2025. Transect A is located near the railroad crossing while transect D is located downstream of the tide gate. Error bars represent standard error.

Water Level Hydrodynamic Model Validation

ADCIRC simulated water levels generally agree with observations at both a long-term tide gage: Fort Pulaski, Georgia (Figures 3.10a and 3.11) and at a site within our area of interest (Figure 3.10b). There were mismatches towards the end of the simulations, which might likely be due to unaccounted wind effects. However, the Root Mean Square Error (RMSE) for both the tide and storm simulations were calculated to quantify the differences between the observed and modeled water levels as well as differences between the pressure-derived water depths and the modeled water levels.

$$RMSE = \sqrt{\left(\frac{1}{N}\sum_i (Oi - Si)^2\right)} \quad \text{.....Equation 3.6}$$

where, N is the number of data points used in the comparison, O_t is the observed water levels, and S_t is the simulated water levels.

The RMSE for tidal water levels at Fort Pulaski (Figure 3.10a) was 0.3401 m, while the RMSE for the derived water depths from the sensor I deployed (Figure 3.10b) was 0.475 m. For the RMSE obtained for the sensor, I only considered water levels where the sensor was inundated. The sensor was in the intertidal zone and cannot record water levels below its elevation, resulting in an apparent truncation of the tidal signal (Figure 3.10b).

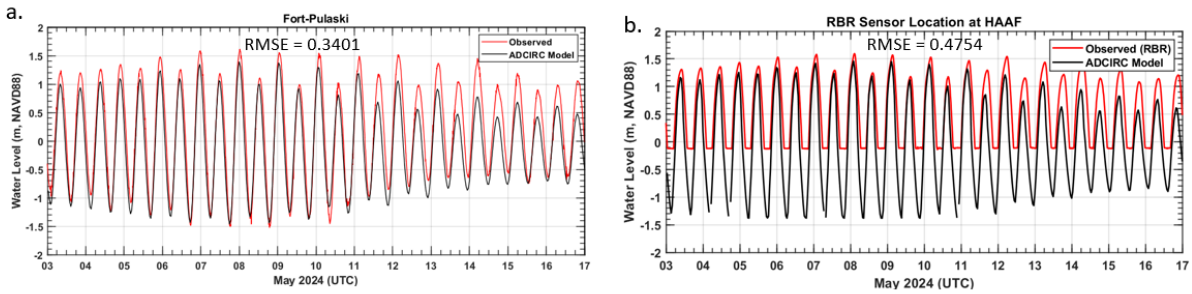

Figure 3.10: Validation of the modeled water level time series (a.) using the observed water levels at Fort Pulaski tide gate, and (b.) at a node near the deployed sensor using pressure-derived water levels from the sensor deployed downstream of the tide gate. The modeled water level time series used in (b.) was obtained from the present condition, as the gate was in place when the sensors were deployed at the site.

The storms used in this study were validated as well, using the Fort Pulaski tide gage. For Hurricane Matthew, the RMSE is 0.3690 m, and the modeled water levels align well with the observed water levels (Figure 3.11a), as well as closely capturing the rising limb, falling limb, magnitude and timing of the peak surge hydrograph (October 8th, 2016). Hurricane Irma (September 11th, 2017) has an RMSE of 0.3151 m and the modeled water levels showed close alignment with the observed water levels throughout the simulation period (Figure 3.11b). The

RMSE values obtained fall within the range reported in previous studies, indicating that the model performance is reasonable and acceptable (Forbes et al., 2008; Asher et al., 2019).

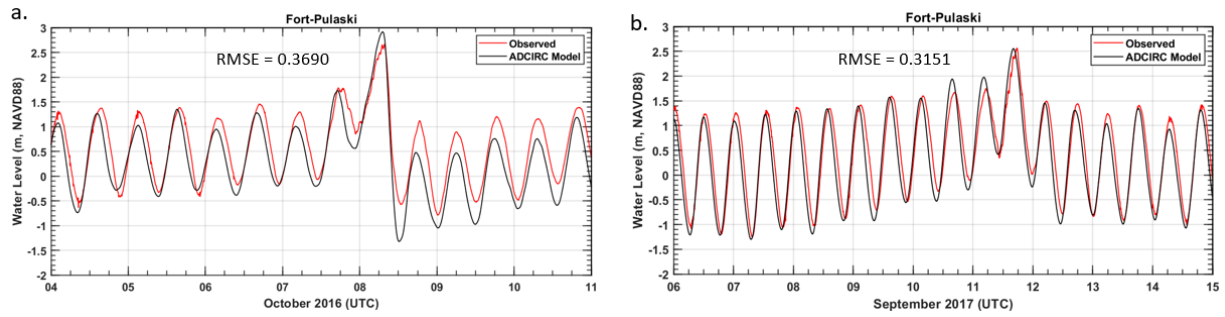

Figure 3.11: Water level validation illustrates model performance during storm simulation for (a.) Hurricane Matthew and (b.) Hurricane Irma with RMSE values of 0.3690 m and 0.3151 m respectively.

Simulated Tidal Water Levels

Modeled water surface elevation (WSE) at the base of the railroad crossing reveals the effect of the different landscape conditions on upstream flow (Figures 3.12). Presented here is WSE in the channel adjacent to the base of the railroad crossing, which is considered the critical infrastructure in need of protection. The damaged tide gate (Figure 3.12a) and natural (Figure 3.12b) landscape conditions have semi-diurnal tidal fluctuations ranging from approximately -1.5 m NAVD88 to 1.5 m NAVD88. However, in the present and potential conditions, water levels did not change at the railroad crossing due to the presence of the tide gate which was blocking tidal exchange between the upstream and downstream. This sharp contrast between the presence and absence of the tide gate demonstrates the strong hydraulic control of the tide gate in preventing downstream saline water from propagating into the upstream area.

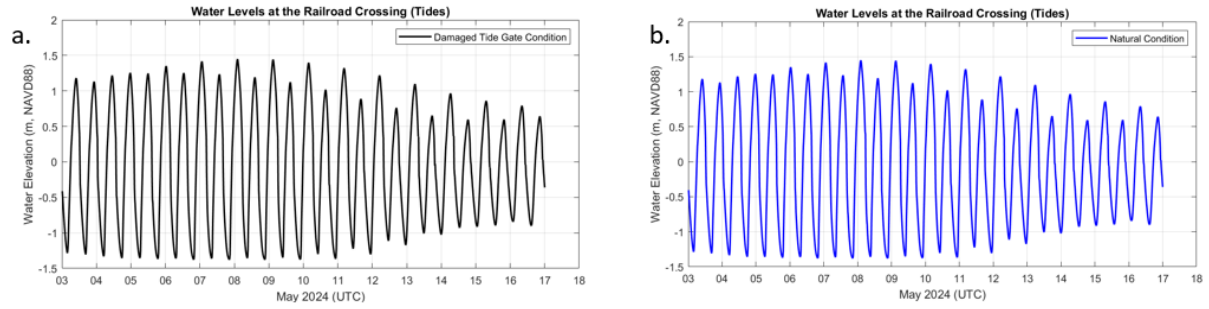

Figure 3.12: The damaged tide gate and natural condition water levels showing full tidal signals at the railroad crossing.

Simulated Tidal Flow Velocities

ADCIRC-simulated tidal flow velocities at the base of the railroad crossing vary with the state of the tide gate (Figures 3.13a and 3.13b). The damaged tide gate (Figure 3.13a) had velocities up to 0.41 m/s at the start of the simulation, with an isolated peak approaching 0.6 m/s. In contrast, the natural condition (Figure 3.13b) exhibited tidal velocities below 0.3 m/s at the start of the observation period, and reached a peak of ~0.8 m/s. Furthermore, the flow velocities for the potential and present conditions were essentially zero at the railroad crossing, reflecting the effective suppression of tidal flow by the tide gate.

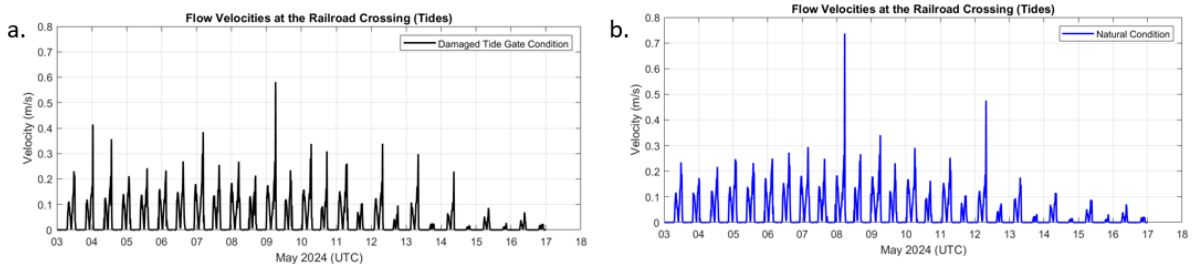

Figure 3.13: Flow velocities at the base of the railroad crossing for the damaged tide gate and natural conditions.

Simulated Storm Surge (Hurricane Matthew)

Differences in simulated storm water levels demonstrate the effect of the various landscape conditions during Hurricane Matthew at the railroad crossing located upstream (Figure 3.14). The ADCIRC-simulated storm surge for Hurricane Matthew peaked at ~2 m NAVD88 in both the damaged tide gate (Figure 3.14a) and natural (Figure 3.14b) conditions. These peaks occurred on October 8th, which coincides with the day Hurricane Matthew passed through the Georgia coast. The water levels for days before and after the storm fluctuated between -1.5 m and 1.5 m NAVD88 when the tide gate was absent and damaged. In contrast, the potential and present conditions, where the tide gate was fully functional, had water levels that remained near zero from the start to the end of the simulation period at the railroad crossing. This means Hurricane Matthew did not overtop the tide gate so there was no significant change in the water levels upstream.

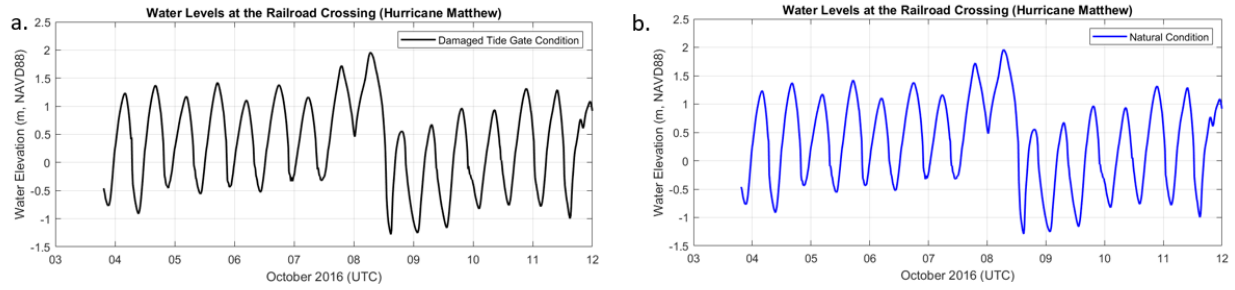

Figure 3.14: ADCIRC-simulated storm water levels at the railroad crossing for the damaged tide gate and natural conditions. Hurricane Matthew was observed on the 8th of October, 2016, with a storm peak of ~2 m NAVD88.

Modeled Storm Flow Velocities (Hurricane Matthew)

Storm currents in Hurricane Matthew simulations revealed oscillatory flow patterns at the railroad crossing under the damaged and natural conditions (Figure 3.15). In the damaged tide gate condition (Figure 3.15a), velocities fluctuated throughout the observation period, with a mean flow

velocity of 0.023 m/s and a peak reaching approximately ~0.35 m/s at the railroad crossing, whereas the natural condition (Figure 3.15b) had a mean flow velocity of 0.036 m/s and peaked at ~0.5 m/s. Flow speeds for the potential and present conditions remained near zero throughout the simulation period, which is to be expected since water did not overtop the tide gate.

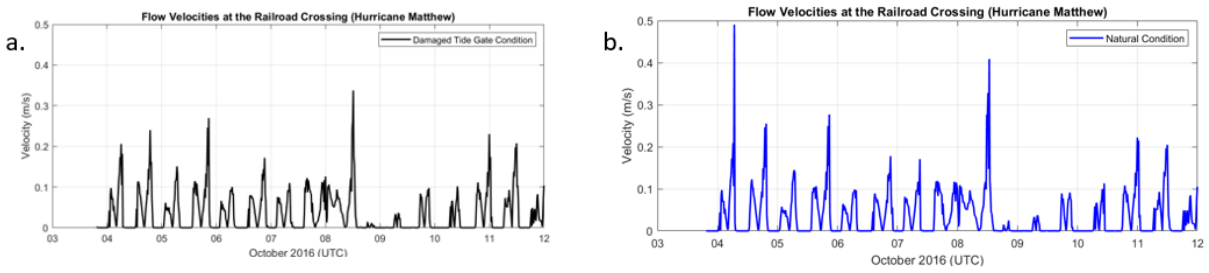

Figure 3.15: Storm currents during Hurricane Matthew at the base of the railroad crossing for the damaged tide gate and natural conditions.

Simulated Storm Surge (Hurricane Irma)

Water levels for Hurricane Irma showed contrasting hydrodynamics between the different landscape conditions at the railroad crossing situated upstream (Figure 3.16). In the damaged tide gate (Figure 3.16a) and natural (Figure 3.16b) conditions, water levels fluctuated between -1.5 m and 3 m NAVD88, reflecting surge-driven exchange between upstream and downstream. Also, on the day of the storm, the water levels remained elevated at low tide, likely due to delayed drainage of stormwater, which remained in the upstream system for roughly 24 hours before receding and returning to normal tidal conditions. However, in the potential (Figure 3.16c) and present (Figure 3.16d) conditions, the tide gate acted as a barrier that restricted water from flowing upstream during the normal tidal flows. As a result, water levels at the railroad crossing remained near zero prior to the storm event. On the day of the storm, water overtopped the tide gate, with stormwater levels spiking up to ~3 m NAVD88 at the upstream. Thereafter, water levels dropped to 1.9 m NAVD88 and remained at that level. It is important to note that this impounding of water is due

to the model configuration since it does not incorporate drainage pipes found in the real-life design.

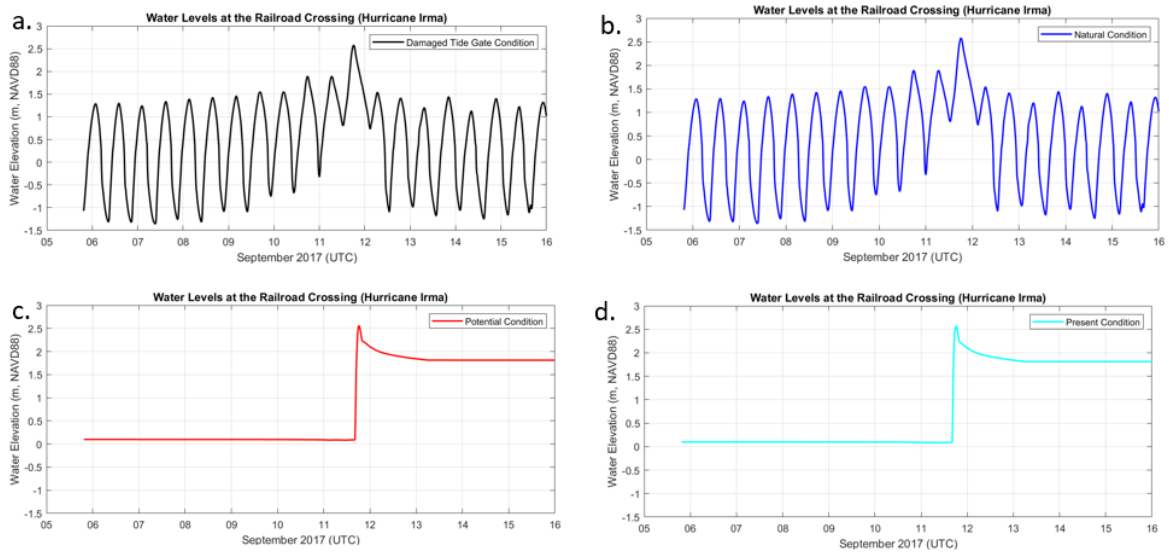

Figure 3.16: WSE time series for all four conditions showing the impact of Hurricane Irma at the base of the critical rail line located upstream. The storm graphs show a peak of 2.7 m NAVD88 on the day of the storm, followed by a decline and water impoundment after the storm for the potential and present conditions.

Simulated Storm Flow Velocities (Hurricane Irma)

Storm-driven currents in Hurricane Irma varied considerably between scenarios with and without/damaged tide gate at the railroad crossing (Figure 3.17). In the damaged tide gate (Figure 3.17a) and natural (Figure 3.17b) conditions, flow velocities remained low, fluctuating below 0.5 m/s throughout the entire simulation duration. In contrast, the present (Figure 3.17c) and potential (Figure 3.17d) conditions maintained near-zero flow before and after the storm, but produced a sharp spike on the day of the storm, with flow velocities reaching up to 3 m/s.

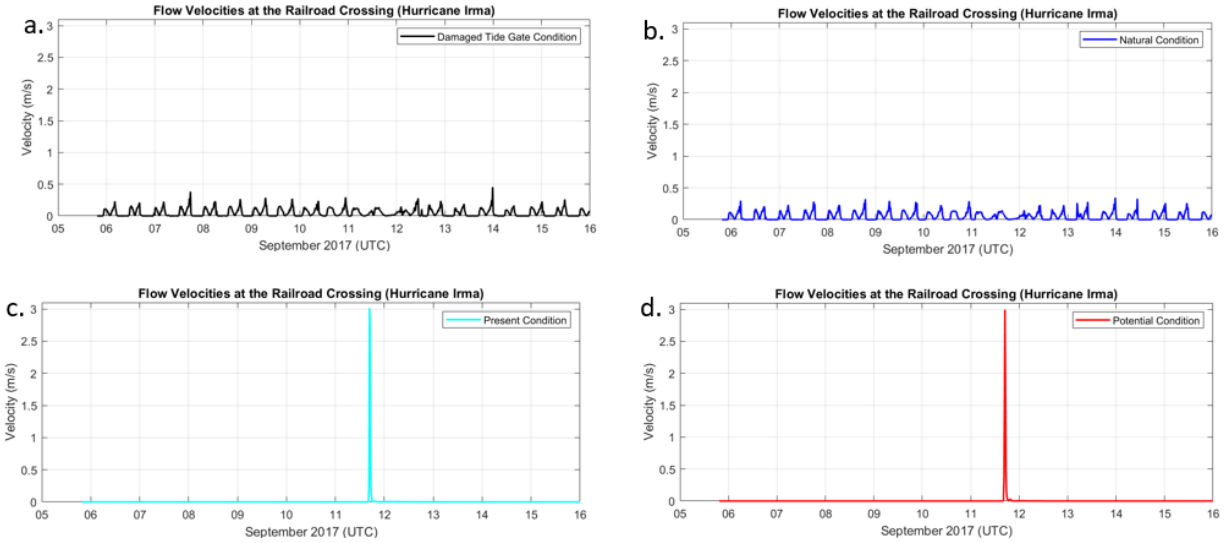

Figure 3.17: Flow velocities in Hurricane Irma simulation at the base of the railroad crossing for all landscape conditions, with peak velocities in the potential and present conditions reaching up to 3 m/s while the natural and the damaged tide gate conditions fluctuated below 0.5 m/s.

Simulated Spatial Variation in Maximum Water Levels

Maximum water surface elevation observed across all landscape conditions in both tide and storm simulations showed a mix of dry, shallow and deep-water level areas throughout the study site (Figure 3.18 to Figure 3.20). For the tides, the damaged tide gate (Figure 3.18a) and natural (Figure 3.18b) conditions generally reached a maximum water level of ~1.60 m NAVD88 throughout the study site but had locations in the downstream with maximum water levels at ~1.75 m NAVD88. The potential (Figure 3.18c) and present (Figure 3.18d) conditions displayed a contrasting water level gradient from the natural and damaged conditions upstream of the study site. The range, which is between 0 to 0.50m NAVD88, for the potential and the present conditions were likely reflecting the effect of the tide gate in restricting tidal exchange upstream. Downstream water

levels in these conditions were comparable to those of the natural and the damaged tide gate conditions.

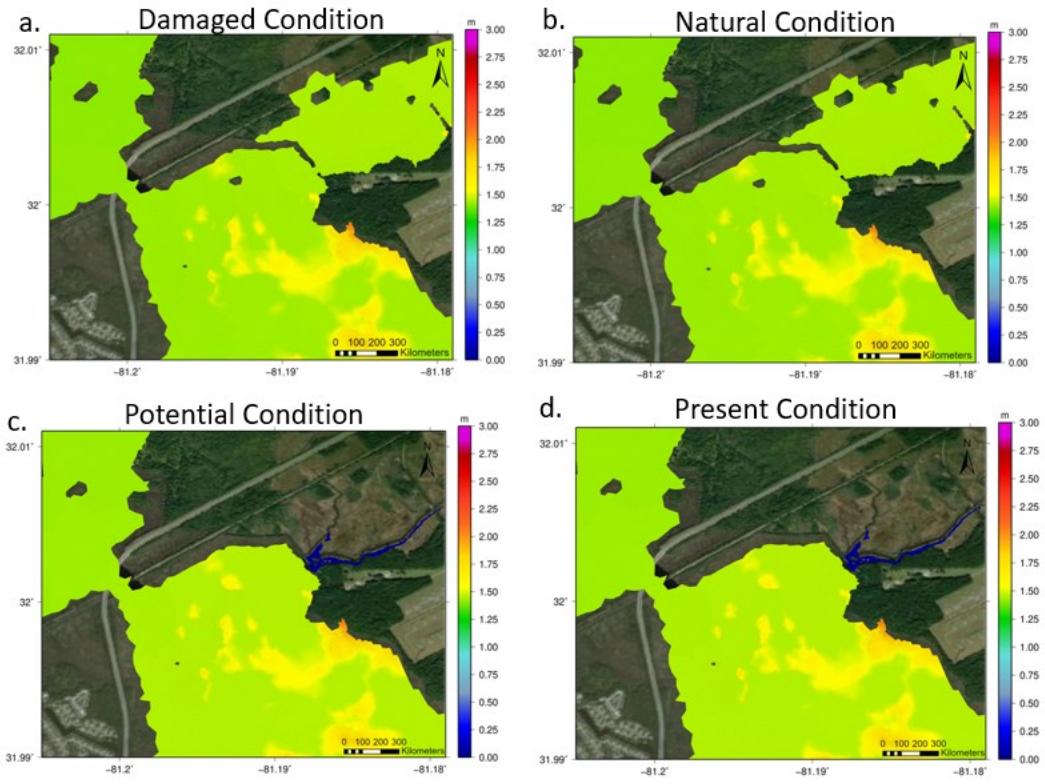

Figure 3.18: Spatial plots of the maximum water levels obtained from ADCIRC tidal simulation for the various landscapes in this study.

For Hurricane Matthew, maximum stormwater levels in the damaged tide gate and natural conditions (Figures 3.19a and 3.19b respectively) ranged from 1.80 m NAVD88 to 2.00 m NAVD88 both upstream and downstream. However, maximum water levels in the potential and present conditions (Figures 3.19c and 3.19d respectively) mostly were between 0 m NAVD88 to 0.5 m NAVD88 at the upstream and between 1.80 m NAVD88 to 2.00 m NAVD88 at the downstream.

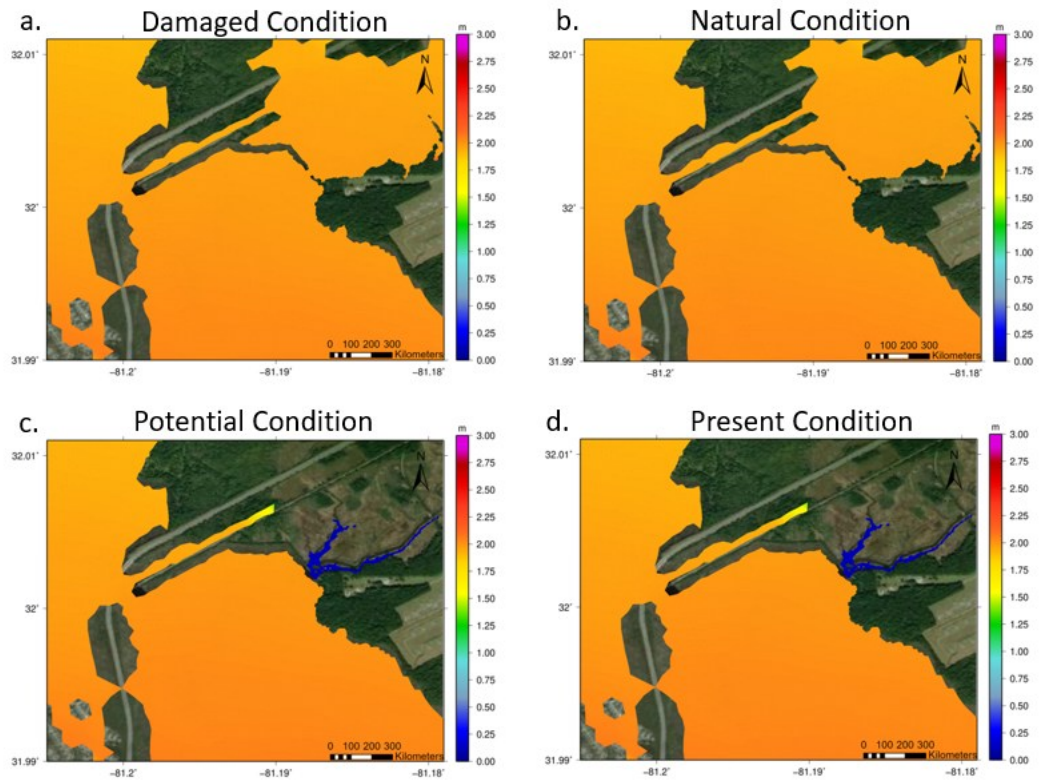

Figure 3.19: Spatial plots of ADCIRC maximum water levels obtained from Hurricane Matthew simulation.

For Hurricane Irma, the damaged tide gate (Figure 3.20a), natural (Figure 3.20b), potential (Figure 3.20c) and present (Figure 3.20d) conditions displayed maximum water levels at ~2.7 m NAVD88 both upstream and downstream of the study site. For the potential and present conditions, which include the tide gate, downstream and upstream water levels were nearly the same, likely because water overtopped the gate and flowed upstream.

While the main difference across runs, particularly for the tide and Hurricane Matthew simulation were due to the presence or absence of the tide gate, subtle differences such as in the damaged tide gate condition produced similar maximum water level results with the natural condition that contains no tide gate. Similarly, upstream vegetation types varied across the landscapes, but these variations also did not translate into meaningful differences in maximum water level.

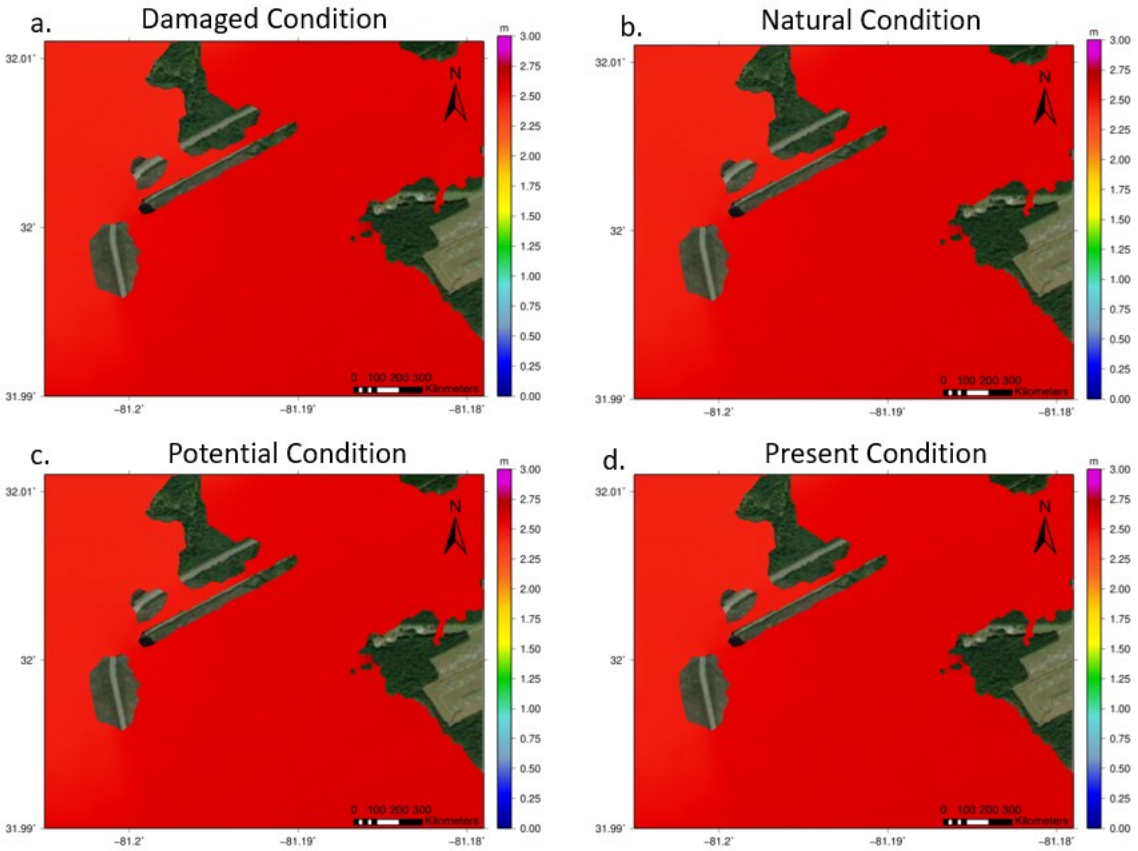

Figure 3.20: Spatial plots of ADCIRC maximum water levels obtained from Hurricane Irma simulation. All four landscape conditions exhibited a water level of approximately 2.7 m NAVD88 both at the upstream and downstream.

Soil Shear Strength Measurements

Field-based soil shear strength readings used to obtain the depth-averaged critical velocity was higher at the upstream than at the downstream. For the river channel, where in-situ shear strength measurements were not feasible, the critical shear stress value was obtained from Thoman & Niezgoda (2008) (Table 3.8).

Table 3.3: The area of the study site and the corresponding soil shear strength, average shear stress values and standard errors. The river channel in the study site had average shear velocity values

that were computed from a critical shear stress value obtained from a paper by Thoman & Niezgoda, 2008.

Study Site	Positions	Soil shear strength (kPa)	Average Shear Velocity (m/s)
Upstream	edge	19.66 ± 1.83	0.0681 ± 0.0028
	interior	17.40 ± 1.56	0.0661 ± 0.0026
Downstream	edge	4.09 ± 0.27	0.0313 ± 0.0012
	interior	4.12 ± 0.27	0.0333 ± 0.0009
*River Channel	upstream	0.00011	0.0105
	downstream	0.00011	0.0104

**The critical shear stress value of the river channel, 0.11 Pa, was obtained from (Thoman & Niezgoda, 2008).*

At the upstream site, the measured soil shear strength had higher mean values of 19.66 ± 1.83 kPa at the marsh edge and 17.40 ± 1.56 kPa in the interior, with corresponding average shear velocities of 0.068 m/s and 0.066 m/s at the marsh edge and marsh interior respectively. At the downstream, I obtained the mean soil shear strength along the marsh edge to be 4.09 ± 0.27 kPa and 4.12 ± 0.27 kPa at the marsh interior, with corresponding shear velocities of 0.031 m/s and 0.033 m/s respectively. For subsequent calculations, the lower value between the marsh edge and interior was taken to be the shear velocity for the upstream, and the same procedure was applied to the downstream (Table 3.3). For the river channel, the critical shear stress value obtained from Thoman & Niezgoda, (2008) was added in equation 3.2 to obtain an average shear velocity of 0.0105 m/s for the upstream and 0.0104 m/s for the downstream.

Critical Velocity Exceedance

Modeled depth-averaged velocities exceeded the calculated critical depth-averaged velocity under the present and natural conditions (Figure 3.21) mostly within the river channel, little to no exceedance in the adjacent marsh areas. The present and natural conditions were the only two landscapes considered because I was able to directly measure soil shear strength in the corresponding ecosystems. The present condition (Figure 3.21a) showed that modeled velocities exceeded the critical depth-averaged velocities for up to 40% of the simulation period along the downstream channel, while minimal to no exceedance was observed in the upstream river channel. In contrast, the natural condition exhibited much greater exceedance, with the modeled velocity at the downstream channel exceeding the critical velocity up to 90% of the simulation time whereas the upstream channel had percentage exceedance ranging between 30% to 70% of the simulation time (Figure 3.21b). The contrasting result between the two landscape conditions indicates that the tide gate substantially reduces the potential for sediment mobility, particularly along the upstream channel.

For Hurricane Matthew, the present condition (Figure 3.21c) displayed minimal to no exceedance at the railroad crossing on the day of the storm but had the downstream channel exceedance for about 33% of the simulation time on the storm day. The natural condition (Figure 3.21d) produced about 85% exceedance along the downstream channel on the day of the storm, whereas the exceedance at the upstream river channel was about 65%. The difference in both landscape exceedance percentages indicates that the tide gate limited the potential for storm-driven sediment movement along the upstream channel, while its absence allowed prolonged exceedance and greater erosive potential along the downstream and upstream channel. Regardless of the condition of the tide gate, very little exceedance was observed in the marsh (Figure 3.21). For Hurricane

Irma, the present condition (Figure 3.21e) showed little to no exceedance along the upstream river channel, while the downstream river channel had about 42% exceedance during the day of the storm. The natural condition (Figure 3.21f) exhibited prolonged exceedance, with the downstream channel producing about 92% exceedance for the day of the storm and the upstream channel exceedance at 62% during the storm. Like Hurricane Matthew, exceedance was rare in the marsh, and the presence of the tide gate appeared to reduce exceedance duration within the upstream channel.

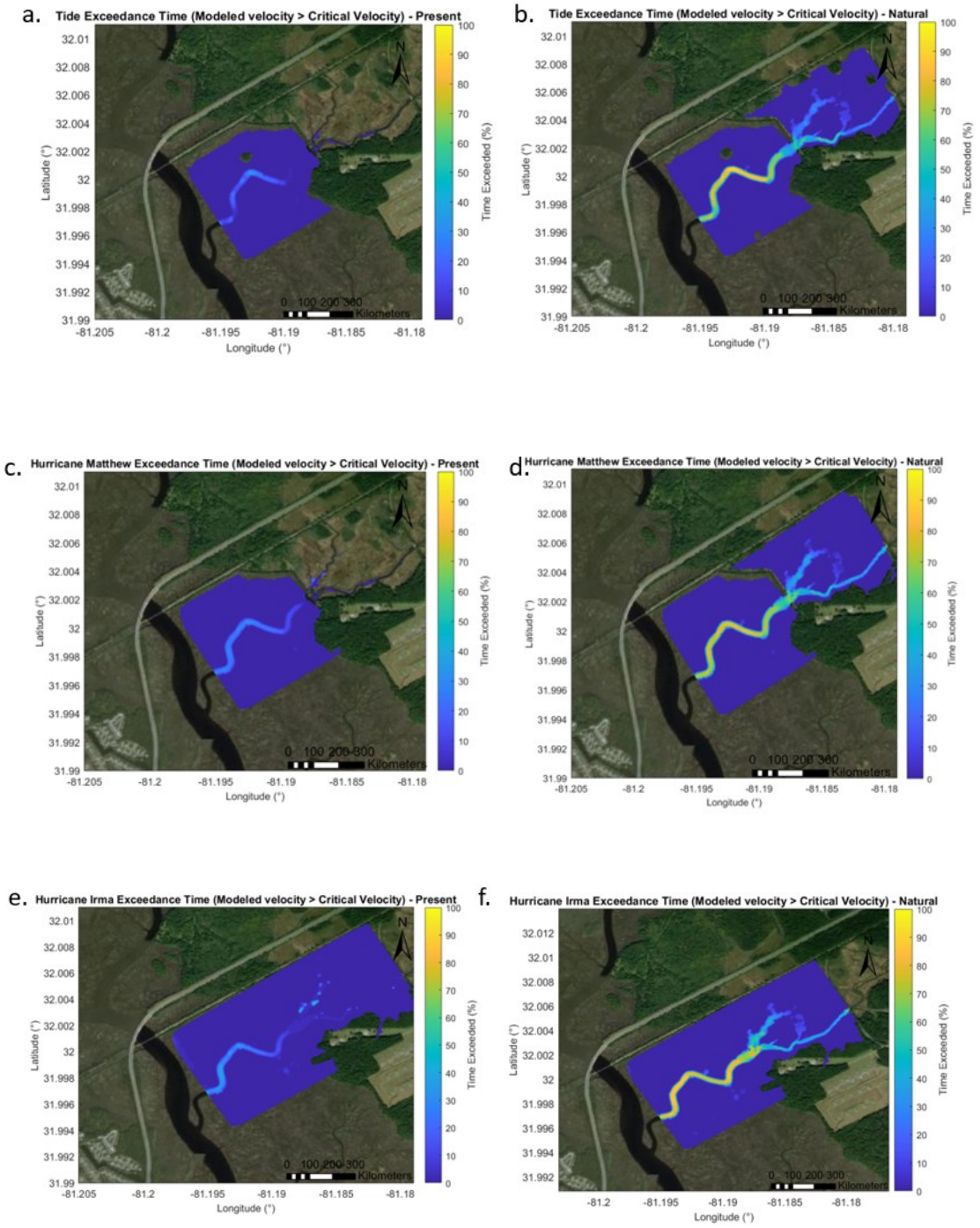

Figure 3.21: Spatial distribution of areas where the modeled velocities are greater than the critical depth-averaged velocities under the present and natural conditions for the tidal and storm simulations. The exceedance is expressed in percentage of time.

Hydroperiod

Modeled water level results display the effects of barriers on upstream ecosystem inundation patterns at the study site (Figure 3.22). Ponds that appeared in the inundation maps, caused by low mesh resolution in tiny creeks, were removed from the spatial plots by identifying nodes where the water levels remained artificially constant across multiple consecutive time steps, indicating unrealistic ponding. These nodes were then masked out to provide a realistic representation of inundation patterns. Upstream flooding in Figure 3.22a reflects partial restriction of tidal exchange. Inundation in the marsh platform mostly ranged between (0-20) % while the river channel areas maintained 100% inundation. The natural condition (Figure 3.22b), which contained no barrier, exhibited unrestricted flow. The marsh platform was inundated about 0-20% of the time while the river channel remained at a 100% inundation. For the potential (Figure 3.22c) and present (Figure 3.22d) conditions, the presence of the tide gate caused a minimal to no inundation at the upstream. However, the downstream displayed 0-20% marsh platform inundation. The river channel both upstream and downstream was at a 100% inundation.

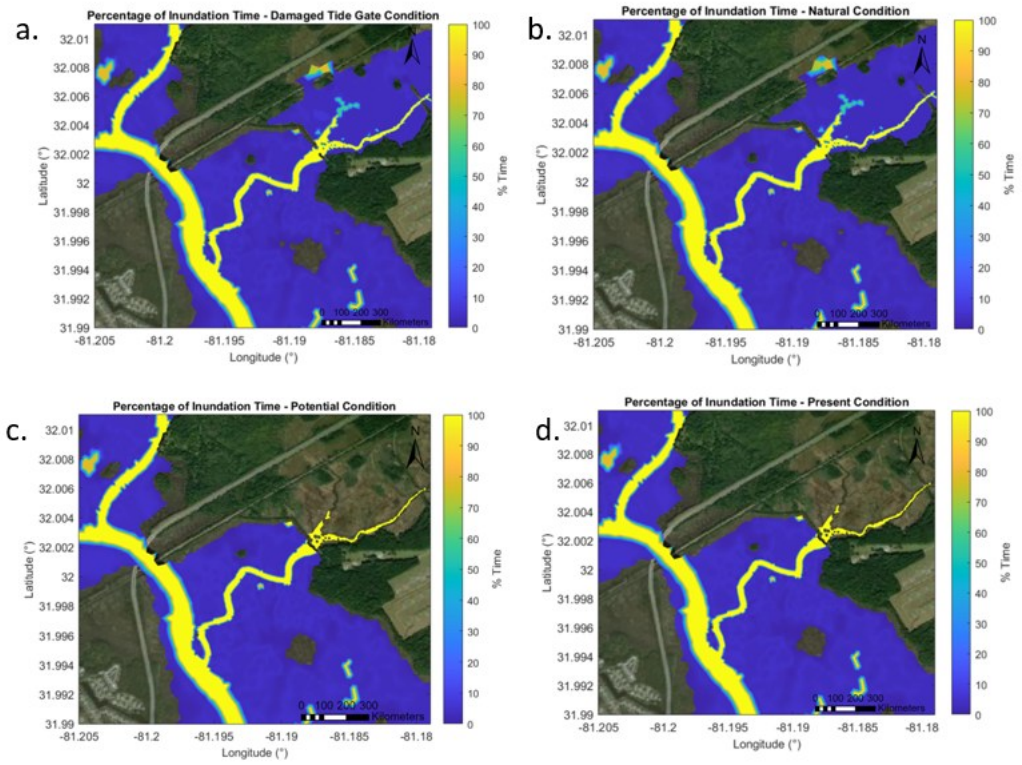

Figure 3.22: Spatial distribution of the percentage of inundation time across the four landscape conditions during tide simulation. The color scale represents the proportion of time the land surface remains inundated over the simulation period. 100% indicates that the area is always wet.

DISCUSSION

This research evaluated how tide gate conditions impact the upstream ecosystem and infrastructure, particularly near the railroad crossing. By integrating field data and hydrodynamic modeling, I found that changes in tide gate functionality significantly affected tidal exchange and flow velocities at the upstream. Field data collection characterized existing marsh conditions by documenting the vegetation structure and soil resistance, both at the upstream and downstream. Hydrodynamic modeling was used to simulate and evaluate how different landscape conditions influenced water levels and flow velocities across the study site using four landscape conditions –

natural, present, potential, and damaged tide gate. These conditions were developed to represent different states of the tide gate and marsh platform across the study site. Our findings revealed that variations in tide gate functionality overwhelmed variations in vegetation upstream in terms of hydrodynamic impact (upstream water levels, flooding, water velocities). Additionally, sediment movement exceedance results indicating greater risk of erosion at the downstream channel than at the upstream channel even when tide gate is damaged or not present.

Differences in vegetation between the upstream and downstream marshes led to differences in the capacity of the natural infrastructure to protect the railroad crossing against coastal hazards. While our plant measurements were limited to plant height, stem diameter, and plant density, they still provide useful insight into how the tide gate may be affecting the upstream ecosystem. While plant height and stem diameter were comparable between upstream (A) and downstream (D) transects, plant density was generally lower upstream than downstream. Denser vegetation generates greater drag and flow resistance (Nepf, H., 2012), resulting in slower water movement (Xu et al., 2019) and increased energy dissipation across the marsh surface (Shepard et al., 2011; Möller et al., 2014). Given the relationship between vegetation density and flow resistance, the lower vegetation density observed upstream of the tide gate implies reduced capacity to slow flow, stabilize sediment, and protect the railroad crossing from erosion and scour. The removal of the tide gate would allow for the re-introduction of saline water upstream, promoting conditions favorable for the re-establishment of salt marsh vegetation like the healthy salt marsh vegetation currently present downstream of the tide gate. A reversion to saltwater vegetation would likely increase vegetation density and thus dissipate more energy.

The operational condition of the tide gate significantly affected tidal flow response at the railroad crossing (Figures 3.11 and 3.12). Tidal flow was not present upstream at the railroad crossing under fully functional tide gate conditions. This caused the reduction in salinity levels (e.g., conversion to freshwater) upstream and allowed for colonization by low-lying maritime forest/non-salt-tolerant vegetation (Bice et al., 2023). However, these freshwater forested wetlands tend to recover more slowly following disturbance and are highly sensitive to shifts in hydrology and salinity (Temmerman et al., 2023) with significant reductions in the protective capacity of the upstream area to reduce water levels and erosion, which could pose challenges for the military installation. When the tide gate fails (Figures 3.11a, 3.12a, and 3.13a), saline water is re-introduced upstream, killing the upstream non-salt-tolerant plants e.g., trees (Figure 3.4). The widespread collapse of the upstream ecosystem leads to standing dead trees that can attract large birds, posing bird-strike hazards for HAAF. A meta-analysis conducted by Gutzat & Dormann (2018) demonstrated that large birds tend to select large, dead trees with broken crowns for nesting, hence increasing avian activity at HAAF after saltwater intrudes upstream.

Modeled stormwater simulations indicate that flow barriers such as tide gates limit upstream erosion and flooding during moderate storm events but become less effective under higher surge conditions (Figures 3.13 to 3.16). Present and potential conditions blocked the impact of Hurricane Matthew upstream since the peak water level of the storm (Figure 3.13) was below the height of the tide gate which is 2.1 m NAVD88. However, Hurricane Irma, with peak water levels ~3 m NAVD88, overtopped the tide gate (Figures 3.15c and 3.15d) and flooded the upstream. Upstream water was also impounded for a much longer period, although this is partially because our mesh did not include the culverts present in the real-life structure. Additionally, prolonged inundation beyond threshold levels can lead to significant declines in species abundance and productivity

(Delgado et al., 2018). As such, it is important to estimate the amount of time it will take for the saline water to drain through the four culverts in the tide gate design. To provide a rough estimate of the time for storm surge waters to drain out of the upstream area, the volume of stagnant water upstream after the storm, upstream, was obtained using:

$$Vol_{up} = A_{up}H_{up} \text{ ……Equation 3.7}$$

where A_{up} is the upstream inundate area, and H_{up} is the average depth of the retained storm surge water level.

Also, the discharge, Q, of the storm surge through the four tide gate conduits (fitted with duckbill valves) was estimated using equations for the discharge of flow through an orifice, like calculations provided in ADCIRC as:

$$Q_{tide\ gate} = C_d A\sqrt{2gH} \text{ ……..Equation 3.8}$$

Where C_d is the coefficient of discharge (0.7-0.9), A is the area of the orifice in m^2 (pipe diameters of 24", 36", 48"), g is the acceleration due to gravity, and H is the head difference between upstream water level and downstream water level. The time to drain the upstream area is then:

$$T_{drain} = V_{up}/Q_{tide\ gate} \text{ ……..Equation 3.9}$$

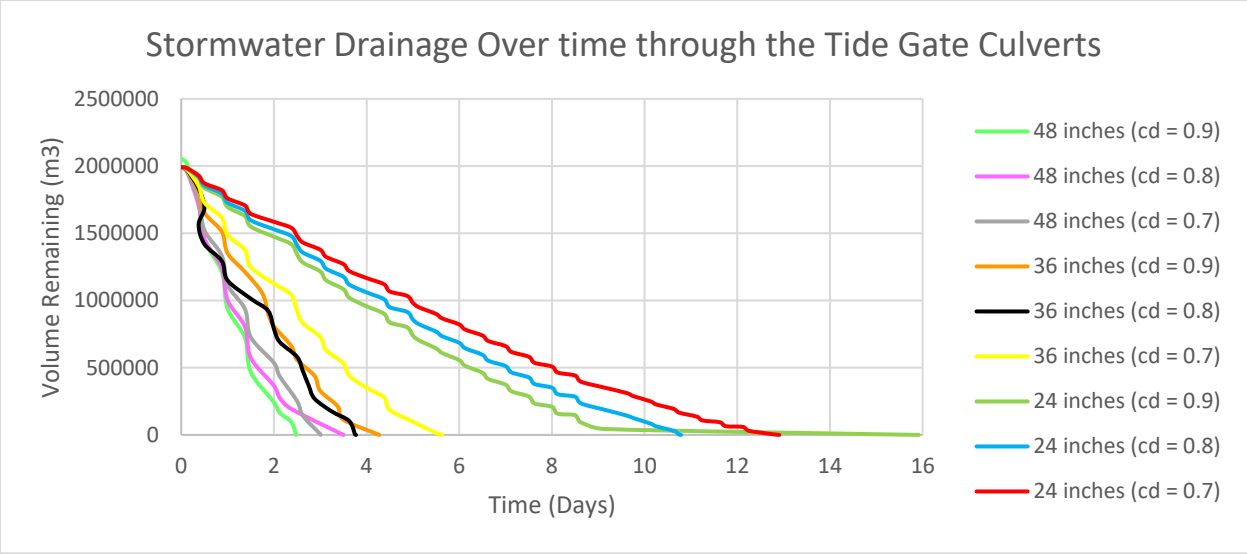

Figure 3.23: The discharge timeline for the modeled stormwater impounded upstream following Hurricane Irma (2017).

Using these conditions, the time for storm surge (impounded saline waters) to drain out of the upstream area in the presence of the tide gate was estimated between 2 to 16 days as compared to less than about one day in the case of the natural condition.

The observed amplification of storm-driven currents under the present and potential conditions for Hurricane Irma suggests that flow barriers can intensify flow and potentially increase scour at the railroad crossing (Figures 3.16c and 3.16d). According to the U.S. Department of Defense, (2021), the tide gate had undergone extensive repairs by the military installation that costs several million dollars multiple times since the first installation. However, restoring and maintaining natural conditions by removing the tide gate (Figure 3.16b) could potentially result in reduced storm surge damage and erosion risk at the upstream and this landscape condition could be a more favorable solution for the military installation. Additionally, maintaining natural conditions support ecosystem stability by allowing unrestricted tidal exchange as opposed to the potential and present

conditions that does not support tidal pulsing and flushing. These latter conditions leave the upstream ecosystem more vulnerable during intense storm events, should the tide gate fail.

The erosion potential across the study site showed higher periods of critical velocity exceedance in channels (Figures 3.21c and 3.21d) compared to the intermittently flooded marsh platform (Figure 3.22). Channels are deeper with fewer obstructions and less vegetation leading to higher flow velocities and therefore had the highest potential for sediment movement. Field observations by Temmerman et al., (2003) in tidal marshes demonstrated that suspended sediment concentration and deposition increase when tides are higher (spring tides). This supports the finding that the river channel has greater potential for sediment mobility compared to the marsh platform.

Another factor limiting sediment movement on the marsh platform could be vegetation. Vegetation increases sediment deposition and reduces resuspension and soil erosion (Ge et al., 2021). Figure 3.20e shows that there might have been less time for the flow to potentially erode sediments at the upstream river channel. A similar outcome was observed by Hung et al. (2025), whose experiments demonstrated that coastal defense structures can suppress sediment movement under extreme hydrologic conditions. In contrast, the natural condition (Figure 3.20f) is comparable to the no-structure case in Hung et al. (2025), where sediments were more mobile. Just as their experiments showed that in the absence of coastal defense structures, more sediments were mobilized, the natural condition in my study exhibited higher potential for sediment movement along the river channel. However, the potential for sediment movement was higher at the downstream channel than at the upstream channel where the railroad crossing is located.

The field-based soil shear strength measurements were for fine-grain sediments as opposed to angular cobbles (> 0.18m, van Rijn, 2019) that are currently used by the army as protection for the railroad crossing (Figure 1.1). Natural conditions could still provide protection as the armoring

placed at the base of the railroad crossing would require a much higher velocity than the velocity I obtained from our critical depth averaged velocity calculations before sediment displacement would take place. Additionally, Hurricane Irma simulations for the potential and present conditions produced flow velocities approaching approximately 3 m/s near the base of the railroad crossing, and based on van Rijn (2019), velocities of this magnitude are sufficient to mobilize angular cobbles. This demonstrates that during extreme storms, the big boulders may be displaced when the tide gate is present. Under natural condition, marsh stability is also maintained as the salinity level of the ecosystem will remain unaltered during and after storm events.

Model Assumptions and Interpretations

Vegetation and Relative Insensitive Nature of ADCIRC with Implications

ADCIRC is not very sensitive to small variations in Manning's *n*. This means that subtle changes in flow resistance estimates have limited influence on model outcomes. This could be the reason why the condition of the tide gate became the dominating factor affecting the changes observed in the flow velocity and water level results of the four landscape conditions. Moreover, the physical condition of the tide gate determines the type of vegetation that can persist upstream. In the model, the tide gate functions as an impermeable barrier, so its influence would naturally outweigh that of vegetation.

Testing the Tide gate's Resilience under Stronger Synthetic Storm Events

Research has shown that hydrologic events are likely to become more intense in the future (NASA., 2024). As a result, there is need to evaluate the resilience of the tide gate under stronger storm events to observe how the tide gate would perform. Additionally, the current model did not include culvert modules, which contributes to stormwater discharge at the upstream during

extreme events. Incorporating these culverts in future simulations while applying stronger synthetic storms would help refine the assessment of tide gate performance at the military base and provide a more realistic representation of upstream inundation timeline under stronger storm forcing.

Lack of Rainfall in the Model and How Stormwater Discharges

The model did not include rainfall events which is the primary source of inflow for the upstream channel and marsh platform. By omitting the rainfall events, the model could have underestimated the total water depth and water volume, particularly at the upstream. Runoff is collected throughout the base via a well-developed stormwater drainage system and this collected stormwater drains into the upstream part of the study site. This inflow could have a significant impact by increasing the upstream water volume and slowing down drainage even further. Since neither rainfall nor stormwater drainage were represented in the model, the upstream hydrodynamics likely underestimate actual water levels and duration of inundation which are usually very critical during design.

Broader Implications and Conclusions of the Research Study

The tide gate at HAAF serves protective purposes but also presents certain unintended challenges. While it limits flow upstream, thereby reducing erosion and flooding risk at the railroad crossing, our findings indicate that the tide gate may not perform well during extreme storm events. Under such events, the tide gate could fail and allow saline water from downstream to re-enter the upstream ecosystem, potentially destabilizing soil conditions and compromising ecosystem health.

Installing a higher and stronger tide gate capable of withstanding future climate conditions may help maintain long-term ecosystem stability. Alternatively, the tide gate could be removed entirely to restore natural hydrologic conditions. Maintaining a stable salt marsh ecosystem would benefit

the base by reducing nesting habitats for large birds which limits bird-strike collision, stabilizing the fish population that allows for recreation and maintaining marsh resilience. In summary, balancing infrastructure protection with ecosystem stability is essential for long-term coastal resilience at HAAF and the knowledge gained from this study can help inform decisions at other military installations facing similar challenges.

CHAPTER FOUR

At HAAF, I observed that the tide gate could have substantial negative impact on the upstream natural infrastructure. This observation is a major challenge that usually arises when engineered and natural systems are combined (Smith et al., 2021). Although engineered structures such as tide gates provide protection against coastal hazards, they can also limit the ability of adjacent marshes to provide ecosystem services. Results from this study therefore highlight an existing knowledge gap in understanding the interaction between engineered and natural infrastructures before implementation, as these infrastructure interactions often lead to unintended ecological and management outcomes.

My coupled field and modeling study of HAAF indicated that the natural infrastructure upstream was altered by the condition of the tide gate. Under current conditions, the upstream had lower plant density than the natural infrastructure downstream. Simulations demonstrated that the effectiveness of the tide gate is dependent on the severity of the storm. The model simulations suggest that the tide gate could exacerbate flooding and erosion in the upstream during the most extreme conditions. This could pose challenges for the military base as the essence of the tide gate is to protect the railroad crossing and the upstream area from flooding and erosion. Also, there was more potential for sediment mobility at the downstream than at the upstream. Moreover, the sediments being considered to move were silt and clay sediment particles as opposed to the rip rap that were placed by the army in 2025 to provide protection to the railroad crossing. The armoring would require a much higher velocity like the flow velocity under the present and potential condition under Hurricane Irma simulation to be displaced.

In summary, the tide gate proved to be beneficial to the base as it created flow restrictions upstream when functional which protected the railroad crossing from flooding and erosion risks. However, the absence of the tide gate may not necessarily mean more intense flooding or erosion. Instead, the absence of the tide gate could provide ecosystem stability, fewer hazardous bird-strikes, and aquatic population increase- all which were factors of concern for the military prior to the study.

Future Work

Incorporating culvert modules into future mesh designs would allow for a more realistic simulation of how water moves through the tide gate, particularly during storm events. This refinement would provide a more accurate estimate of upstream inundation and drainage timelines after a storm. Additionally, rainfall data could be included into the model to aid in a better estimation of total water depth and water volume, particularly at the upstream. These two parameters can enhance the ability of the model to produce results that are more reliable for design applications.

Future work could focus on testing the resilience of the tide gate under more severe conditions. This test could be achieved by running synthetic storm events with much higher storm categories to represent future climate scenarios. These simulations would be very beneficial in understanding how extreme surges would interact with the tide gate during overtopping, structural damage, etc., as projections show increase in intensity of hydrologic events in the future (NASA, 2024). Results for this would not only help assess tide gate design limits but also inform strategies to optimize tide gate performance and improve coastal protection under changing climate conditions.

While this study showed that the condition of the tide gate largely controls water level and flow velocity changes upstream, future work could focus on using a model that with more realistic representation of vegetation. This would help capture how the flow entering through the tide gate

is further influenced by the vegetation and aid in a better understanding of how different landcovers influence flow dynamics, which can be applied in future restoration projects.

REFERENCES

ADCIRCWiki., C. (2020). Bibliographic details for Manning's n at sea floor. doi: https://wiki.adcirc.org/index.php?title=Manning%27s_n_at_sea_floor&oldid=781.

Abelson, A., Reed, D., Edgar, G., Smith, C., Kendrick, G., Orth, R., . . . Nelson, P. (2020). Challenges for restoration of coastal marine ecosystems in the anthropocene. *Frontiers in Marine Science*, Vol. 7 | https://doi.org/10.3389/fmars.2020.544105.

Adam, P. (2015). Salt marshes. *Encyclopedias of Estuaries*, pp. 515-535.

Adams, J., Raw, J., Riddin, T., Wasserman, J., & Van Niekerk, L. (2021). Salt marsh restoration for the provision of multiple ecosystem services. *Diversity*, 1-20.

Albert, C., Brillinger, M., Guerrero, P., Gottwald, S., Henze, J., Schmidt, S., . . . Schroter, B. (2020). Planning nature-based solutions: Principles, steps, and insights. *Ambio*, Vol. 50 | pp. 1446-1461.

Alizard, K., Hagen, S., Medeiros, S., Bilskie, M., Morris, J., Balthis, L., & Buckel, C. (2018). Dynamic responses and implications to coastal wetlands and the surrounding regions under sea level rise. *PLOS ONE*, 13(12).

Airoldi, L., Abbiati, M., Beck, M., Hawkins, S., Jonsson, P., Martin, D., . . . Aberg, P. (2005). An ecological perspective on the deployment and design of low-crested and other hard coastal defense structures. *Coastal Engineering*, pp. 1073-1087 | Vol. 52 | No. 10 - 11.

Anderson, M., & Smith, J. (2014). Wave attenuation by flexible, idealized salt marsh vegetation. *Coastal Engineering*, Vol. 83 | pp. 82-92.

Anderson, M., & Smith, J. M. (2015, January 15). Quantifying Wave Damping in Spartina alterniflora. *Ocean waves*. Retrieved from https://scholarworks.uno.edu/cgi/viewcontent.cgi?article=1048&context=oceanwaves

Antuna-Rozado, C., Herzog, C., Freitas, T., Cagnin, C., & Wiedman, G. (2019). Nature-based Solutions (NbS) for sustainable and resilient cities: Experiences from Europe and Brazil. *Emerging Concepts for Sustainable Built Environment* (pp. DOI 10.1088/1755-1315/297/1/012001). Helsinki, Finland: Purpose-Led Publishing.

Appelo, C., & Willemsen, A. (1987). Geochemical calculations and observations on salt water intrusions, I. A combined geochemical/minxing cell model. *Journal of Hydrology*, 313-330.

Armitage, A., Weaver, C., & Pennings, S. (2020). Resistance to hurricane effects varies among wetland vegetation types in the marsh-mangrove ecotone. *Estuaries and Coasts*, pp. 960 - 970 | Vol. 43.

Arnaud, G., Krien, Y., Abadie, S., Zahibo, N., & Dudon, B. (2021). How would the potential collapse of the Cumbre Vieja Volcano La Palma Canary Islands impact the Guadeloupe Islands? Insights into the consequences of climate change. *Geosciences*, Vol. 11 | https://doi.org/10.3390/geosciences11020056.

Asher, T., Luettich, R., Fleming, J., Blanton, B. (2019). Low frequency water level correction in storm surge models using data assimilation. *Ocean Modelling*. Vol 144

Balaji, R., Kumar, S., & Misra, A. (2017). Understanding the effects of seawall construction using a combination of analytical modeling and remote sensing techniques: Case study of Fansa, Gujarat, India. *Journal of Ocean and Climate: Science, Technology and Impacts*, https://journals.sagepub.com/doi/full/10.1177/1759313117712180.

Ban, Y., Lei, T., Gao, Y., & Qu, L. (2017). Effect of stone content on water flow velocity over loess slope: non-frozen soil. *Journal of Hydrology*, pp. 525-533 | Vol. 549.

Barbier, E. (2011). *Capitalizing on Nature: Ecosystem as natural assets.* Cambridge, UK: Cambridge University Press.

Barbier, E., Hacker, S., Kennedy, C., Koch, E., Stier, A., & Silliman, B. (2011). The value of estuarine and coastal ecosystem services. *Ecological Monographs*, pp. 169 - 193 | Vol. 81 | No. 2.

Barlow, P., & Reichard, E. (2010). Saltwater intrusion in coastal regions of North America. *Hydrogeology Journal*, 247-260.

Bechauf, R., Cutler, E., Bassi, A., Casier, L., Kapetanakis, M., Pallaske, G., & Simmons, B. (2022). *The value of incorporating nature in urban infrastructure planning.* Global Resource Centre.

Beck, M., Losada, I., Menendez, P., Reguero, D.-S. P., & Fernandez, F. (2018). The global flood protection savings provided by coral reefs. *Nature Communications*, https://www.nature.com/articles/s41467-018-04568-z.

Beeftink, W. (1977). coastal salt marshes of western and northern Europe: an ecological and phytosociological approach. *AGRIS*, 109-155.

Bernard, E., Mofjeld, H., Titov, V., Synolakis, C., & Gonzalez, F. (2006). *Tsunami: scientific frontiers, mitigation, forcasting and policy implications.* London: The Royal Society.

Bertness, M., & Shumway, S. (1993). Competition and Facilitation in Marsh Plants. *The American Naturalist*, Vol. 142, No 4.

Bergeron, N., & Abrahams, A. (1992). Estimating shear velocity and roughness length from velocity profiles. *Water Resources Research*, pp. 2155-2158 | Vol. 28 | No. 8.

Bhable, S., Kayte, S., Mali, S., Kayte, J., & Maher, R. (2015). A Review Paper on Coastal Hazard. *International Journal of Engineering Research and Applications*, 83-93.

Bhattacharya, A., Papakonstantinou, K., Warn, G., McPhillips, L., Bilec, M., Forest, C., . . . Chavda, D. (2025). Optimal life-cycle adaptation of coastal infrastructure under climate change. *Nature Communications*, Vol. 16 | No. 1076.

Bice, C., Huisman, J., Kimball, M., Mallen-Cooper, M., Zampatti, B., & Gillanders, B. (2023). Tidal barriers and fish- Impacts and remediation in the face of increasing demand for freshwater and climate change. *Estuarine, Coastal and Shelf Science.*, pp. 1-16 | Vol. 289.

Biehn, K. (1997). Water control structures used in the restoration and creation of wetlands. *Restoration and Reclamation Review*, Vol. 2 | No. 4 | pp. 1-6.

Billah, M., Bhuiyan, K., Islam, M., Das, J., & Hoque, R. (2022). Salt marsh restoration: An overview of techniques and success indicators. *Environmental Science and pollution Research*, Vol. 29 | pp. 15347-15363.

Bilskie, M., & Hagen, S. (2013). Topographic accuracy assessment of bare earth lidar-derived unstructured meshes. *Advances in Water Resources*, pp. 165-177.

Bilskie, M., Coggin, D., Hagen, S., Medeiros, S. (2015). Terrain-driven unstructured mesh development through semi-automatic vertical feature extraction. *Advances in Water Resources,* Vol. 86 | pp. 102-118

Blain, C., & Rogers, W. (1998). Coastal tide prediction using the ADCIRC-2DDI hydrodynamic finite element model: Model Validation and sensitivity analyses in the Southern North sea/english channel. *Naval Research Laboratory*, pp. 1-96.

Blott, S., & Pye, K. (2012). Particle size scales and classification of sediment types based on particle size distributions: Review and recommended procedures. *Sedimentology*, pp. 2071 - 2096 | Vol. 59 | No. 7 | https://doi.org/10.1111/j.1365-3091.2012.01335.x.

Bo, T., & Ralston, D. (2020). Flow separation and increased drag coefficient in estuarine channels with curvature. *Journal of Geophysical Research: Oceans*, pp. 1-25 | Vol. 125 | No. 10.

Borelli, P., Robinson, D., Panagos, P., Lugato, E., Yang, J., Alewell, C., . . . Ballabio, C. (2020). Land use and climate change impacts on global soil erosion by water (2015-2070). *Proceeding of the National Academy of Sciences of the United States of America*, 21994-22001.

Bordoni, M., Persichillo, P., Meisina, C., Crema, S., Cavalli, M., Bartelletti, C., . . . Avanzi, G. (2018). Estimation of the susceptibility of a road network to shallow landslides with the integration of the sediment connectivity. *Natural Hazards and Earth System Sciences.*, pp. 1735-1758.

Brears, R. (2023). From Traditional Grey Infrastructure to Blue-Green Infrastructure. *Blue and Green Cities*, pp. 5-42 | https://doi.org/10.1007/978-3-031-41393-3_2.

Bridges, T., Wagner, P., Burks-Corpes, K., Bates, M., Coller, Z., Fischenich, C., . . . Wamsley, V. (2015). *Use of Natural and Nature-Based Features (NNBF) for Coastal Resilience.* Vicksburg: U.S. Army Engineer Research and Development Center, Environmental Laboratory, Coastal and Hydraulics Laboratory.

Bridges, T., Smith, J., King, J., Simm, J., Dillard, M., deVries, J., . . . Cairns. (2022). Coastal Natural and Nature-based Features: International Guidelines for Floofd Risk Management. *Sec. Coastal and Offshore Engineering*, https://www.frontiersin.org/articles/10.3389/fbuil.2022.904483/full.

Brinson, M., Lugo, A., & Brown, S. (1981). Primary productivity, decomposition, and consumer activity in freshwater wetlands. *Annual Review of Ecology and Systematics.*, pp. 123-161 | Vol. 12.

Brooks, H., Moller, I., Carr, S., Chirol, C., Christe, E., Evans, B., . . . Royce, K. (2020). Resistance of salt marsh substrates to near-instantaneous hydrodynamics forcing. *Earth Surface Processes and Landforms.*, Vol. 46 | No. 1 | pp. 67-88.

Broome, S., Craft, C., & Burchell, M. (2019). Tidal Marsh Creation. *Coastal Wetlands (Second Edition)*, 789-816.

Burdick, D., Dionne, M., Boumans, R., & Short, F. (1997). Ecological responses to tidal restorations of two Northern New England salt marshes. *Special Issue: Hydrologic Restoration of Coastal Wetlands. Wetland Ecology and Management*, Vol. 4 | No. 2 | pp. 129-144.

Cahoon, D., Hensel, P., & Spencer, T. (2006). Coastal wetland vulnerability to relative sea-level rise: Wetland elevation trends and process controls. In *Wetlands and Natural Resource Management* (pp. 272 - 292). Edgewater: Springer.

Cai, X., Shen, J., Zhang, Y., Oin, Q., & Linker, L. (2023). The roles of tidal marshes in the estuarine biochemical processes: A numerical modeling study. *JGR Biogeosciences*, Vol. 128 | No. 2 | https://doi.org/10.1029/2022JG007066.

Cai, Z., Wang, J., Yang, Y., & Zhang, R. (2021). Influence of vegetation coverage on hydraulic characteristics of overland flow. *MDPI: Water*, Vol. 13 | No. 8 | https://doi.org/10.3390/w13081055.

Caltrans Division of Research, & Information, I. a. (2016). *Tide gates: Technical and ecological considerations.* https://dot.ca.gov/-/media/dot-media/programs/research-innovation-system-information/documents/preliminary-investigations/tide-gates-pi-a11y.pdf: CTC & Associates LLC.

Cameron, W., & Pritchard, D. (1963). *Estuaries.* New York: M.N. Hill, Ed., The Sea, Vol. II, Jogn Wiley and Sons.

Cattrijsse, A., & Hampel, H. (2006). European intertidal marshes: A review of their habitat functioning and value for aquatic organisms. *Marine Ecology Progress Series*, Vol. 324 | pp. 293-307.

Chanson, H. (2021). *The Hydraulics Of Open Channel Flow: An Introduction.* ELSEVIER Butterworth Heinemann.

Chapman, M., & Bulleri, F. (2003). Intertidal seawalls-new features of landscape in intertidal environments. *Landscape and Urban Planning*, 159-172.

Chapman, M., & Underwood, A. (2011). Evaluation of ecological engineering of "armored" shorelines to improve their value as habitat. *Journal of Experimental Marine Biology and Ecology.*, Vol. 400 | No. 1-2 | pp. 302-313.

Coch, N., & Wolff, M. (1991). Effects of Hurricane Hugo Storm Surge in Coastal South Carolina. *Journal of Coastal Research*, 201-226.

Cohen-Shacham, E., Janzen, C., Maginnis, S., & Walters, G. (2016). Nature-based solutions to address global societal. *International Union for Conservation of Nature (IUCN)*, (p. https://doi.org/10.2305/IUCN.CH.2016.13.en). Switzerland.

Coleman, D., Cassalho, F., Miesse, T. (2022). The role of invasive phragmites australis in wave attenuation in the Eastern United States. *Ecological Engineering,* Vol. 35 | No 6 | pp. 961-970.

Coleman, D., Gittman, R., Landry, C., Byers, J., Alexander, C., Coughlin, P., & Woodson, B. (2024). Quantifying the impacts of future shoreline modification on biodiversity in a case study of coastal Georgia, United States. *Conservation Biology*, pp. 1-10 .

Constantine, J., & Anderson, I. (2002). Sediment deposition and accretion in a mid-atlantic (U.S.A.) tidal freshwater marsh. *Estuarine, Coastal and Shelf Science.*, pp. 1-15 | https://doi.org/10.1006/ECSS.2001.0854.

Cooke, S., Bergman, J., Nyboer, E., Reid, A., Gallagher, A., Hammerschlag, N., . . . Vermaire, J. (2020). Overcoming the concrete conquest of aquatic ecosystems. *Biological Conservation*, https://www.sciencedirect.com/science/article/pii/S0006320719318518.

Cooper, J., O'Conner, M., & McIvor, S. (2020). Coastal Defences versus Coastal Ecosystems: A Regional Appraisal. *Marine Policy*, Vol. 111 | .

Costanza, R., Farber, S., Grasso, M., Hannon, B., . . . van den Belt, M. (1997). The value of the world's ecosystem services and natural capital. *Nature*, 253-260.

Currin, C., Delano, P., & Valdes-Weaver, L. (2008). Utilization of a citizen monitoring protocol to assess the structure and function of natural and stabilized fringing salt marshes in North Carolina. *Wetlands Ecology and Management*, Vol. 16 | pp. 97-118.

Dai, W., Li, H., Gong, Z., Zhou, Z., Li, Y., Wang, L., . . . Pei, H. (2021). Self-organization of salt marsh patches on mudflats: Field evidence using the UAV technique. *Estuaries, Coastal and Shelf Science*, 107608.

Dalrymple, R., Kirby, J., & Hwang, P. (1984). Wave diffraction dur to areas of energy dissipation. *Journal of Waterw. Port Coast. Ocean Eng.,*, 67-79.

Darnault, C., & Uyusur, B. (2008). Mixing and Transport. *Water Environmental Research*, 1883-1924.

Day, J., Boesch, D., Clairain, E., Kemp, P., Laska, S., Mitsch, W., . . . Whigham, d. (2007, March 23). Restoration of the Mississippi Delta: Lessons from Hurricanes Katrina and Rita. *Science*, 1679-1684. Retrieved from https://www.science.org/doi/full/10.1126/science.1137030

Day, J., Burdick, D., Ibanez, C., Mitsch, W., Elsey-Quirk, T., & Rivaes, S. (2021, June 19). Restoration of Tidal Marshes. In D. FitzGerald, & Z. Hughes, *Salt Marshes function, Dynamics, and Stresses* (pp. 443-475). Cambridge, England: Cambridge University Press. Retrieved from https://doi.org/10.1017/9781316888933.020

Delgado, P., Hensel, P., & Baldwin, A. (2018). Understanding the impacts of climate change: an analysis of inundation, marsh elevation, and plant communities in a tidal freshwater marsh. *Estuaries and Coasts*, Vol. 41 | pp. 25-35.

Department of Defense (2021). Draft finding of no practicable alternative repair tide gate on Hunter Army Airfield, Georgia. https://home.army.mil/stewart/5316/2801/0304/Draft_FONPA_Repair_Tide_Gate_on_HAAF_GA_v29MAR21.pdf

Dietrich, J., Kolar, R., & Luettich, R. (2004). Assessment of ADCIRC's wetting and drying algorithm. *Developments in Water Science*, Vol. 55 | No 2 | pp. 1767-1778.

Dietrich, J., Westerink, J., Kennedy, A., Smith, J., Jensen, R., Zijlema, M., . . . Powell, M. (2011). Hurricane Gustav (2008) waves and storm surge: Hindcast, synoptic analysis, and validation in Southern Louisiana. *Monthly Weather Review*, pp. 2488-2522.

Dick, J., Carruther-Jones, J., Carver, S., Dobel, A., & Miller, J. (2020). How are nature-based solutions contributing to priority societal challenges surrounding human well-being in the United Kingdom: a systematic map. *Environmental Evidence*, https://environmentalevidencejournal.biomedcentral.com/articles/10.1186/s13750-020-00208-6#citeas.

D'Ippolito, A., Calomino, F., Alfonsi, G., & Lauria, A. (2021). Flow resistance in open channel due to vegetation at reach scale: A review. *Water*, Vol. 13 | No. 2.

Duarte, C. (2017). Reviews and syntheses: Hidden forests, the role of vegetated coastal habitats in the ocean carbon budget. *European Geosciences Union*, Vol. 14 | No. 2 | pp. 301-310.

Dokou, Z., & Karatzas, G. (2012, May 24). Saltwater intrusion estimation in a karstified coastal system using density-dependent modelling and comparison with the sharp-interface approach. *Hydrological Sciences Journal*, 985-999.

Drake, S., Halifax, H., Adamowicz, S., & Craft, C. (2015, June 25). *Carbon Sequestration in Tidal Salt Marshes of the Northeast United States*. Retrieved from https://link.springer.com/article/10.1007/s00267-015-0568-z

Duan, J., French, R., & Miller, J. (2002). The lodging velocity for emergent aquatic in open channels. *J. Am. Water Resources Assoc.*, 255-263.

Eekhout, J., & de Vente, J. (2022). Global impact of climate change on soil erosion and potential for adaptation through soil conservation. *Earth-Science Reviews*, https://www.sciencedirect.com/science/article/pii/S0012825222000058.

Eggermont, H., Balian, E., Azevedo, J., Beumer, V., Brodin, T., Claudet, J., . . . Le Roux, X. (2015). Nature-Based Solutions: new influence for environmental management and research in Europe. *Ecological Perspectives for Science and Society*, Vol. 24 | No. 4 | pp. 243-248(6) | https://doi.org/10.14512/gaia.24.4.9.

Elliot, M., Burdon, D., Hemingway, K., & Apitz, S. (2007). Estuarine, coastal and marine ecosystem restoration: Confusing management and science - A review of concepts. *Estuarine, Coastal and Shelf Science*, Vol. 74 | Issue 3 | pp. 349-366.

European Communities. (2015). *Towards an EU research and innovation policy agenda for nature-based solutions & re-naturing cities. Final report of the Horizon 2020 expert group on nature-based solutions and re-naturing cities.* http://bookshop.europa.eu/en/towards-an-eu-research-and-innovation-policy-agenda-for-nature-based-solutions-re-naturing-cities-pbKI0215162/.

Environmental Protection Agency. (2020). *Tidal Restrictions Synthesis Review: An analysis of U.S tidal restrictions and opportunities for their avoidance and removal.* Washington D.C.

European Commission. (2021). The Solution is in Nature: Future Brief 24. *Science Communication Unit*, https://knowledge4policy.ec.europa.eu/publication/future-brief-solution-nature_en.

FEBA. (2022). Nature-based Solutions and the global goal on adaptation. *FEBA adaptation brief on nature-based solutions released at COP27.*

Fegherazzi, S., Anisfeld, S., Blum, L., Long, E., Feagin, R., . . . Williams, K. (2019). Sea level rise and the dynamics of the marsh-upland boundary. *Frontiers in Environmental Science*, https://www.frontiersin.org/articles/10.3389/fenvs.2019.00025/full.

Follett, E., & Nepf, H. (2012). Sediment patterns near a modle patch of reedy emergent vegetation. *Geomorphology*, 141-151.

Forbes, C., Luettich, R., Mattocks, C., Westerink, J. (2010). A retrospective evaluation of the storm surge produced by Hurricane Gustav (2008): Forecast and hindcast results.

Foster-Martinez, M., Lacy, J., Ferner, M., & Variano, E. (2018). Wave attenuation actoss a tidal marsh in San Francisco Bay. *Coastal Engineering* , Vol. 136 | pp. 26-40.

Galea, S., Nandi, A., & Vlahov, D. (2005). The epidemology of post-traumatic stress disorder after disasters. *Epidemiologic Reviews*, 27:78-91.

Gang, C., Pan, S., Hanqin, T., Wang, Z., Rongting, X., Pan, N., . . . Shi, H. (2020). Satellite observations of forest resilience to hurricanes along the North Gulf of Mexico. *Forest Ecology and Management*, pp. 1 - 12 | Vol. 472.

Garzon, J., Maza, M., Ferreira, C., Lara, J., & Losada, I. (2019, April). Wave Attenuation by Spartina Salt marshes in the Chesapeake Bay Under Storm Surge Conditions. *JGR Oceansd*, 5220-5243. Retrieved from https://www.sciencedirect.com/science/article/pii/S0378383918302175

Ge, F., T., B., Zhou, Y., He, Q., & Qian, W. (2018). Analyzing the role of salt marshes on attenuating waves with Rb16-2050 measures in changjiang estuary. *Resour. Environ. Yangtze Basin 27*, pp. 1784-1792 | doi: 10.11870/cjlyzyyhj201808014.

Ge, J., Yi, J., Zhang, J., Wang, X., Chen, C., Yuan, L., . . . Ding, P. (2021). Impact of vegetation on lateral exchanges in a salt marsh-tidal creek system. *Advancing Earth and Space Sciences*.

Gedan, B., Silliman, R., & Bertness, D. (2008). Centuries of Human-Driven Change in Salt Marsh Ecosystems. *Annual Reviews of Marine Science*, 117-141.

Gedan, K., Kirwan, M., Wolanski, E., Barbier, E., & Silliman, B. (2011). The present and future role of coastal wetland vegetation in protecting shorelines: answering recent challenges to the paradigm. *Climate Change*, pp. 7-29 | Vol. 106 .

Georgia Department of Natural Resources. (2006). Wetland Monitoring. *Environmental Protection Division*, 1-45.

Giannico, G., & Souder, J. (2005, January). *Tide Gates in the Pacific: Operation, Types and Environmental Effects*. Retrieved from https://www.researchgate.net/publication/233758070_Tide_Gates_in_the_Pacific_Operation_Types_and_Environmental_Effects

Girardin, C., Jenkins, S., Seddon, N., Allen, M., Lewis, S., Wheeler, C., . . . Malhi, Y. (2021). Nature-based solutions can help cool the planet- if we act now. *Nature*, 593(7858): 191-194 | doi:10.1038/d41586-021-01241-2.

Giuliani, S., & Bellucci, L. (2019). Chapter 4 - Salt marshes: Their role in our society and threats posed to their existence. In C. Sheppard, *World Seas: An Environmental Evaluation (Second Edition)* (pp. 79-101). Academic Press.

Gosselink, J., & Mitsch, W. (2015). Wetlands. *New Jersey*.

Grant, A., & Cooker, M. (2023). Reductions in water level over coastal wetlands during storm surges and tsunamis: An analytical result and a critical review of the literature. *Coastal Engineering*, pp. 1-7 | Vol. 183.

Golitaleb, M., Mazaheri, E., Bonyadi, M., & Sahebi, A. (2022). Prevalence of Post-traumatic Stress Disorder after Flood: A systematic review and meta-analysis. *Frontiers in Psychiatry*, 10.3389/fpsyt.2022.890671.

Grant, W., & Madsen, O. (1982). Movable bed roughness in unsteady oscillatory flow. . *Journal of Geophysical Research*, pp. 469-481.

Griggs, G. (2005). The Impacts of Coastal Armoring. *Shore & Beach*, Vol. 73 | No 1 | pp. 13-22.

Griggs, G., & Patsch, K. (2019). The Protection/Hardening of California's Coast: Times are Changing. *Journal of Coastal Res.*, http://doi:10.2112/JCOASTRES-D-19A-00007.1.

Gutzat, F., & Dormann, C. (2018). Decaying trees improve nesting opportunities for cavity-nesting birds in temperate and boreal forests: A meta-analysis and implications for retention forestry. *Ecology and Evolution*, pp. 8616 - 8626 | Vol. 8 | No. 6.

Hadja, K., & Kharchi, F. (2017). The erosion of reinforced concrete walls by the flow of rainwater. *International Journal of Concrete Structures and Materials.*, pp. 151 - 159 | Vol. 11.

Hagen, S., Zundel, A., & Kojima, S. (2006). Automatic, unstructured mesh generation for tidal circulation in a large domain. *International Journal of Computational Fluid Dynamics*, Vol. 20 | No. 8 | pp. 593 - 608.

Haigh, R., Amaratunga, D., & Hemachandra, K. (2018). A capacity analysis framework for multi-hazard early warning in coastal communities. *7th International Conference on Building Resilience; Using scientific knowledge to inform policy and practice in disaster risk reduction, ICBR2017, 27-29 November 2017, Bangkok, Thailand* (pp. 1139-1146). United Kingdom: Elsevier.

Hanson, H., & Lindh, G. (1993). Coastal Erosion: An escalating environmental threat. *AMBIO*, Vol. 22, No. 4 (Jun 1993), pp. 188-195.

Harrington, R., & Harrington, E. (1982). Effects on fishes and their forage organisms of impounding a Florida salt marsh to prevent breeding by salt marsh mosquito. *Bull. Mar. Sci.*, Vol. 32 | No. 2 | pp. 523 - 531.

Hautier, Y., Tilman, D., Isbell, F., Seabloom, E., Borer, E., & Reich, P. (2015). Anthropogenic environmental changes affect ecosystem stability via biodiversity. *Science*, 336-340.

Hewett, C., Simpson, C., Wainwright, & Hudson, S. (2018). Communicating risks to infrastructure due to soil erosion: A bottom-up approach. *Land Degradation & Development*, https://doi.org/10.1002/ldr.2900.

Hinkel, J., Lincke, D., Vafeidis, A., Perrette, M., Nicholls, R., Tol, R., & Levermann, A. (2014). Cpastal flood damage and adaptation costs under 21st century sea-level rise. . *Proceedings of the National Academy of Sciences.*, pp. 3292-3297 | Vol. 111.

Horstman, E., Bryan, K., & Mullarney, J. (2021). Drag variations, tidal assymetry and tidal range changes in a mangrove creek system. *Earth Surface Processes and Landforms*, pp. 1-1846 | Vol. 46.

Houser, C., Trimble, S., & Morales, B. (2015). Influence of blade flexibility on the drag coefficient of aquatic vegetation. *Estuarines and Coasts*, Vol. 38 | pp. 569-577.

Hovis, M., Hollinger, J., Cubbage, F., Shear, T., Doll, B., Kurki-Fox, J., . . . Potter, T. (2021). Natural infrastructure practices as potential flood storage and reduction for farms and rural communities in the North Carolina coastal plain. *Sustainability*, Vol. 13 | No. 16 | https://doi.org/10.3390/su13169309.

Huang, R., Zeng, Y., Zha, W., & Yang, F. (2022). Investigation of flow characteristics in open channel with leaky barriers. *Journal of Hydrology*, 1-9.

Huge, J. (2025). Understanding coastal modeling: Techniques and applications for shoreline management and protection. *Journal of Coastal Zone Management*, Vol. 28 | No. 2.

Hung, H., Chen, H., & Yang, R. (2025). Experimental study on the sediment-trapping performance of different coastal protection structures in a high-tidal range area. *Journal of Marine Science and Engineering*, Vol. 13 | No. 6.

International Code Council. (2021). The use of climate data and assessment of extreme weather event risks in building codes around the world: Survey findings from the Global Resiliency Dialogue. pp. 1-10.

Irish, J., Lynett, P., Weiss, R., Smallegan, S., & Cheng, W. (2013). Buried relic seawall mitigates Hurricane Sandy's impacts. *Coastal Engineering*, 79-82.

Irwin, N., Irwin, E., Martin, J., & Aracena, P. (2018). Constructed wetlands for water quality improvements: Benefits transfer analysis from Ohio. *Journal of Environmental Management*, 1063-1071.

Jafari, N., Harris, B., Morris, J., & Cadigan, J. (2024). Interplay of hydroperiod on root shear strength for coastal wetlands. *Geophysical Research Letters*, Vol. 51 | No. 11.

Jing, X., Zhuo, Y., Xu, Z., Chen, Y., Li, G., & Wang, X. (2023). Coastal wetland restoration strategies based on ecosystem service changes: A case study of the south bank of Hangzhou Bay. *MDPI: Land*, Vol. 12 | No. 5 | https://doi.org/10.3390/land12051110.

Johnson, M., & Hutchins, E. (2023). The effects of tide gate on New England Wetlands and other tidal resources. *NOAA FISHERIES*, Vol. 23 | No. 1 | https://orcid.org/0000-0003-0846-7978.

Kawabata, Y., Takimoto, K., Nishida, T., Koshikawa, Y., & Aizawa, A. (2024). Integration of green and gray infrastructures - Conceptualization from the perspective of gray engineers. *Structural Engineering International*, Vol. 35 | pp. 125-133 |.

Kemp, J., Harper, D., & Crosa, G. (2000). The Habitat-scale ecohydraulics of rivers. *Ecological Engineering* , 17-29.

Kennedy, A., Gravois, U., Zachry, B., Westerink, J., Hope, M., Dietrich, C., & Powell, M. (2011). Origin of the Hurricane Ike forerunner surge. *Advancing Earth and Space Sciences*, https://doi.org/10.1029/2011GL047090 | Vol. 38 | No. 8.

Kentula, M. (2000). Perspectives on setting success criteria for wetland restoration. *ELSEVIER: Ecological Engineering*, Vol. 15 | No. 3-4 | pp. 199-209.

Kimball, M., Rozas, L., Boswell, K., & Cowna Jr., J. (2015). Effects of slotted water control structures on Nekton movement within salt marshes. *Marine and Coastal Fisheries*, Vol. 7 | pp. 177-189.

Knutson, P., Brochu, R., Seelig, W., & Inskeep, M. (1982). Wave damping in Spartina alterniflora marshes. *Wetlands*, 87-104.

Kolar, R., Westerink, J., Cantekin, M., & Blain, C. (1994). Aspects of nonlinear simulations using shallow-water models based on the wave continuity equation. *Computers & Fluids*, pp. 523-538 | Vol. 23 | No. 3.

Kranenburg, W., Geyer, W., Garcia., & Ralston. (2019). Reversed lateral circulation in a sharp estuaring bend with weak stratification. *Journal of Physical Oceanography*, pp. 1619-1637 | Vol. 49 | No. 9.

Krauss, K., Doyle, T., Doyle, T., Swarzenski, C., From, A., Day, R., & Conner, W. (2009). Water level observations in mangrove swamps during two hurricanes in Florida. *Wetlands*, pp. 142-149 | Vol. 29 | No. 1.

Krebs, S., Limburg, K., & Schummer, M. (2023). Reduction in coastal salt marsh habitat fro wildlife from sea-level rise in the United States. *Case Studies in the Environment*, 1-17.

Knutson, P., Brochu, R., Seelig, W., & Inskeep, M. (1982). Wave damping in Spartina alterniflora marshes. *Wetlands*, 87-104.

Kumar, A., Thakur, T., & Yu, Z. (2023). Editorial: Wetland ecosystems as important greenhouse hotspots. *Frontiers in Environmental Science*, Vol. 10 | https://doi.org/10.3389/fenvs.2022.1127269.

Kurth, M., Piercy, C., Jackson, C., Lemasson, B., & Harris, B. (2024). Life cycle management of natural infrastructure: Assessment of state of practice and current tools. . *Frontiers in Built Environment*, https://www.frontiersin.org/articles/10.3389/fbuil.2023.1181835/full.

Kuwae, T., & Crooks, S. (2021). Linking climate change mitigation and adaptation through coastal green-gray infrastructure: a perspective. *Coastal Engineering Journal*, 188-199.

Lakshmi, A. (2021). Coastal ecosystem services & human wellbeing. *Indian Journal of Medical Research*, 382-387.

Leonard, J., & Richard, G. (2004). Estimation of runoff critical shear stress for soil erosion from soil shear strength. *CATENA*, Vol. 57 | No 3 | pp. 233 - 249.

Li, H. (2019). Coastal Modeling. In H. Li, *Encyclopedia of Coastal Science. Encyclopedia of Earth Sciences Series.* (pp. http://doi.org/10.1007/978-3-319-93806-6_368). Switzerland: Springer Cham.

Li, F., Angelini, C., Byers, J., Craft, C., & Pennings, S. (2022). Responses of a tidal freshwater marsh plant community to chronic and pulsed saline intrusion. *Journal of Ecology*, pp. 1508 - 1524 | Vol. 110 | No. 7.

Lim, C., Kim, T., Lee, S., Yeon, Y., & Lee, J. (2021). Assessment of potential beach erosion risk and impact of coastal zone development: A case study on Bongpo-Cheonjin Beach. *Natural Hazards and Earth System Sciences*, 21, 3827-3842. https://nhess.copernicus.org/articles/21/3827/2021/nhess-21-3827-2021.pdf.

Liu, C., & Nepf, H. (2016). Sediment deposition within and around a finite patch of model vegetation over a range of channel velocity. *Water Resources Research*, 606-612.

Liu, H., Jay, M., & Chen, X. (2021). The role of nature-based solutions for improving environmental quality, health and well-being. *Sustainability*, 13(19) | https://doi.org/10.3390/su131910950.

Loder, N., Irish, J., Cialone, M., & Wamsley, T. (2009). Sensitivity of hurricane surge to morphological parameters of coastal wetlands. *Estuarine, Coastal and Shelf Science*, pp. 625-636 | Vol. 84.

Long Island Sound Habitat Restoration Manual. (2004). *Habitat - The environment in which an organism or biological population usually lives or grows.*

Longman, J., Rahman, K., & Bennett-Levy, J. (2023). Research Letter: Flooding, displacement, peritraumatic experience and disaster-related PTSD in Northern New South Wales - The critical need for quality data to plan mental health support. *Australian & New Zealand Journal of Psychiatry*, 10.1177/00048674231203901.

Lopez-Ortega, A., Bayon, R., & Arana, J. (2018). Evaluation of protective coating for offshore applications. Corrosion and tribocorrosion behavior in synthetic seawater. *Surface Coating Technology*, pp. 1083 - 1097 | Vol. 349.

Luettich, R., & Westerink, J. (1992). *ADCIRC: An advanced three-dimensional circulation model for shelves, coasts, and estuaries.* https://apps.dtic.mil/sti/tr/pdf/ADA261608.pdf.

Luettich, R., & Westerink, J. (1995). An assessment of flooding and drying techniques for use in the ADCIRC hydrodynamic model: Implementation and performance in one-dimensional flows. pp. 1-55.

Luettich Jr., R., & Westerink, J. (1995, July 14). *Implementation and testing of elemental flooding and drying in the ADCIRC hydrodynmaic model.* Retrieved from https://adcirc.org/wp-content/uploads/sites/2255/2018/11/1995_Luettich03.pdf

Luettich, R., & Westerink, J. (1999). *Elemental Wetting and Drying in the ADCIRC Hydrodynamic Model: Upgrades and Documentation for ADCIRC Version 34.XX.* Vicksburg.

Luettich, R., & Westerink, J. (2004). Formulation and numerical implementation of the 2D/3D ADCIRC finite element model version 44.XX. pp.1-74.

Luhar, M., & Nepf, H. (2013). From the blade scale to the reach scale: A characterization of aquatic vegetative drag. *Advances in Water Resources*, 305-316.

Lynn, L., & Reed, D. (2002). Hydrodynamics and sediment transport through tidal marsh canopies. *Journal of Coastal Research*, pp. 459 - 469 | Vol. 36 | https://doi.org/10.2112/1551-5036-36.sp1.459.

Ma, Y., Zhu, L., Peng, Z., Xue, L., Zhao, W., Li, T., . . . Li, X. (2023). Wave attenuation by flattened vegetation (Scirpus mariqueter). *Frontiers in Marine Science*, Vol. 10 | https://doi.org/10.3389/fmars.2023.1106070.

MacKinnon, K., Sobrevila, C., & Hickey, V. (2008). *Biodiversity, Climate Change and Adaptation: Nature-based Solutions from the World Bank Portfolio.* Washington D.C.: The International Bank for Reconstruction and Development.

Malone, S., Staudhammer, C., Loescher, H., Olivas, P., Oberbauer, S., Ryan, M., . . . Starr, G. (2014). Seasonal patterns in energy partitioning of two freshwater marsh ecosystems in the Florida Everglades. *Journal of Geophysical Research: Biogeosciences.*, pp. 1487 - 1505.

Manis, J., Garvis, S., Jachec, S., & Walters, L. (2015). Wave attenuation experiments over living shorelines over time: a wave tank study to assess recreational boating pressures. *Journal of Coastal Conservation*, Vol. 19 | pp. 1-11.

Marshall, S. (2011). The water crisis in Kenya: causes, effects and solutions. *Global Majority E-Journal*, Vol. 2 | No. 1 | pp. 31-45.

Marsooli, R., & Wu, W. (2014). Numerical investigation of wave attenuation by vegetation using a 3D RANS model. *Advanced Water Resources*, 245-257.

Mazhar, S., Pellegrini, E., Contin, M., Bravo, C., & De Nobili, M. (2022). Impacts of salinization caused by sea level rise on the biological processes of coastal soils- A review. *Frontiers in Environmental Sciences*, Vol. 10 | doi: https://doi.org/10.3389/fenvs.2022.909415.

Mcowen, C., Weatherdon, L., Van Bochove, J., Sullivan, E., Blyth, S., Zockler, C., . . . Fletcher, S. (2017). A global map of salt marshes. *Biodiversity Data Journal*, 10.3897/BDJ.5.e11764.

Middleton, B. (1999). Disturbance dynamics in wetlands. In B. Middleton, *Wetland Restoration: Flood pulsing and Disturbance Dynamics* (pp. pp. 1-61). New York: John Wiley & Sons, Inc.

Mishra, A., & Rai, S. (2017). Comparative Performance Assessment of Eco-Friendly Buildings and Conventional Buildings of Kathmandu Valley. *International Journal of Current Research* , pp. 62958 - 62973.

Mitsch, W., & Gosselink, J. (2015). *Wetlands, 5th ed.* New York, NY, USA.: John Wiley and Sons Inc. | ISBN 978-1118676820.

Möller, I., & Spencer, T. (2002). Wave dissipation over macro-tidal salt marshes: Effects of marsh edge typology and vegetation change. *Jounal of Coastal Research*, 506-521.

Moller, I., Kudella, M., Rupprecht, F., Spencer, T., Paul, M., van Wesenbeeck, B., . . . Schimmels, S. (2014). Wave attenuation over coastal salt marshes under storm surge conditions. . *Nature Geoscience*, 727-731.

Molnar, M. (2016). Tide Gates: Technical and Ecological Considerations. *Caltrans Division of Research, Innovation and System Information*, 1-54.

NASA. (2024, October 23). *The effects of climate change.* Retrieved from National Aeronautics and Space Administration: https://science.nasa.gov/climate-change/effects/

Nash, L., van Putten, I., Alexander, K., Bettiol, S., Cvitanovic, C., Farmery, A., . . . Vince, J. (2022). Oceans and society: feedbacks between ocean and human health. *Reviews in Fish Biology and Fisheries*, 161-187.

National Weather Service. (2020, May 1). *Tropical Cyclone History for Southeast South Carolina and Northern Portions of Southeast Georgia*. Retrieved from National Oceanic and Atmospheric Administration.

Nepf, H. (1999). Drag, turbulence and diffusion in flow through emergent vegetation. *Water Resources Research* , 479-489.

Nepf, H. (2012). Flow and transport in regions with aquatic vegetation. *Annual Review of Fluid Mechanics*, 123-142.

Nepf, H. (2012). Hydrodynamics of vegetated channels. *Journal of Hydraulic Research*, 262-279.

Nesshover, C., Assmuth, T., Irvine, K., Rusch, G., Waylen, K., Delbaere, B., . . . Wittmer, H. (2017). The science, policy and practice of nature-based solutions: An interdisciplinary perspective. *Science of the Total Environment*, 1215-1227.

Newton, A., Icely, J., Cristina, S., Perillo, G., Turner, R., Ashan, D., . . . de Lima, R. (2020). Anthropogenic, direct pressures on coastal wetlands. *Frontiers in Ecology and Evolution: Sec. Conservation and Restoration Ecology*, https://doi.org/10.3389/fevo.2020.00144.

Nichols, R., Wright, L., Bainbridge, S., Cosby, A., Henaff, A., Loftis, J., . . . Zarillo, G. (2019). Collaborative science to enhance coastal resilience and adaptation. *Frontiers in Marine Science*, https://www.frontiersin.org/articles/10.3389/fmars.2019.00404/full.

NOAA. (2015). Guidance for considering the use of living shorelines. https://www.habitatblueprint.noaa.gov/wp-content/uploads/2018/01/NOAA-Guidance-for-Considering-the-Use-of-Living-Shorelines_2015.pdf .

NOAA. (2020). Hurricanes in History. *National Hurricane Center and Center Pacific Hurricane Center*, https://www.nhc.noaa.gov/outreach/history/.

NOAA. (2021, February 26). *Exploring the secrets of marsh happiness*. Retrieved from National Ocean Service: https://oceanservice.noaa.gov/ecosystems/estuaries/happy-marsh.html

NOAA. (2024). Costliest U.S. Tropical Cyclones. pp: 1-5 | doi:https://www.ncei.noaa.gov/access/billions/dcmi.pdf.

NOAA. (2024). Natural Infrastructure. *Office for Coastal Management Digital Coast*, https://coast.noaa.gov/digitalcoast/topics/green-infrastructure.html.

NOAA. (2024, March 14). *Natural Infrastructure*. Retrieved from Office for Coastal Management Digital Coast: https://coast.noaa.gov/digitalcoast/topics/green-infrastructure.html

North Carolina Wetlands. (2017). *Freshwater vs. Saltwater wetlands in North Carolina.* www.ncwetlands.org.

Nunn, P., & Kumar, R. (2018). Understanding climate-human interactions in Small Island Developing States (SIDS): implications for future livelihood sustainability. *International Journal of Climate Change Strategies and Management.*, pp. 245-271.

Nunn, P., Klock, C., & Duvat, V. (2021). Seawalls as maladaptations along island coasts. *Oceans & Coastal Management.*, https://www.sciencedirect.com/science/article/pii/S0964569121000399.

Odum, E. (1988). Comparative Ecology of Tidal Freshwater and Salt Marshes. . *Annual Review of Ecological Systems*, 147-176.

Oppenheimer, M., Glavovic, B., Hinkel, J., van de Wal, R., Magnan, A., Abd-Elgawad, A., . . . Sebesvari, Z. (2019). *Sea level rise and implications for low-lying islands, coasts and communities.* United Kingdom: Cambridge University Press.

Orescanin, M., Elgar, S., & Raubenheimer, B. (2016). Changes in bay circulation in an evolving multiple inlet system. *Continental Shelf Research*, Vol. 124 | pp. 13-22.

Organization, W. M. (2023, December 5). *Rate and impact of climate change surges dramatically in 2011-2020.* Retrieved from https://wmo.int/news/media-centre/rate-and-impact-of-climate-change-surges-dramatically-2011-2020

Ortals, C., Cordero, O., Valle-Levinson, A., & Angelini, C. (2021). Flows, Transport, and Effective Drag in Intertidal Salt Marsh Creeks. *JGR Oceans*, Volume 126 issue 11.

Orton, P., Ralston, D., van Prooijen, B., D., S., Ganju, N., Chen, Z., . . . Marcell, K. (2023). Increased Utilization of storm surge barriers: A research agenda on estuary impacts. *Advancing Earth and Space Science*, pp. 1-10 .

Osman, A., Ansah-Mensah, K., Amoah-Nuamah, J., & Atanga, R. (2023). Flood related depression and replacement of damaged household items. *Progress in Disaster Science*, https://www.sciencedirect.com/science/article/pii/S2590061723000078#bb0005.

Pandoe, W., & Edge, B. (2008). Case study for a cohesive sediment transport model for Matagorda Bay, Texas, with coupled ADCIRC 2D-Transport and SWAN wave models. *Journal of Hydraulic Engineering*, Vol. 134 | No. 3 | doi: 10.1061/(ASCE)0733-9429(2008)134:3(303).

Paola, G., Rodriquez, G., & Rosskopf, C. (2023). Shoreline dynamics and beach erosion. *Geosciences*, 13(3), 74; https://doi.org/10.3390/geosciences13030074.

Passeri, D., Hagen, S., Smar, D., Alimohammadi, N., Risner, A., White, R. (2011). Sensitivity of ADCIRC tide and storm surge model to Manning's n. Estuarine and Coastal Modelling. pp. 457- 475.

Pe Kinnmark, I., & Gray, W. (1985). Stability and accuracy of spatial approximations for wave equation tidal models. *Journal of Computational Physics*, Vol. 60 | No. 3| pp. 447-466.

Pearlstine, G., Kitchens, W., Latham, P., & Bartleson, R. (1993). Tide gate influences on a tidal marsh. *Water Resources Bulletin*, Pp. 1009-1019 | Vol. 29 | No 6.

Perry, J., & Atkinson, R. (2009). York River Tidal Marshes. *Journal of Coastal Research.*, pp. 43-52.

Perry, J., Bilkovic, D., Havens, K., & Hershner, C. (2009). Tidal freshwater wetlands of the mid-atlantic and southeastern united states. In A. Barendregt, D. Whigham, & A. Baldwin, *Tidal freshwater wetlands.* (pp. 158-310). Margraf Publishers, Weikersheim.

Piggot-Mckellar, A., Nunn, P., McNamara, K., & Sekinini, S. (2020). Dam(n) Seawalls: A case of climate change maladaptation in Fiji. *Managing Climate Change Adaptation in the Pacific Region*, pp. 69-84.

Pirro, E., Roebeling, P., Sallustio, L., Marchetti, M., & Lasserre, B. (2023). Cost-effectiveness of nature-based solutions under different implementation scenarios: A national perspective for italian urban areas. *MDPI: Land*, Vol. 12 | No. 3 | https://doi.org/10.3390/land12030603.

Portnoy, J., & Giblin, A. (1997). Effects of historic tidal restrictions on salt marsh sediment chemistry. *Biogeochemistry*, pp. 275 - 303 | Vol. 36.

Powell, E., Tyrell, M., Milliken, A., Tirpak, J., & Staudinger, M. (2019). A review of coastal management approaches to support the integration of ecological and human community planning for climate change. *Journal of Coastal Conservation*, 1-18.

Purcell, A., Khanal, P., Straka, T., & Willis, D. (2020). Valuing ecosystem services of coastal marshes and wetlands. *Clemson (SC) Cooperative Extension, Land-Grant Press by Clemson Extension*, https://doi.org/10.34068/report4.

Ralston, D., & Geyer, W. (2019). Response to channel deepening of the salinity intrusion, estuarine circulation, and stratification in an urbanized estuary. *Journal of Geophysical Research: Oceans*, pp. 4784 - 4802 | Vol. 124 | No. 7.

Reimann, L., Vafeidis, A., & Honsel, L. (2023). Population development as a driver of coastal risk: Current trends and future pathways. *Cambridge Prisms: Coastal Futures*, 1:e14. doi:10.1017/cft.2023.3.

Rizalihadi, M., Ziana, & Shaskia, N. (2019). Approaching model of Manning's coefficient due to an effect of density and height of vegetation in open channel. *IOP Conference Series: Materials Science and Engineering* (pp. pp. 1-8). IOP Publishing Ltd.

Rogers, B., Herke, W., & Knudsen, E. (1992). Effects of three different water-control structures on the movements and standing stocks of coastal fishes and macrocrustaceans. *Journal of the Society of Wetland Scientists*, Vol. 12 | pp. 106-120.

Rothenberger, M., Armstrong, A., & Spitz, M. (2018). Social-ecological system responses to Hurricane Sandy in the Hudson-Raritan Estuary. *Ambio*, doi: 10.1007/s13280-017-0949-z.

Rozas, L. (1995). Hydroperiod and its influence on nekton use of the salt marsh: A pulsing ecosystem. *Estuaries*, pp. 579 -590 | Vol. 18.

Rupprecht, F., Moller, I., Paul, M., Kudella, M., Spencer, T., van Wesenbeeck, B., . . . Schimmels, S. (2017). Vegetation-wave interactions in salt marshes under storm surge conditions. *Ecological Engineering*, 301-315.

Rytwinski, T., Taylor, J., & Cooke, S. (2017). What are the impacts of flow regime changes on fish productivity in temperate regions? A systematic map protocol. *Environmental Evidence*.

Sandifer, P., Braud, A., Knapp, L., & Taylor, J. (2012). Is Living in a U.S. Coastal City good for one's health? *International Journal of Environmental Research and Public Health*, https://www.ncbi.nlm.nih.gov/pmc/articles/PMC8393764/.

Sandifer, P., & Scott, G. (2021). Coastlines, coastal cities, and climate change: A perspective on urgent research needs in the United States. *Frontiers in Marine Science*, https://www.frontiersin.org/articles/10.3389/fmars.2021.631986/full.

Sanitwong-Na-Ayutthaya, S., Saengsupavanich, C., Ariffin, E., Ratnayake, A., & Yun, L. (2023). Environmental Impacts of Shore Revetment. *PMCID*, doi: 10.1016/j.heliyon.2023.e19646.

Schoonees, T., Mancheno, G., Scheres, B., Bouma, T., Silva, R., Schlurmann, T., & Schuttrumpf, H. (2019). Hard structures for coastal protection, towards greener designs. *Environmental Fluid Mechanics*, Vol. 42 | No. 7.

Schoutens, K., Heuner, M., Minden, V., Ostermann, T., Silinski, A., Belliard, J., & Temmerman, S. (2019). How effective are tidal marshes as nature-based shoreline protection throughout seasons? *Association for the Science of Limnology and Oceanography*, Vol. 64 | pp. 1750-1762 | doi: 10.1002/lno.11149.

Schuerch, M., Mossman, H., Moore, H., Christe, E., & Kiesel, J. (2022). Invited perspectives: Managed realignment as a solution to mitigate coastal flood risks - optimizing success through knowledge co-production. *Natural Hazards and Earth System Sciences*, 2879-2890.

Seara, T., Clay, P., & Colburn, L. (2016). Percieed adaptive capacity and natural disasters: A fisheries case study. *Global Environmental Change*, 38: 49-57.

Seddon, N., Sengupta, S., Garcia-Espinosa, M., Hauler, I., Herr, D., & Rizvi, A. (2019). *Nature-based Solutions in nationally determined contributions: Synthesis and recommendations for enhancing climate ambition and action by 2020.* Gland Switzerland: IUCN: University of Oxford, UK.

Seddon, N. C., Berry, P., Girardin, C., Smith, A., & Turner, B. (2020). Understanding the value and limits of nature-based solutions to climate change and other global challenges. *Biological Sciences*.

Shepard, C., Crain, C., & Beck, M. (2011). The protective role of coastal marshes: A systematic review and meta-analysis. *PLOS One*, Vol. 6 | No. 11.

Sherman, S., & Hartman, R. (2021, August 16). Marsh Madness: Restoring Tidal Wetlands in our Estuaries. *Frontiers for Young Minds*, 10.3389/frym.2021.607674.

Simelton, E., Carew-Reid, J., Coulier, M., Damen, B., Howell, J., Pottinger-Glass, C., . . . van Der Meiren, M. (2021). NbS framework for agricultural landscapes. *Frontiers in Environmental Science*, 9, 678367.

Simpson, G., & Castelltort, S. (2006). Coupled model of surface water flow, sediment transport and morphological evolution. *Computers & Geosciences*, pp. 1600-1614 | Vol. 32 | No. 10.

Singhvi, A., Luijendijk, A., & Oudenhoven, A. (2022). The grey-green spectrum: A review of coastal protection interventions. *Journal of Environmental Management*, Vol. 311.

Small, C., & Nicholls, R. (2003). A Global Analysis of Human Settlement in Coastal Zones. *Journal of Coastal Research*, 584-599.

Smith, C., Rudd, M., Gittman, R., Melvin, E., Patterson, V., Renzi, J., . . . Silliman, B. (2020). Coming to terms with living shorelines: A scoping review of novel restoration strategies for shoreline protection. *Frontiers in Marine Science: Sec. Marine Conservation and Sustainability*, Vol. 7 | https://doi.org/10.3389/fmars.2020.00434.

Song, C., Park, S., & Shin, J. (2024). An experimental study of flow and turbulence properties near the rising sector gate mouth considering the gate opening with a PIV measuring system. *MDPI: Water*, Vol. 16 | No. 20 | https://doi.org/10.3390/w16203004.

Souder, J., Tomarco, L., Giannico, G., & Behan, J. (2018). *Ecological effects of Tide gate upgrade or removal: A literature review and knowledge synthesis. Report to Oregon Watershed Enhancement Board.* Corvallis: Institute for Natural Resources, Oregon State University.

Sowinska-Swierkosz, B., & Garcia, J. (2021). A new evaluation framework for nature-based solutions (NbS) projects based on the application of performance questions and indicators approach. *Science of the Total Environment*, 1-15.

Spalding, M., Ruffo, S., Lacambra, C., Meliane, I., Hale, L., Shepard, C., & Beck, M. (2014). The role of ecosystem in coastal protection. Adapting to climate change and coastal hazards. *Ocean and Coastal Management*, pp. 50-57 .

Spano, G., Dadvand, P., & Sanesi, G. (2021). Editoral: The benefits of Nature-based Solutions to Psychological Health. *Frontiers in Psychology*, 12, 646627 | doi: 10.3389/fpsyg.2021.646627.

Stewart, R., H. (2007). Introduction to physical oceanography.

Stanley, R., Bilskie, M., Woodson, C., Byers, J. (2024). A model for understanding the effects of flow conditions on oyster reef development and impacts to wave attenuation. *Ecological Modelling*, Vol. 489.

Steven, A., Appeaning Addo, K., Llewellyn, G., & Vu, C. (2020). *Coastal development: Resilience, restoration and infrastructure requirements.* Washington D.C.: www.oceanpanel.org/blue-papers/coastal-development-resilience-restoration-and-infrastructure-requirements.

Stark, J., Oyen, V., Meire, P., & Temmerman, S. (2015). Observations of tidal and storm surge attenuation in a large tidal marsh. *Limnology and Oceanography*, Pp. 1371-1381 | Vol. 60.

Sturm, T., Hong, S., & Hobson, P. (2008). Estimating critical shear stress of bed sediment for improved prediction of bridge contraction scour in Georgia. *Digital Library of Georgia*.

Suedel, B., Calabria, J., Bilskie, M., Byers, J., Broich, K., Mckay, K., . . . Dolatowski, E. (2022). Engineering coastal structures to centrally embrace biodiversity. *Journal of Environmental Management.*, pp. 1-10 .

Survey., U. G. (2021). National Land Cover Database (NLCD) 2021 land cover and Imperviousness. . *Multi-Resolution Land Characteristics (MRLC) Consortium.*, https://www.mrlc.gov/viewer/.

Sutton-Grier, A., Wowk, K., & Bamford, H. (2015). Future of our coasts: The potential for natural and hybrid infrastructure to enhance the resilience of our coastal communities, economies and ecosystems. . *Environmental Science & Policy*, pp. 137-148 | Vol. 51.

Sutton-Grier, A., Gittman, R., Arkema, K., Bennett, R., Benoit, J., Blitch, S., . . . Grabowski, J. (2018). Investing in natural and nature-based infrastructure: Building better along our coasts. *MDPI: Sustainability*, Vol 10 | No. 2 | https://doi.org/10.3390/su10020523.

Taylor, M., Baker, R., Simenstad, C., & Weinstein, M. (2021). Concepts and Controversies in tidal marsh ecology revisited. *Estuaries and Coasts*, 1493-1496.

Temmerman, S., Govers, G., Wartel, S., Meire, P. (2003). Spatial and temporal factors controlling short-term sedimentation in a salt and freshwater tidal marsh, Scheldt estuary, Belgium, SW Netherlands. *Earth Surface Processes and Landforms*, Vol.28 | No. 7 |.

Temmerman, S., Horstman, E., Krauss, K., Mullarney, J., Pelckmans, I., & Schoutens, K. (2023). Marshes and mangroves as nature-based coastal storm buffers. *Annual Review of Marine Science*, pp. 95 - 118 | Vol. 15.

The American Littoral Society. (2012). Assessing the impacts of Hurricane Sandy on Coastal Habitats. https://www.nrc.gov/docs/ML1409/ML14094A367.pdf.

Thoman, R., & Niezgoda, S. (2008). Determining erodibility, critical shear stress, and allowable discharge estimates for cohesive channels: Case study in the Powder River Basin of Wyoming. *Journal of Hydraulic Engineering*, Vol. 34 | No. 12.

TNC. (2021). Nature's role in Mitigating damages from storms, wildfires - TNC Guidebook promotes nature-based solutions. *The Nature Conservancy*, https://www.nature.org/en-us/what-we-do/our-priorities/tackle-climate-change/climate-change-stories/nature-based-fema-hazard-mitigation-guidebook/?vu=femaguide.

Turner, R., Swenson, E., Milan, C., Lee, J., & Oswald, T. (2004). Below-ground biomass in healthy and impared salt marshes. *Ecol Res*, 29-35.

U.S.A.C.E. (2021). *River Analysis System.* https://rashms.com/wp-content/uploads/2021/06/HEC-RAS-2D-Mannual-Mannings-n.pdf.

U.S.A.C.E. (2022, October 21). *Advanced Circulation Model*. Retrieved from Engineer Research and Development Center Website: https://www.erdc.usace.army.mil/Media/Fact-Sheets/Fact-Sheet-Article-View/Article/476698/advanced-circulation-model/

U.S.G.S. (2018). Multi-Resolution Land Characteristics Consortium. https://www.mrlc.gov/viewer/.

United Nations Environment Programme (UNEP). (2022, October 12). *Nature-based Solutions: Opportunities and challenges for scaling up.* Retrieved from United Nations: https://www.unepfi.org/nature/nature/nature-based-solutions/

United Nations Framework Convention on Climate Change. (1999). Coastal Adaptation Technologies.

United Nations: Climate Change. (2022, September 13). *United in Science: We are Heading in the Wrong Direction*. Retrieved from https://unfccc.int/news/united-in-science-we-are-heading-in-the-wrong-direction

U.S. Army. (2025). Fort Stewart-Hunter Army Airfield. https://home.army.mil/stewart/about/history/hunter-army-airfield-history

Van Coppenolle, R., & Temmerman, S. (2020). Identifying global hotspots where coastal wetland conservation can contribute to nature-based mitigation of coastal flood risks. *Global and Planetary Change, Elsevier*, 103125.

van der Wulp, S., Dsikowitzky, L., Hesse, K., & Schwarzbauer, J. (2016). Master Plan Jakarta, Indonesia: The Giant Seawall and the need for structural treatment of municipal waste water. *Marine Pollution Bulletin*, 686-693.

Van Proosdij, D., Lundholm, J., Neatt, N., Bowron, T., & Graham, J. (2010, October). Ecological re-engineering of a freshwater impoundment for salt marsh restoration in a hypertidal system. *Ecological Engineering*, 1314-1332. Retrieved from https://www.sciencedirect.com/science/article/pii/S092585741000162X

van Rijn, L. (2019). Critical movement of large rocks in currents and waves. *International Journal of Sediment Research*, 1-21.

van Zelst, V., Dijkstra, J., van Vesenbeeck, B., Eilander, D., Morris, E., Winsemius, H., . . . de Vries, M. (2021). Cutting the costs of coastal protection by integrating vegetation in flood defences. *Nature Communications*, Vol. 12 | No. 6533.

Visser, J. M., Midway, S., Baltz, D. M., & Sasser, C. E. (2019). Ecosystem Structure of Tidal Saline Marshes. In G. M. Perillo, E. Wolanski, D. Cahoon, & C. Hopkinson, *Coastal Wetlands: An Integrated Ecosystem Approach* (pp. 1-75). Elsevier.

Vurilj, M., Antolinez, J., Muis, S., & Napoles, O. (2025). Storm surge hydrographs from historical observations of sea level along the Dutch North Sea coast. *Natural Hazards*, pp. 1 - 29.

Waite, T., Chaintarli, K., Beck, C., Bone, A., Amlot, R., Kovats, S., . . . Oliver, I. (2017). The English national cohort study of flooding and health: cross-sectional analysis of mental health outcomes at year one. *BMC Public Health*, https://doi.org/10.1186/s12889-016-4000-2.

Walsh, S., & Miskewitz, R. (2013). Impact of sea level rise on tide gate function. *Journal of Environmental Science and Health*, Vol. 48 | No. 4.

Wamsley, V., Cialone, M., Smith, J., Atkinson, J., & Rosati, J. (2010). The potential of wetlands in reducing storm surge. *Ocean Engineering*, pp. 59 - 68 | Vol. 37 .

Wang, Y., Yin, Z., & Liu, Y. (2021). Predicting the bulk drag coefficient of flexible vegetation in wave flows based on a genetic programming algorithm. *Ocean Engineering*, Vol. 223 | https://www.sciencedirect.com/science/article/abs/pii/S0029801821001293.

Warner, S., & MacCready, P. (2014). Headland: Internal waves versus eddies. *Journal of Geophysical Research: Oceans*, pp. 1554-1571.

Waryszak, P., Gavoille, A., Whitt, A., Kelvin, J., & Macreadie, P. (2021). Combining gray and green infrastructure to improve coastal resilience: lessons learnt from hybrid flood defenses. *Coastal Engineering Journal*, 335-350.

Watson, I., & Finkl Jr., C. (1990). State of the Art in Storm-Surge Protection: The Netherlands Delta Project. *Journal of Coastal Research*, 739-764.

Welch-Devine, M., & Orland, B. (2020). Is It Time to Move Away? How Hurricanes Affect Future Plans. *International Journal of Mass Emergencies and Disasters*, 54-76.

Westerink, B., Luettich, R., & Scheffner, N. (1994). *ADCIRC: An advanced three-dimensional circulation model for shelves, coasts, and estuaries.*

Westerink, J., Blain, C., Luettich, R., & Scheffner, N. (1994). ADCIRC: An advanced three-dimensional circulation model for shelves, coasts, and estuaries. pp. 1-168.

Wheeler, B., White, M., Stahl-Timmins, W., & Depledge, M. (2012). Does living by the coast improve health and wellbeing? *Health & Place*, 1198-1201.

Whigham, D., & Simpson, R. (1978). The relationship between aboveground and belowground biomass of freshwater tidal wetland macrophytes. *Aquatic Botany*, pp. 355 - 364 | Vol. 5.

Williams, P., Thornton, E., & Monismith, S. (2008). *Elkhorn slough tidal wetland project. Hydrodynamic modeling and morphologic projections of largs-scale restoration actions.* San Francisco: Philip Williams & Associates.

Woods, H. (2021, March 17). *Assessing Salt Marsh Vulnerability Nationwide*. Retrieved from United States Geological Survey (USGS): https://www.usgs.gov/news/assessing-salt-marsh-vulnerability-nationwide

Wright, L. (1977). Sediment transport and deposition at river mouths: A synthesis. *GSA Bulletin*, pp. 857-868 | Vol. 88 | No. 6.

Wu, W., & Marsooli, R. (2012). A depth-averaged 2-D shallow water model for breaking and non-breaking long waves affected by rigid vegetation. *Journal of Hydraulic Resources*, 558-575.

Yasmin, M., Razali, S., Sharil, S., Mohtar, W., & Saadon, K. (2022). Effectiveness of tidal control gates in flood-prone areas during high tide appearances. *Sec. Interdisciplinary Climate Studies*.

Yu, S., Cui, B., Xie, T., Wang, Q., Yan, J., & Ning, Z. (2022). Research progress and development trend of coastal wetland restoration in Greater Bay areas. *Watershed Ecology and the Environment*, Vol. 4 | pp. 177-187.

Zhang, H., Wang, Z., Dai, L., & Xu, W. (2015). Influence of vegetation on turbulence characteristics and Reynolds shear stress in partly vegetated channels. *Journal of Fluids Engineering*, Vol. 137 | No. 6 | doi: https://doi.org/10.1115/1.4029608.

Zhang, K., Douglas, B., & Leatherman, S. (2004). Global Warming and Coastal Erosion. *Climate Change*, pp. 41-58 | Vol. 64.

Zhang, X., & Nepf, H. (2021, October 13). Wave damping by flexible marsh plants influenced by current. *Physical Review Fluids*. Retrieved from https://journals.aps.org/prfluids/abstract/10.1103/PhysRevFluids.6.100502

Zhang, X., & Nepf, H. (2021). Wave-induced reconfiguration of and drag on marsh plants. *Journal of Fluids and Structures*, 1-20. Retrieved from https://doi.org/10.1016/j.jfluidstructs.2020.103192

Zhang, X., & Nepf, H. (2024). Laboratory data linking the reconfiguration of and drag on individual plants to the velocity structure and wave dissipation over a meadow of salt marsh plants under waves with and without current. *Earth System Science Data*, Vol. 26 | No. 2 | pp. 1047-1062.

Zhao, C., Yang, H., Fan, Z., Zhu, L., Wang, W., & Zeng, F. (2020). Impacts of Tide Gate Modulation on Ammonia Transport in a Semi-closed Estuary during the Dry Season—A Case Study at the Lianjiang River in South China . *MDPI*, 12(7).

Zhao, Q., Bai, J., Huang, L., Gu, B., Lu, Q., & Gao, Z. (2016). A review of methodologies and success indicators for coastal wetland restoration. *ELSEVIER: Ecological Indicators*, Vol. 60 | pp. 442-452.

Zhu, L., Chen, Q., Ding, Y., Jafari, N., Wang, H., & Johnson, B. (2023, November 27). Towards a unified drag coefficient formula for quantifying wave energy reduction by salt marshes. *Coastal Engineering*, 10.1016/j.coastaleng.2022.104256. Retrieved from https://www.usgs.gov/publications/towards-a-unified-drag-coefficient-formula-quantifying-wave-energy-reduction-salt